

Award Number: W81XWH-05-1-0390

TITLE: Chemoprevention of breast cancer by mimicking the protective effect of early first birth.

PRINCIPAL INVESTIGATOR: Malcolm C. Pike, PhD

CONTRACTING ORGANIZATION: University of Southern California
Los Angeles, CA 90089

REPORT DATE: March 2013

TYPE OF REPORT: Final addendum

PREPARED FOR: U.S. Army Medical Research and Materiel Command
Fort Detrick, Maryland 21702-5012

DISTRIBUTION STATEMENT: Approved for Public Release;
Distribution Unlimited

The views, opinions and/or findings contained in this report are those of the author(s) and should not be construed as an official Department of the Army position, policy or decision unless so designated by other documentation.

REPORT DOCUMENTATION PAGE			<i>Form Approved</i> <i>OMB No. 0704-0188</i>		
Public reporting burden for this collection of information is estimated to average 1 hour per response, including the time for reviewing instructions, searching existing data sources, gathering and maintaining the data needed, and completing and reviewing this collection of information. Send comments regarding this burden estimate or any other aspect of this collection of information, including suggestions for reducing this burden to Department of Defense, Washington Headquarters Services, Directorate for Information Operations and Reports (0704-0188), 1215 Jefferson Davis Highway, Suite 1204, Arlington, VA 22202-4302. Respondents should be aware that notwithstanding any other provision of law, no person shall be subject to any penalty for failing to comply with a collection of information if it does not display a currently valid OMB control number. PLEASE DO NOT RETURN YOUR FORM TO THE ABOVE ADDRESS.					
1. REPORT DATE March 2013		2. REPORT TYPE Final addendum		3. DATES COVERED 2 May 2012 – 2 February 2013	
4. TITLE AND SUBTITLE Chemoprevention of breast cancer by mimicking the protective Effect of early first birth				5a. CONTRACT NUMBER	
				5b. GRANT NUMBER W81XWH-05-1-0390	
				5c. PROGRAM ELEMENT NUMBER	
6. AUTHOR(S) Malcolm C. Pike, PhD, Anna H. Wu, PhD, Celeste Leigh Pearce, PhD E-Mail: mcpike@usc.edu				5d. PROJECT NUMBER	
				5e. TASK NUMBER	
				5f. WORK UNIT NUMBER	
7. PERFORMING ORGANIZATION NAME(S) AND ADDRESS(ES) University of Southern California Los Angeles, CA 90089				8. PERFORMING ORGANIZATION REPORT NUMBER	
9. SPONSORING / MONITORING AGENCY NAME(S) AND ADDRESS(ES) U.S. Army Medical Research and Materiel Command Fort Detrick, Maryland 21702-5012				10. SPONSOR/MONITOR'S ACRONYM(S)	
				11. SPONSOR/MONITOR'S REPORT NUMBER(S)	
12. DISTRIBUTION / AVAILABILITY STATEMENT Approved for Public Release; Distribution Unlimited					
13. SUPPLEMENTARY NOTES					
14. ABSTRACT Breast terminal duct lobular unit tissue cell proliferation and estrogen and progesterone receptor expression (ER α and both PRA and PRB) have been studied by immunohistochemistry in four protocols relating to chemoprevention: (1) parous and nulliparous women; (2) women in the first trimester of pregnancy; (3) women briefly exposed to high levels of estrogen secondary to ovarian stimulation; and (4) women using oral contraceptives (OCs) with the same estrogen dose but markedly different doses of the progestin, norethisterone. Further related studies are currently being completed. Pregnancy reduced PRA expression (and cell proliferation) and lower PRA distinguished parous from nulliparous women, but PRA levels were not reduced with short-term high levels of estrogen. Results from our study of high levels of progestin exposure will be available shortly. Most importantly, reducing the dose of the progestin in an OC by 60% failed to reduce cell proliferation, due it appears to marked increases in receptor levels. Results from our study of reducing the estrogen dose while keeping the progestin dose constant in an OC will be available shortly. Early in this grant we showed that breast tissue was overwhelmingly concentrated in dense tissue. Pregnancy reduces mammographic density and long-term breast cancer risk; study of a large autopsy series and the results discussed above suggest that the protection is due to a reduction in breast tissue and in its cell proliferation rate. We successfully identified a set of breast tissue gene expression changes that distinguish parous from nulliparous rats and mice: a critical step in the testing of possible experimental chemoprevention approaches. We showed that, in the rat, estradiol, estradiol plus progesterone, and β -HCG are protective against carcinogen-induced mammary cancer. Progesterone alone was not. We are currently testing this effect of β -HCG in women funded by another grant.					
15. SUBJECT TERMS					
16. SECURITY CLASSIFICATION OF:			17. LIMITATION OF ABSTRACT	18. NUMBER OF PAGES	19a. NAME OF RESPONSIBLE PERSON USAMRMC
a. REPORT U	b. ABSTRACT U	c. THIS PAGE U			19b. TELEPHONE NUMBER (include area code)
			UU	111	

Table of Contents

	<u>Page</u>
Introduction.....	4
Body.....	4 - 33
Key Research Accomplishments.....	34 - 35
Reportable Outcomes.....	36
Conclusion.....	37
References.....	38
List of Personnel.....	39 - 40
Appendices.....	41 - 111

INTRODUCTION: This Innovator Award is designed to provide insight into the ways in which a chemoprevention regimen can mimic the protective effect of a full-term pregnancy (a birth) against breast cancer. In addition, we are aiming to understand the mechanisms underlying the risk associated with increased mammographic density, the strongest known risk factor for breast cancer after the highly penetrant genetic risk factors of BRCA1 and BRCA2 mutations. Mammographic densities are permanently reduced by births; and this relationship is being explored in order to determine if this is an important part of the mechanism by which births provide protection against breast cancer. This work is being conducted both in humans and rodents.

BODY: The Innovator Award consists of four projects (Projects 1 and 2 are being completed through a subcontract to Dr. Lewis Chodosh at the University of Pennsylvania, and Projects 3 and 4 are being completed by the team at USC).

Projects 1 and 2

Task 1: Months 1-12: Treat rats with different hormonal chemoprevention regimens, harvest mammary tissue, and isolate RNA.

Groups of Lewis rats have been treated with pellets containing either estradiol, progesterone, estradiol and progesterone, β -hCG, or perphenazine. Animals were treated for 21 days. Pellets were then removed and animals sacrificed 28 days later. Control groups consisted of parous animals allowed to undergo a single round of pregnancy, lactation, and 28 days of involution, as well as age-matched nulliparous controls. For all groups, total RNA was prepared from mammary glands by ultracentrifugation through a CsCl/guanidinium isothiocyanate cushion.

The effects of each of these hormonal treatments on the susceptibility to MNU-induced mammary tumorigenesis was tested using standard protocols either with MNU administered before hormonal treatments or after. Similar results were obtained and confirmed that treatment with estradiol, estradiol and progesterone, or β -hCG is protective against mammary tumorigenesis, whereas treatment with progesterone is not. Additionally, we found that treatment with perphenazine was partially protective against MNU-induced tumorigenesis.

Task 2: Months 6-24: Analyze morphological changes and determine global gene expression profiles for rat mammary gland samples from rats treated with different hormonal chemoprevention regimens.

Analysis of mammary gland morphology by carmine stained whole mounts as well as by hematoxylin and eosin-stained sections indicated that after 21 days of hormone treatment with estradiol, estradiol and progesterone, β -hCG, or perphenazine, each gave rise to mammary epithelial differentiation comparable to that observed in mid-pregnant animals. In contrast, treatment with progesterone had no effect on mammary epithelial morphology.

Mammary gland morphology was also examined following 28 days of involution following treatment termination. This analysis revealed that mammary gland morphology was extremely similar among all groups and that there were not obvious

differences in the amount of epithelium present.

RNA prepared from each of these experimental groups was used to generate biotinylated cRNA suitable for hybridization to Affymetrix oligonucleotide microarrays. Each of these samples was subsequently hybridized to Affymetrix microarrays. Array results have been analyzed and quality control parameters have confirmed successful hybridization and scanning of the arrays. Analyses of these microarray data sets have also been performed to identify genes that are differentially expressed as a consequence of each hormonal treatment regimen.

All hormone treatments, in addition to pregnancy, led to significant gene expression changes in the mammary gland after 4 weeks of regression (Table 1). The number of differentially expressed genes in response to pregnancy and progesterone treatment was relatively small, while estradiol, estradiol plus progesterone, β -hCG, and perphenazine treatment led to more widespread gene expression changes.

Experimental condition	Baseline condition	Differentially Expressed Genes (Experimental/Baseline)		
		Total	Up-regulated	Down-regulated
G1P1	G0P0	314	137	177
P	G0P0	294	132	162
E	G0P0	1613	905	708
E+P	G0P0	1559	655	904
HCG	G0P0	1206	443	763
PPZ	G0P0	1431	565	866

Table 1. Differentially expressed genes in response to various hormone treatments. Rats were treated with the indicated hormones for 21 days, and the mammary gland was allowed to regress for 28 days following treatment termination. Genes differentially expressed in response to each treatment compared to nulliparous controls (G0P0) were identified by microarray analysis. Differentially expressed genes were identified by CyberT at an FDR <10%.

We next sought to identify genes that are differentially expressed in response to protective, but not non-protective, hormonal treatments. Perphenazine treatment conferred only partial protection against MNU-induced tumorigenesis and elicited variable degrees of mammary epithelial differentiation. To avoid confounding effects of this heterogeneity, we excluded perphenazine-treated rats from this analysis. We compared genes commonly up- or down-regulated by protective (G1P1, E, E+P, and β -hCG) but not non-protective (P) regimens. This analysis identified 47 genes commonly upregulated (Table 2) and 28 genes commonly downregulated (Table 3) in protective hormone treatments, but that were unaltered in the non-protective treatment. These represent promising candidates for genes that are responsible for the chemopreventive effects of these hormonal regimens.

Gene ID	Symbol	Name
29173	Csn2	casein beta
114595	Csng	casein gamma
114596	Wap	whey acidic protein

314487		Partial mRNA for immunoglobulin alpha heavy chain (partial), complete constant region
394266	Gjb2	gap junction membrane channel protein beta 2
54231	Ca2	carbonic anhydrase 2
29229	Spt1	salivary protein 1
117033	Mmp12	matrix metalloproteinase 12
24903	Kng	T-kininogen
24284	Csn1	Casein, alpha
Gene ID	Symbol	Name
54231	Ca2	carbonic anhydrase 2
24567	Mt1a	Metallothionein
29469	Lbp	lipopolysaccharide binding protein
24528	Lalba	lactalbumin, alpha
24567	Mt1a	Metallothionein
64669	Mch	medium-chain S-acyl fatty acid synthetase thio ester hydrolase (MCH)
24567	Mt1a	Metallothionein
170496	Lcn2	lipocalin 2
79131	Fabp3	fatty acid binding protein 3
29188	Csn10	casein kappa
171578	Muc4	mucin 4
24571	Muc1	mucin 1
24191	Aldoc	aldolase C, fructose-biphosphate
25046	Pigr	polymeric immunoglobulin receptor
24191	Aldoc	aldolase C, fructose-biphosphate
81503	Gro1	gro
24825	Tf	Transferrin
361725	MGC72333	similar to PROSTATIC STEROID-BINDING PROTEIN C3 CHAIN PRECURSOR (PROSTATEIN PEPTIDE C3)
25717	Tgfb3	transforming growth factor, beta 3
24825	Tf	Transferrin
83497	Ocln	occludin
25145	Cd24	CD24 antigen
83497	Ocln	occludin
29285	Rps15	ribosomal protein S15
362350		Rat T-cell receptor active beta-chain C-region mRNA, partial cds, clone TRB4
25277	Mfge8	milk fat globule-EGF factor 8 protein
60350	Cd14	CD14 antigen
25717	Tgfb3	transforming growth factor, beta 3
24268	Cp	ceruloplasmin
25055	Lipa	lipase A, lysosomal acid
294257	Bf	B-factor, properdin
60350	Cd14	CD14 antigen
25275	Cnp1	cyclic nucleotide phosphodiesterase 1
298199	ADRP	adipose differentiation-related protein
24767	Scnn1b	sodium channel, nonvoltage-gated 1 beta
54410	LOC54410	alkaline phosphodiesterase
25279	Cyp24	cytochrome P450, subfamily 24

Table 2. Genes commonly and uniquely upregulated in response to protective hormonal regimens (E, E+P, HCG) or parity compared to nulliparous rats.

Gene ID	Symbol	Name
50561	Resp18	regulated endocrine-specific protein 18
25492	Nfia	nuclear factor I/A
94339	Mmp23	Matrix metalloproteinase 23
50658	Mapk9	stress activated protein kinase alpha II
Gene ID	Symbol	Name
81008	Itga7	integrin alpha 7
29637	Hmgcs1	3-hydroxy-3-methylglutaryl-Coenzyme A synthase 1
60627	LOC60627	component of rsec6/8 secretory complex p71 (71 kDa)
140808	Enman	endo-alpha-mannosidase
25157	Plagl1	pleiomorphic adenoma gene-like 1
24472	Hspa1a	heat shock 70kD protein 1A
64030	Kit	c-kit receptor tyrosine kinase
65028	Hsj2	DnaJ-like protein
83626	Ugcg	UDP-glucose:ceramide glycosyltransferase
29650	Adam10	a disintegrin and metalloprotease domain 10
309798		Similar to Golgi coiled coil protein GCC185 (LOC309798), mRNA
64831	Ireb2	iron-regulatory protein 2
24848	Tph	tryptophan hydroxylase
25230	Add3	adducin 3, gamma
117255	Ptpn12	protein tyrosine phosphatase, non-receptor type 12
29416	Kat2	kynurenine aminotransferase 2
25382	Aplp2	amyloid beta (A4) precursor-like protein 2
24553	Met	met proto-oncogene
25510	Pcp4	Purkinje cell protein 4
54245	Crko	avian sarcoma virus CT10 (v-crk) oncogene homolog
24679	Prkar2b	protein kinase, cAMP dependent regulatory, type II beta
25404	Cav	caveolin
79124	Anxa4	ZAP 36/annexin IV
25705	Tcf8	transcription factor 8

Table 3. Genes commonly and uniquely downregulated in response to protective hormonal regimens (E, E+P, β -hCG) or parity compared to nulliparous rats.

We next wished to assess the overlap between these lists and the gene signature ('core parous signature') that we identified as being conserved across multiple rat strains, as is described in Tasks 3 and 4. We focused our initial efforts on genes that are upregulated in response to parity or protective hormone treatments. The core parous signature contains 17 up-regulated genes, and there are 39 genes whose expression is commonly up-regulated among protective hormonal treatments. There is a statistically significant overlap of 8 genes between these two lists ($p < 1 \times 10^{-10}$, hypergeometric test).

The core parous signature was identified by comparing gene expression changes common across several rat strains, while the protective hormone signature was generated in Lewis rats. When we limited our analysis to Lewis rats, the intersection of the lists increased to 23 of the 39 genes ($p < 1 \times 10^{-12}$). Global analysis of gene expression using principal component analysis (PCA) revealed that β -hCG treatment elicited distinct gene expression changes as compared to pregnancy, E, or E+P (Fig. 1). Thus we considered that eliminating β -hCG from the analysis might further increase the overlap between the two signatures. Indeed, comparing only genes altered in response to pregnancy, E, and E+P with the Lewis-only signature described above yielded the most significant overlap

($p < 1 \times 10^{-16}$).

These results suggest that gene expression changes that are a common end-point of protective hormonal changes are very similar to pregnancy-induced changes that are conserved across multiple rat strains.

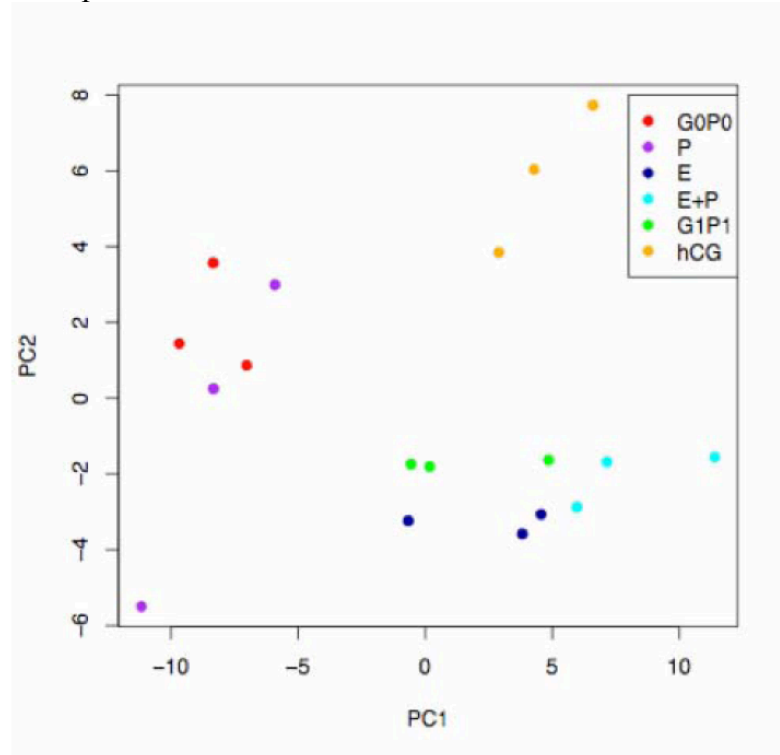


Figure 1. Principal component analysis of hormonal treatments or pregnancy showing that hCG elicits distinct gene expression patterns compared to other protective conditions.

Task 3: Months 6-36: Identify genes that are expressed in a parity-specific manner in the rat.

This task was completed and published in *Cancer Research* (Blakely et al., 66:6421-6431, 2006; erratum in 67:844-846), where it was featured on the cover.

A major challenge posed by global gene expression surveys is the large number of differentially expressed genes that are typically identified, only a few of which may contribute causally to the phenomenon under study. Consequently, we considered approaches to identifying parity-induced changes in the rat mammary gland that would permit the resulting list of expressed genes to be narrowed to those most robustly associated with parity-induced protection against mammary tumorigenesis. Given the marked genetic and biological heterogeneity between different inbred rat strains, we reasoned that identifying expression changes that are conserved across multiple strains exhibiting hormone-induced protection against mammary tumorigenesis would facilitate the identification of a core set of genes associated with parity-induced protection against breast cancer.

To achieve this goal, we focused on gene expression changes that are conserved among different strains of rats that exhibit hormone-induced protection against mammary tumorigenesis. Four inbred rat strains that exhibit marked differences in their intrinsic

susceptibilities to carcinogen-induced mammary tumorigenesis were each demonstrated to display significant protection against MNU-induced mammary tumorigenesis following treatment with pregnancy levels of estradiol and progesterone. Microarray expression profiling of parous and nulliparous mammary tissue from these four strains yielded a common 70-gene signature. Examination of the genes constituting this signature implicated alterations in TGF- β signaling, the extracellular matrix, amphiregulin expression, and the growth hormone-IGF1 axis in pregnancy-induced alterations in breast cancer risk. Notably, related changes have been associated with decreased mammographic density, which itself is strongly associated with decreased breast cancer risk. Our findings demonstrate that hormone-induced protection against mammary tumorigenesis is widely conserved among divergent rat strains and define a gene expression signature that is tightly correlated with reduced mammary tumor susceptibility as a consequence of a normal developmental event. Given the conservation of this signature, these pathways may contribute to pregnancy-induced protection against breast cancer.

Task 4: Months 6-36: Identify genes whose expression in rats correlates with protection against breast cancer.

To narrow the list of candidate genes whose regulation might contribute to the protected state associated with parity, we attempted to identify parity-induced gene expression changes that correlated with protection across multiple rat strains. To this end, total RNA was isolated from the mammary glands of nulliparous and parous Wistar-Furth, Fischer 344, and Copenhagen rats and analyzed on RGU34A arrays. This led to the identification of 68, 64 and 92 parity-up-regulated genes and 132, 209 and 149 parity-down-regulated genes in Wistar-Furth, Fischer 344, and Copenhagen rats, respectively.

Unsupervised hierarchical clustering performed using the expression profiles of 1,954 globally varying genes across the nulliparous and parous datasets representing the four rat strains revealed that samples clustered primarily based on strain without regard to parity status. This suggested that the principal source of global variation in gene expression across these data sets was due to genetic differences between strains rather than reproductive history. This observation suggested that determining which parity-induced gene expression changes were conserved among these highly divergent rat strains could represent a powerful approach to defining a parity-related gene expression signature correlated with hormone-induced protection against mammary tumorigenesis.

To identify parity-induced gene expression changes that were conserved across strains, we selected genes that exhibited ≥ 1.2 -fold change in at least of 3 of the 4 strains analyzed. This led to the identification of 24 up-regulated and 46 down-regulated genes. Based on the number of parity-induced gene expression changes observed for each strain, an overlap of this size is highly unlikely by chance (up-regulated: $P < 1 \times 10^{-6}$, FDR $< 1\%$; down-regulated: $P < 1 \times 10^{-6}$, FDR = 4%). As such, this approach led to the identification of a set of genes whose expression is persistently altered by parity across multiple strains of rats that exhibit hormone-induced protection against mammary tumorigenesis.

To confirm the validity of the parity-related gene expression signature derived from the above studies, we performed oligonucleotide microarray analysis on samples from nulliparous and parous Lewis rats that were generated independently from those used to derive this signature. Hierarchical clustering analysis of these independent

samples using the gene signature revealed that the expression profiles of these genes were sufficient to accurately distinguish parous from nulliparous Lewis rat samples in a blinded manner.

To determine whether this parity-related signature could distinguish between nulliparous and parous mammary glands from multiple strains of rats, Lewis, Wistar-Furth, Fischer 344, and Copenhagen microarray data sets were clustered in an unsupervised manner based solely on the expression of the genes comprising the parity signature. In each of the four rat strains examined, the gene expression signature was sufficient to distinguish parous from nulliparous rats. Thus, this signature reflects parity-induced gene expression changes that are highly conserved among four genetically divergent rat strains.

Among the genes that we identified as being consistently regulated by parity, at least five categories were evident. These included the previously identified differentiation, immune, TGF- β , and growth factor categories, as well as an additional category of genes that are involved in extracellular matrix structure and function. We next demonstrated that clustering based upon genes in each of these five categories was sufficient to distinguish between nulliparous and parous mammary samples from each of the four different rat strains, from independent mammary samples derived from nulliparous and parous Lewis rats, and from mammary samples derived from FVB mice. These findings indicate that differential expression of these five subsets of genes represent conserved features of parity-induced changes in the rodent mammary gland. Our findings have now been published in *Cancer Research* (Blakely *et al.*, 66:6421-6431, 2006; erratum in 67:844-846).

Task 5: Months 1-48: Isolate RNA from human mammary gland samples and control epithelial and stromal samples.

RNA was isolated from a large number of the available human specimens. In addition, we prepared RNA from control samples consisting of: intact adipose tissue, intact fibrous (i.e., stromal and epithelial) breast tissue, epithelial organoids isolated by collagenase digestion, cultured epithelial organoids, and cultured fibroblasts from reduction mammoplasty specimens.

To achieve the objectives of this aim, we collected 168 snap-frozen human breast samples (43 nulliparous, 125 parous) from patients who had either undergone reduction mammoplasty or had an excisional biopsy for a lesion that was ultimately determined to be benign (and not associated with elevated breast cancer risk). Tissue was taken from regions determined to be normal, as assessed by a breast pathologist. Women providing samples were interviewed to obtain information on age at the time of biopsy, age at first full-term pregnancy (FFTP), age at last full-term pregnancy, number of pregnancies, number of live births, spacing of live births, lactation history, ages at first miscarriage or abortion, total number of miscarriages and abortions, menopausal status, age at menopause, history of bilateral oophorectomy, history of oral contraceptive use, and history of postmenopausal hormonal replacement therapy. Of the 168 frozen samples that we received from the Mayo Clinic, we found adequate reproductive information for 90 samples (64 parous, 26 nulliparous). Age of individuals ranged from 20 to 79 (median 41) and age at FFTP for parous samples ranged from 16-35 (median 23). RNA was harvested from these samples and its integrity was assessed. We obtained high-quality,

intact RNA from 86 samples (60 parous, 26 nulliparous) for subsequent Affymetrix microarray analysis.

In an effort to perform ‘expression deconvolution’ on our existing data set, we generated a reference data set derived from the various cell types within the breast. We obtained fresh human samples from reduction mammoplasties immediately following surgery. Pieces of tissue were dissected grossly to yield regions enriched for adipose, fibrous tissue, and epithelium (Fig. 2). Additional pieces of fibrous-rich tissue were digested with collagenase, and subject to centrifugation and filtration. Cultures of pure epithelial and fibroblast cells were obtained from flow-thru filtration columns and passaged in culture. Epithelial rich digested organoids were also obtained during the filtration process. Finally, from each mammoplasty we were able to isolate adipose, fibrous, digested organoid and pure populations of epithelial and fibroblast cells from tissue culture. RNA was extracted from each of these reference populations for subsequent Affymetrix microarray analysis.

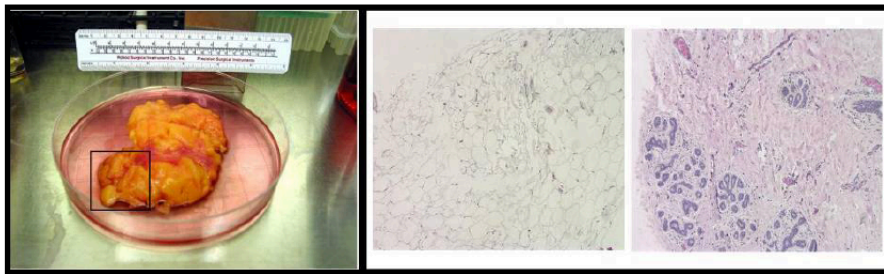


Figure 2. Representative sample from a reduction mammoplasty obtained immediately post-surgery (left). Hematoxylin and Eosin stained sections derived from tissue enriched for adipose (center) and fibrous tissue (right).

Task 6: Months 3-52: Determine global gene expression profiles for human mammary gland samples using oligonucleotide microarrays.

Tissue samples with sufficient RNA yields and quality were labeled according to manufacturer’s protocol for hybridization to Affymetrix U133A GeneChips. Following labeling and hybridization to microarrays, 72 samples (50 parous, 22 nulliparous) passed QC inspection and were appropriate for analysis. For the isolated tissue compartments, we profiled each of the cellular compartments for 8 independent reduction mammoplasties on Affymetrix U133A GeneChips.

The experiments conducted in this Task provided us with gene expression data on a large number of human breast samples with known reproductive history, as well as the expression profiles of isolated tissue compartments from the human breast. Together, this data collection was designed to allow us to identify gene expression changes that correlate with reproductive status, while using the reference data set to correct for changes in epithelial content among samples. These efforts are described in Task 7.

Task 7: Months 12-60: Identify genes whose expression in the mammary gland in

women reflects aspects of reproductive history that impact on breast cancer susceptibility.

Preliminary results suggested that identifying genes whose expression correlated with reproductive history may be confounded by significant variations in epithelial content among breast samples. Below we discuss these results and our attempts to overcome this difficulty.

As a preliminary approach toward completing this task, we explored the use of principal component analysis (PCA) to provide an overview of the variables accounting for global difference in gene expression between these samples. PCA uses the most variant genes among ~6700 based on gene expression. The first two components typically reflect the most robust differences in gene expression among samples. Breast samples for nulliparous (green) and parous (pink) microarrays did not appear to be distinguishable on the basis of the first two components by PCA (Fig. 3). This finding suggests that reproductive history does not explain the most dominant inter-patient differences in gene expression. By comparison, in analogous studies using rodent samples, parity induced gene expression changes typically predominate in the first two components in a PCA, thereby rendering nulliparous and parous samples into unique gene expression space.

In light of this finding, we sought to identify the genes that contribute to the first and second components of the PCA. Genes characteristic of epithelial cells or epithelial content were found to constitute the predominant number of genes identified. Based on this information, we then coded samples from high (red) to low (blue) according to epithelial gene expression using PCA analysis. This analysis confirmed that the pattern observed for our data set could be explained by the relative epithelial content in the original frozen samples (Fig. 4).

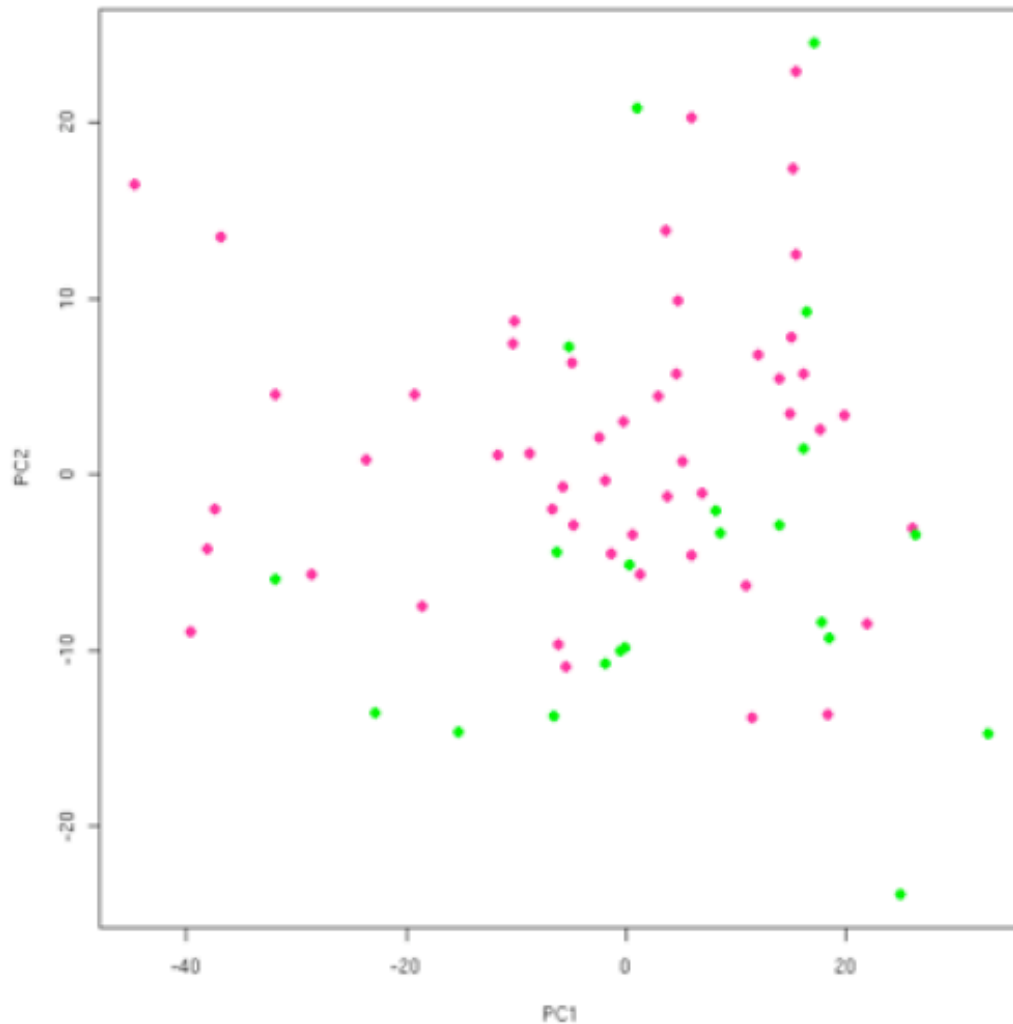


Figure 3: Principal Component Analysis based on the expression of ~6700 variant probe sets demonstrates that nulliparous (green) and parous (pink) samples do not separate by the first 2 components, suggesting that reproductive history is not the largest discriminator for this data set.

The above variability in gene expression patterns based upon epithelial content confounded our ability to address gene expression changes based on reproductive history. To circumvent these issues, we proposed using a mathematical approach termed “expression deconvolution.” Past experience dictated that the interpretation of gene expression data derived from complex organs composed of multiple cell types (like the breast) is complicated by the fact that observed changes in gene expression may be due either to cell-intrinsic changes in gene expression or to changes in the relative abundance of different cell types. Consequently, *bona fide* changes in intrinsic gene regulation can either be mimicked or masked by changes in the relative proportion of different cellular compartments. Therefore, we sought to generate reference expression data from purified populations of constituent cell types within the mammary gland, and to then use this information to computationally adjust for differences in cellular compartments within

samples.

To accomplish this goal, we generated mRNA from purified epithelial, adipose, and fibrous tissue derived from reduction mammoplasties to serve as a reference for compartment adjustment, and profiled each compartments from 8 samples on Affymetrix GeneChips. Samples passing QC were subsequently analyzed by PCA using ~5700 genes with high variance across the data set. With the exception of two adipose samples (which likely contained undetectable fibrous contamination), all cellular subtypes were distinguishable by PCA. Moreover, cell types that were maintained in culture (epithelial and fibroblast) appeared to be distinct from the uncultured tissues obtained from gross dissection (Fig. 5).

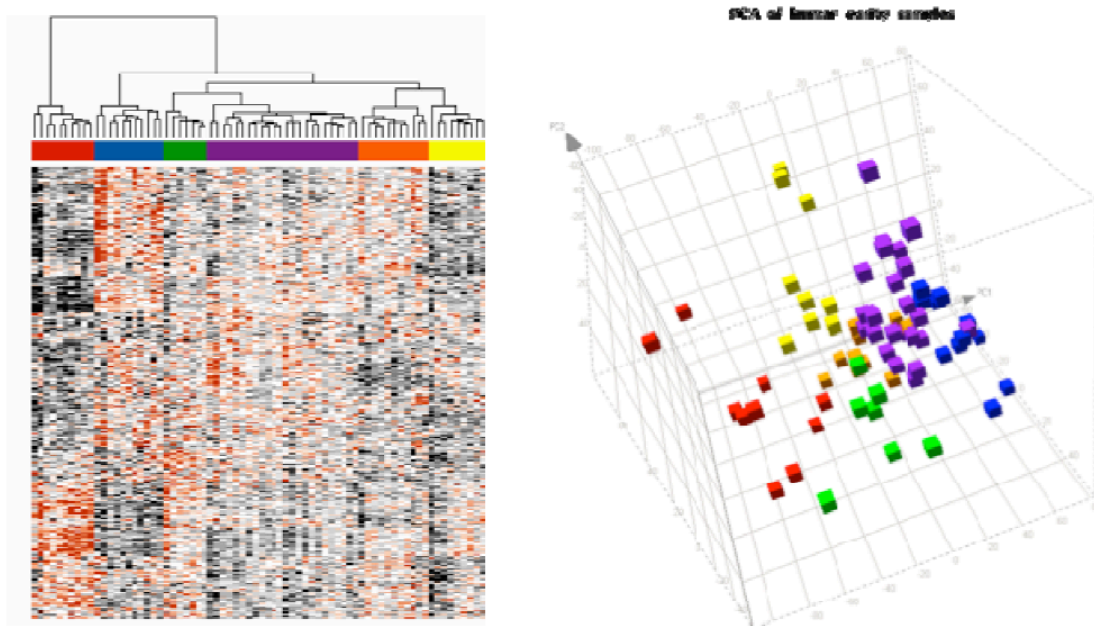


Figure 4. Hierarchical clustering of gene expression data derived from the 72 normal human breast tissue samples demonstrates that epithelial content of the individual samples drives expression to a greater extent than does reproductive history (left). Principal component analysis of individual samples color-coded for high expression of epithelial genes (red) to low expression (blue).

As an initial attempt at defining genes that could serve as discriminators of compartment class, we compiled lists of genes that were unique to adipose, cultured epithelial cells, and cultured fibroblasts. We next used these lists of genes as reference datasets to enable us to estimate the proportion of each cellular compartment present within a complex mixture of cell types.

Initially, we speculated that if we identified samples from our data set that possessed similar epithelial content, we would be able to investigate conserved parity-induced gene expression changes. Accordingly, we selected a subset of samples, from both nulliparous and parous cohorts, that exhibited similar epithelial content. Next, we identified candidate genes from our previously derived core rodent gene signature that were either up- or down-regulated as a result of parity. Consistent with findings in rodents, expression of IGFBP5, a member of the growth hormone IGF1 axis, showed a

trend toward up-regulation in parous as compared to nulliparous women (Fig. 6). Similarly, Kruppel-like factor 9 (KPL9) appeared to have a conserved trend toward higher expression in parous samples (Fig. 6).

To investigate whether genes identified as being down-regulated according to the core rodent signature were conserved, we looked at the expression of Periostin, a gene involved in cell adhesion in the extracellular matrix, as well as the expression of Lumican, a proteoglycan also integral to the extracellular matrix (Fig. 7). For both markers, the trend toward lower expression in parous samples appeared to be conserved. Consequently, we believe that human samples in which we can control for epithelial content can be controlled may in fact maintain gene expression changes that define the parous mammary gland.

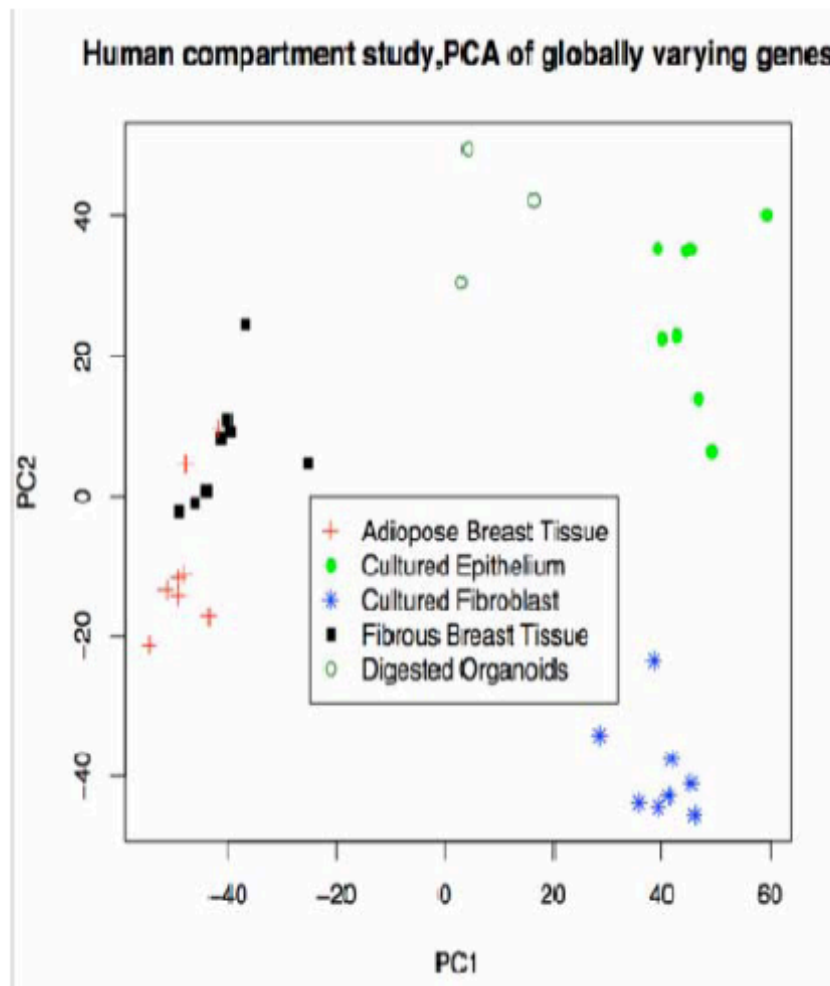


Figure 5. Principal Component Analysis of tissue compartments isolated from human reduction mammoplasties demonstrate almost complete separation by tissue type using ~5700 genes with high variance.

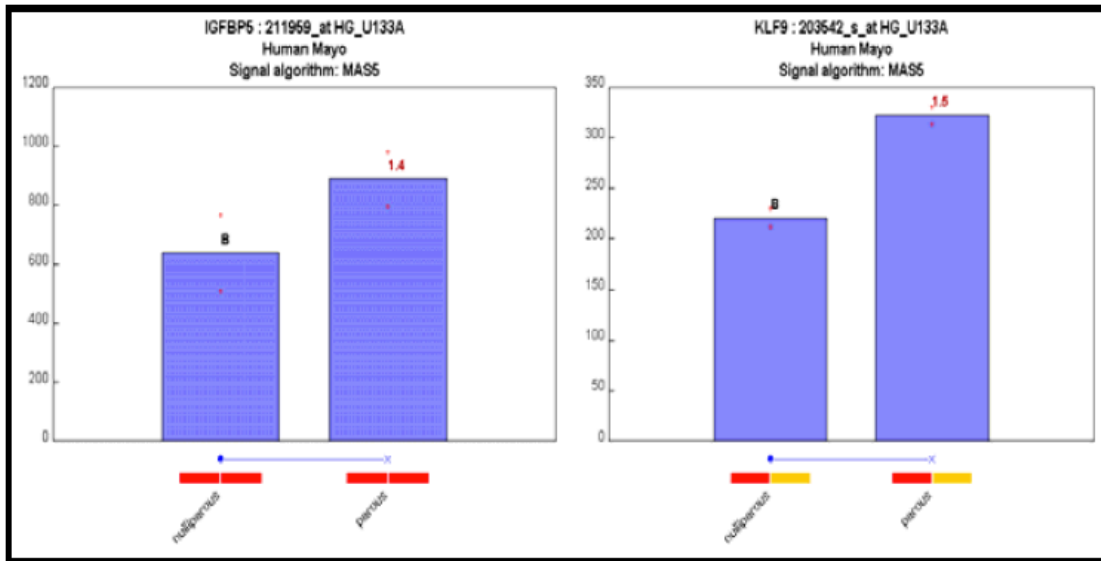


Figure 6: Gene expression analysis of IGFBP5 (left) and KLP9 (right) for a subset of nulliparous and parous samples.

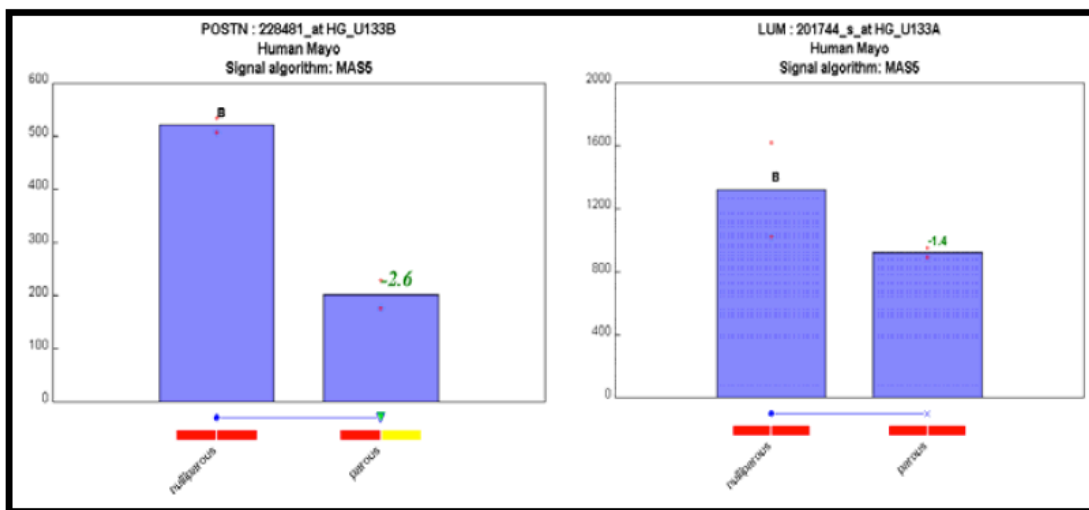
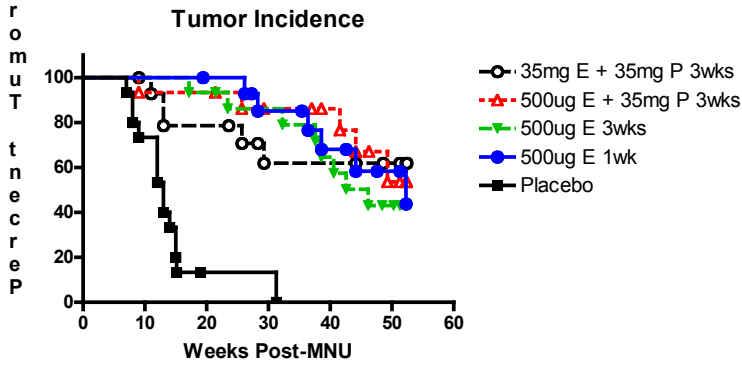


Figure 7: Gene expression analysis of Periostin (left) and Lumican (right) for a subset of nulliparous and parous samples.

Task 8: Months 1-36: Determine the effect of short-term, low-dose estradiol and progesterone treatment on MNU-induced mammary tumor susceptibility.

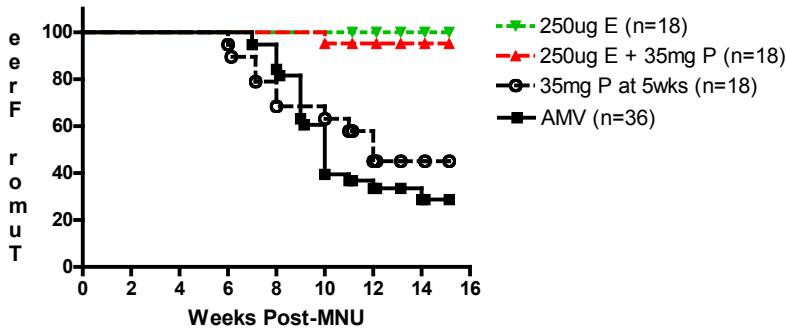
To determine whether lower doses of estradiol and progesterone confer protection against MNU-induced tumorigenesis, rats were treated with MNU followed by various doses of estradiol or estradiol plus progesterone. As expected, treatment of rats with 35mg estradiol plus 35mg progesterone for 3 weeks led to reduced MNU-induced mammary tumor susceptibility; this dose had previously been shown to confer protection against tumorigenesis (Fig. 8). Reducing the dose of estradiol to 500 μ g (Fig. 8) or 250 μ g

(Fig. 9) for 3 weeks also conferred protection, either alone or in conjunction with 35mg progesterone. To determine whether shorter hormone treatment time can also reduce tumor susceptibility, rats were treated with MNU followed by 500µg estradiol for just 1 week. This treatment also conferred protection against mammary tumors (Fig. 8). Thus these results indicate that short-term, low-dose estradiol leads to a reduction in susceptibility to MNU-induced mammary tumors.



	500ug E + 35mg P 3wks	500ug E 3wks	500ug E 1wk	Placebo
35mg E + 35mg P 3wks	0.7962	0.7200	0.9254	0.0002
500ug E + 35mg P 3wks		0.4108	0.7963	<0.0001
500ug E 3wks			0.5345	<0.0001
500ug E 1wk				<0.0001

Figure 8. Short-term and low-dose (500ug) estradiol treatment confers protection against MNU-induced mammary tumorigenesis.



	E+P	P	AMV
E	.3545	.0003	<.0001
E+P		.0007	<.0001
P			.4123

Figure 9. Low-dose (250ug) estradiol treatment confers protection against MNU-induced mammary tumorigenesis.

Task 9: Months 12-60: Determine the effect of hormone treatment on MNU-induced mammary epithelial proliferation.

This work was not completed in order to allow for work on the other tasks.

Task 10: Months 12-60: Determine whether p53 loss abrogates pregnancy-induced protection against carcinogen-induced mammary tumorigenesis.

In order to address this aim, we first needed to demonstrate that the hormone-induced protection against mammary tumors that had been observed in rats was also

operative in mice. This is because mice, but not rats, offer the opportunity to use genetic knockouts, which would be the preferred approach for addressing the involvement of p53 in pregnancy-induced protection, by demonstrating that p53 mutant mice do not exhibit parity-induced protection against breast cancer. During the previous study period we performed a number of experiments to determine whether mice exhibit hormone-induced protection. We tested multiple strains—BALBc/J mice, which have been shown by the Medina lab to be afforded protection by hormone treatment, and FVB mice, which is the strain used in many laboratories for studies of mammary tumorigenesis in genetically engineered mice. We tested BALBc/J mice from a commercial source as well as a BALBc/J substrain obtained directly from the Medina lab. We also tested whether hormone treatment delayed tumorigenesis initiated by the Neu oncogene in MMTV-Neu transgenic mice. Estradiol plus progesterone (E+P) treatment did not afford protection against mammary tumorigenesis in any of these experiments. This result was unanticipated, given that the Medina laboratory had previously demonstrated that E+P treatment confers protection against mammary carcinogenesis in BALBc/J mice. We reasoned that endogenous phytoestrogens present in the mouse diet used in our experiments could have confounded our results by altering the hormonal milieu of experimental mice. To address this issue, in the previous study period we tested whether mice that were maintained on a low phytoestrogen diet exhibited hormone-induced protection. Breeders were fed the low phytoestrogen diet AIN-76 Blue at the time of mating, and female offspring were used for tumorigenesis experiments. Experimental animals were also fed AIN-76 Blue at weaning and throughout the course of experiments. Mice were treated with E+P for 21 days beginning at 7 weeks of age, followed by DMBA administration from 12 to 18 weeks to induce tumorigenesis.

In this experiment E+P treatment caused a modest delay in mammary tumorigenesis, however this delay was not statistically significant (Fig. 10). In addition, interpretation of these results was hampered by the high mortality induced by DMBA in this experiment.

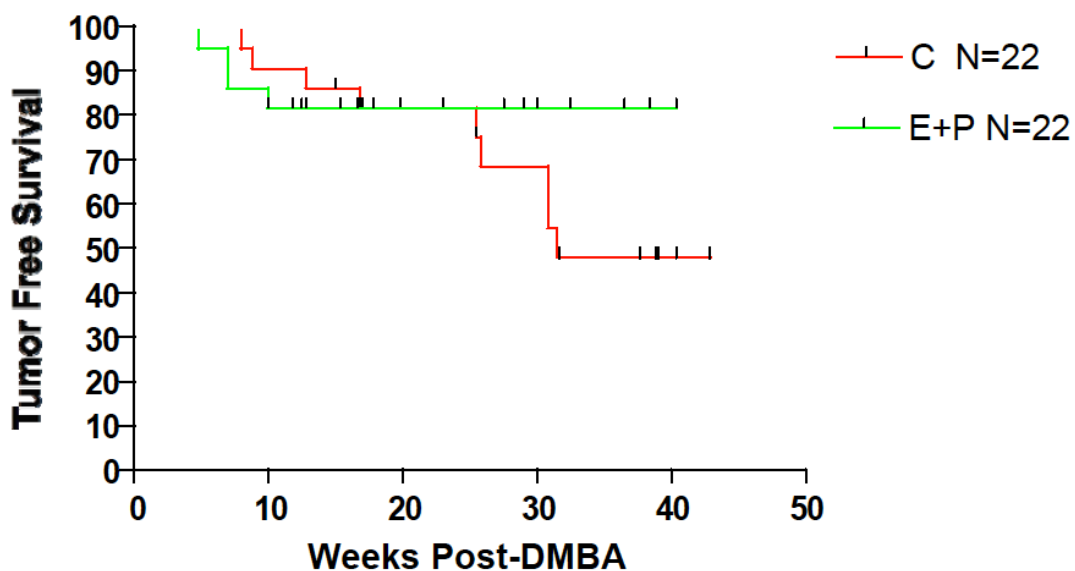


Figure 10. E+P treatment confers a modest delay in DMBA-induced mammary

tumorigenesis in BALBc/J mice on a low phytoestrogen diet. $p=0.32$.

We then performed experiments to confirm this preliminary result and to attempt to circumvent the high mortality that we observed, since this markedly limited the statistical power of our studies. To accomplish this, we first performed the identical experiment in another strain of mice, FVB. Insofar as this is the strain used by our laboratory for all transgenic models of breast cancer, demonstrating hormone-induced protection in this strain would be an important experimental advance.

FVB mice were fed a low phytoestrogen diet, AIN-76 Blue, at weaning and throughout the course of the experiment. Mice were implanted with pellets containing 200 μ g E plus 15mg P) at 7 weeks of age. After 21 days, pellets were removed and glands were allowed to regress for 14 days. Mice were then treated with DMBA weekly for 6 weeks, and monitored for tumor formation. As with BALBc mice, we observed high mortality in FVB mice treated with this experimental regimen. This high rate of mortality again prevented us from determining whether E+P confers protection against DMBA-induced mammary tumors. Although when we compared tumor formation in surviving mice between the two cohorts, we did not observe a statistically significant degree of protection against tumorigenesis by E+P (Fig. 11), the results were similar to those shown in Fig. 10.

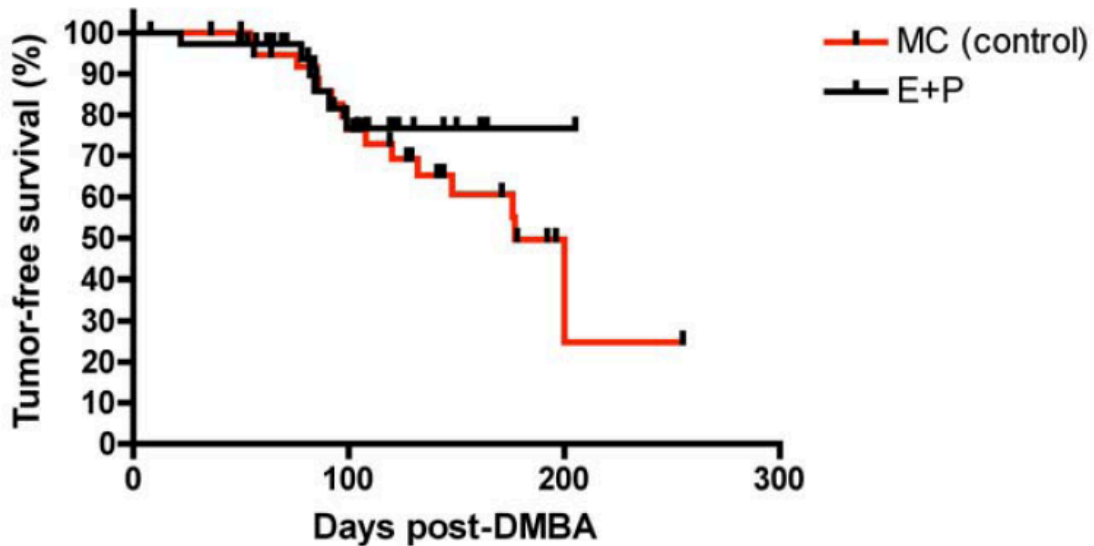


Figure 11. E+P treatment does not delay DMBA-induced mammary tumorigenesis in FVB mice fed a low phytoestrogen diet. $p=0.42$.

In light of the potential protection conferred by E+P treatment when mice are fed a low phytoestrogen diet, we next tested whether E+P could delay tumorigenesis in MMTV-neu mice maintained on this diet. MMTV-neu mice fed AIN-76 Blue were treated with E+P or cellulose control at 7 weeks of age for 21 days, and then monitored for tumor formation. The results of E+P treatment did not show any delay in tumorigenesis in MMTV-neu mice, even when fed a low phytoestrogen diet (Fig. 12). This suggests that this experimental paradigm may not be suitable for studying parity- or hormone-induced protection in mice.

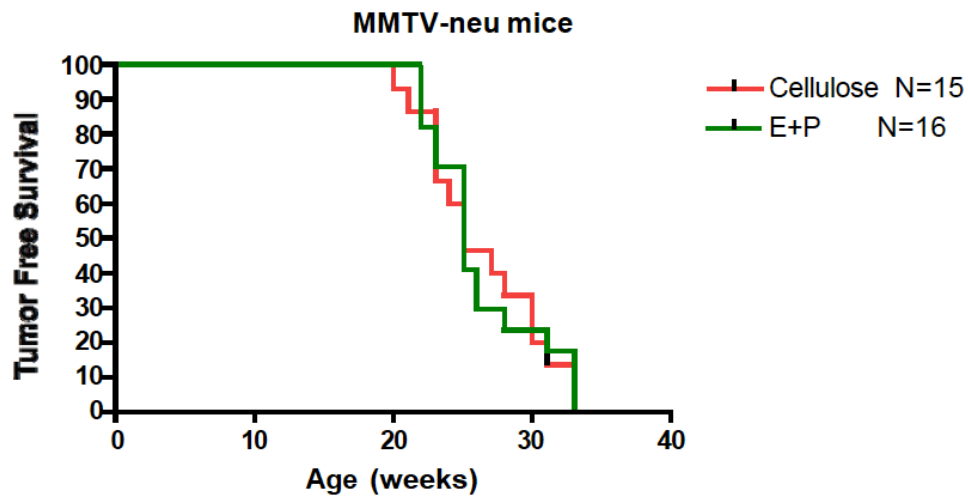


Figure 12. E+P treatment does not delay MMTV-Neu-induced mammary tumorigenesis in mice fed a low phytoestrogen diet. $p=0.91$

In summary, our findings indicate that parity-induced protection in mice is not a robust experimental phenomenon. Given this inability to demonstrate hormone-induced protection in mice, we were not able to address whether the p53 pathway is required for parity-induced protection, since this question can only be addressed directly in genetically engineered animal models deficient for p53, which do not exist in the rat.

Project 3

This project aimed to recruit subjects being treated with a variety of hormonal regimens to have pre- and/or post-treatment breast biopsies. The treatment with the hormonal agents may or may not have been a study procedure. A number of cellular, hormonal and genetic analyses were carried out on the biopsy specimens.

Task 1. Months 1-48: Develop appropriate protocols and treatment regimens.

Completed.

Task 2. Months 24-56: Recruit subjects to the treatment protocols.

Task 2a. Recruit 10 women receiving high dose progestin (Megace) for the treatment of endometrial hyperplasia (as standard of care).

For this research protocol, the subjects were to receive a breast biopsy before Megace treatment, and after three months of Megace treatment. For various reasons, but mainly because USC gynecologists were putting very few women on Megace, we only succeeded in obtaining biopsies on three women on this protocol and discontinued recruitment. Given that the goal of this protocol was to study the effect of high-dose progestins on the breast, we opened the protocol described in Project 3 Task 2c to study women receiving Depot Medroxy-progesterone Acetate.

Task 2b. Recruit 40 women seeking oral contraceptives to be randomized to a low-dose progestin content oral contraceptive or a standard progestin content oral contraceptive and to have a breast biopsy after three months of oral contraceptive use.

Completed. See below for description of the results.

Task 2c. Recruit 36 women receiving Depot Medroxy-progesterone Acetate (DMPA; Depot Provera®) as part of standard of care.

For this research protocol, the subjects received a breast biopsy on day 7±1, day 14±1 or day 21±1 (12 subjects on each of these three days) after their 2nd or subsequent consecutive DMPA injection. This protocol was planned to augment Task 2a as it measures the effect of high levels of progestins. DMPA is a 3-month injectable contraceptive with progestin levels in the first month after injection equivalent to third trimester pregnancy levels. It has proved very difficult to find volunteers for this study.

Our main source of volunteers has been the Love/Avon Army of Women, but volunteers have to be taking DMPA for contraception, *i.e.*, we are not attempting to recruit women to take DMPA, and since the majority of DMPA users are young women the number responding to e-blasts (Love/Avon Army of Women) has been small. However, we have succeeded in recruiting 15 women to the study. This study will be continued using funding providing by the Avon Foundation.

Task 2d. Recruit 50 volunteer women who are not pregnant and not currently receiving any hormonal agents to undergo a breast biopsy. This protocol will specifically recruit women into the following categories: premenopausal, nulliparous – under the age of 30 (5 women)/over the age of 30 (5 women); premenopausal, parous – under the age of 30 (10 women)/over the age of 30 (5 women); and postmenopausal – nulliparous (15 women)/parous (10 women).

This protocol was modified to allow us to recruit additional women to make up for the shortfall in recruitment in Project 4, Task 1. We recruited 60 women into this protocol.

Task 3. Months 30-58: Assay tissue samples* for cellular, hormonal and gene expression markers to determine pre- and/or post-treatment tissue characteristics.

We have completed assays for Ki67 (MIB1), ER, PRA and PRB, by immunohistochemistry (IHC), in the vast majority of the breast biopsy samples we have collected. IHC assays for the remaining samples are ongoing. We also completed assays for γ H2AX on a large number of the samples. γ H2AX measures DNA damage and is being assayed in order to study whether such damage varies with pregnancy, parity, oral contraceptive use and other factors of interest. We are continuing to study this tissue.

Task 4. Months 30-58: Assay blood samples* for hormone levels.

Blood samples taken ‘immediately’ before the prospectively collected breast biopsies have been analyzed for estradiol (E2) and progesterone (P4). See Chung *et al.* (2012; attached). Further assays have been conducted for ethinyl-estradiol (EE2) and norethindrone (NET) to assist with the interpretation of the results described in Hovanessian-Larsen *et al.* (2012, attached).

Task 5. Months 30-60: Conduct data analysis* to compare pre- and/or post-treatment tissue characteristics, to compare these changes to the differences noted between nulliparous and parous women, and to prepare manuscripts as appropriate.

*The tissue and blood assays as well as the subsequent data analysis include specimens (including breast biopsies) collected on protocols funded *via* other mechanisms that directly relate to this Innovator Award. These include specimens from: (1) 33 women undergoing a termination of pregnancy - breast biopsy obtained immediately after the termination and a subsequent biopsy several months later in a small number of them (a source of non-pregnant tissue). This protocol was aimed at measuring the effects of pregnancy levels of estradiol and progesterone. (2) 10 oocyte donors, *i.e.*, women receiving daily injections of follicle stimulating hormone (FSH) which results in the development of multiple ovarian follicles for oocyte donation to other women. This protocol was aimed at measuring the effects of greatly increased circulating estrogen levels without the other changes that occur in pregnancy. The breast biopsy was obtained on the day of, or the day prior to, oocyte retrieval. (3) 37 post-menopausal women receiving menopausal estrogen therapy that also includes intra-vaginal micronized progesterone (E+P) or placebo (E alone). This protocol was aimed at measuring the

effects of low levels of natural progesterone. Nineteen women on E+P were recruited and eighteen women on E alone. Immunohistochemical analysis of the samples is ongoing.

Studies of nulliparous, parous and 'pregnant' breast

We published a manuscript (Taylor *et al.*, 2009; attached) which compares cellular markers in the tissue collected as part of Project 4 with 'pregnant' breast tissue. This manuscript reported our studies of nuclear staining for the progesterone and estrogen receptors (PRA, PRB, ER α) and cell proliferation (Ki67, MIB1) in the epithelium of the breast terminal duct lobular unit (TDLU) of 26 naturally cycling premenopausal women and 30 pregnant women (median 8.1 weeks gestation). Results are shown in Figure 3.5.1. PRA expression decreased from a mean of 17.8% of epithelial cells in cycling subjects to 6.2% in pregnant subjects ($P = 0.013$). Ki67 expression increased from 1.7% in cycling subjects to 16.0% in pregnant subjects ($P < 0.001$). PRB and ER α expression were slightly lower in pregnant subjects but the differences were not statistically significant. Sixteen of the non-pregnant subjects were nulliparous and ten were parous.

PRA was statistically significantly lower in parous women than in nulliparous women (32.2% in nulliparous women vs 10.2%; $P = 0.014$). PRB (23.5 vs 12.9%), ER α (14.4 vs 8.6%) and Ki67 (2.2 vs 1.2%) were also lower in parous women, but the differences were not statistically significant. PRA expression may be a most useful marker of the reduction in risk with pregnancy and may be of use in evaluating the effect of any chemoprevention regimen aimed at achieving a similar reduction in risk. Short-term changes in PRA expression while the chemoprevention is being administered may also be an important marker. A most important aspect of these findings was that the marked decreases in PRA in pregnancy and in parous women have also been found in the rat. This lends much credence to the rat model for studying the protective effect of pregnancy, and suggests that the gene changes found in the rat (Projects 1 and 2 above) may be directly applicable to the human situation.

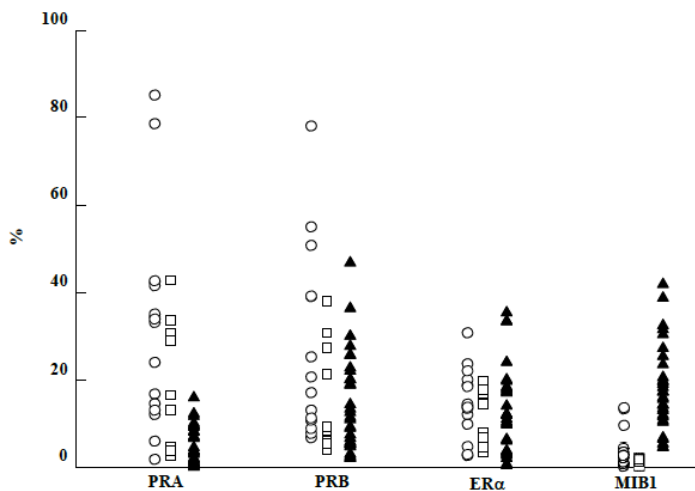


Fig. 1 % of cells expressing nuclear PRA, PRB, ER α and MIB1 in premenopausal nulliparous (○), premenopausal parous (□) and pregnant (▲) women.

Figure 3.5.1. Figure 1 in Taylor *et al.* (2009; attached).

Studies of E2 and P4 effects on the 'pregnant' breast

We have published a manuscript (Chung *et al.*, 2012; attached) which reports our studies of nuclear staining for the progesterone receptors (PRA, PRB) and estrogen receptor (ER α) and cell proliferation (Ki67, MIB1) in the epithelium of the breast terminal duct lobular unit (TDLU) of 30 pregnant women (median 8.1 weeks gestation) as they relate to the levels of serum estradiol (E2) and progesterone (P4). This manuscript also compares these results to what occurs in 26 naturally cycling women and to results obtained from studying the changes in the breast in oocyte donors.

Figure 3.5.2 shows the relationships of serum E2 and P4 to gestational age in the ‘pregnant’ women. E2 increased steadily with gestational age, from ~2,000 pmol/l at 5 weeks gestation to ~27,000 pmol/l at 18 weeks gestation. P4 did not change from the mid-luteal peak of ~40 nmol/l until around week 11 of gestation, after which it increased to ~80 nmol/l. Figure 3.5.3 shows the E2 and P4 values of the individual oocyte donors in the seven days before oocyte retrieval. E2 increased steadily in each subject until the day before oocyte retrieval – on the day of retrieval, E2 had fallen from a median of ~15,300 to ~6,000 pmol/l. P4 also increased steadily in each subject; the median value increased from 1.1 nmol/l at seven days before oocyte retrieval to 4.1 nmol/l at two days before retrieval, and then, after hCG treatment, to 18.0 nmol/l on the day before oocyte retrieval and to 36.3 nmol/l on the day of retrieval. For comparison, in naturally cycling women the follicular phase maximum E2 is ~1,100 pmol/l, the luteal phase maximum E2 is ~510 pmol/l, and the luteal phase maximum P4 is ~40 nmol/l.

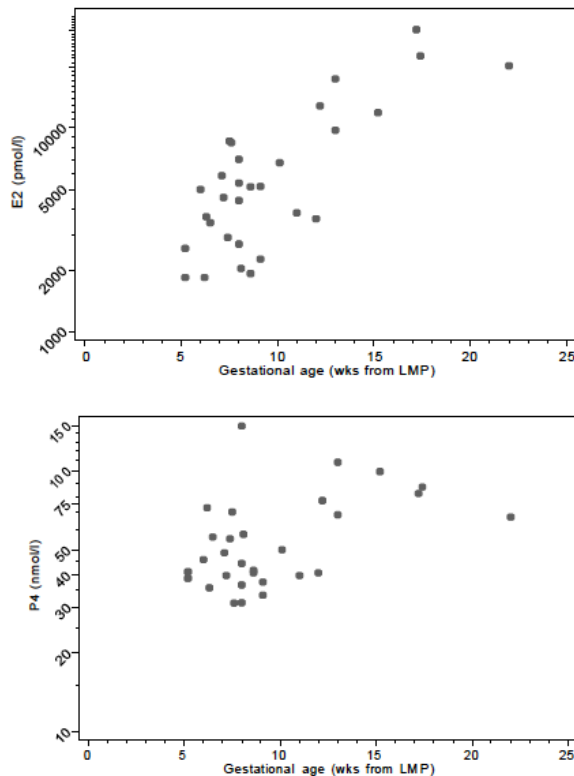


Figure 2. Individual pregnant women estradiol (E2) and progesterone (P4) values vs gestational age.

Figure 3.5.2. Figure 2 in Chung *et al.* (2012; attached).

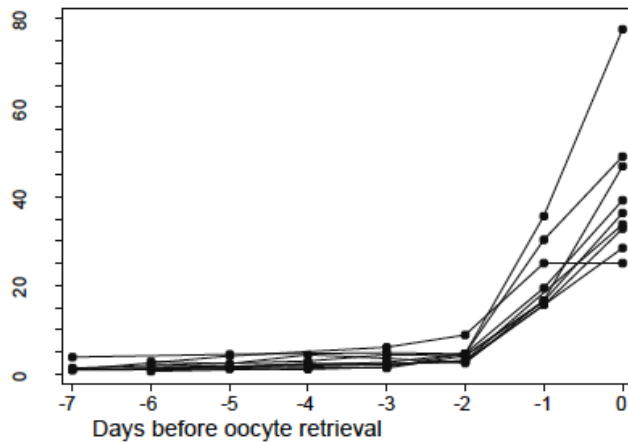
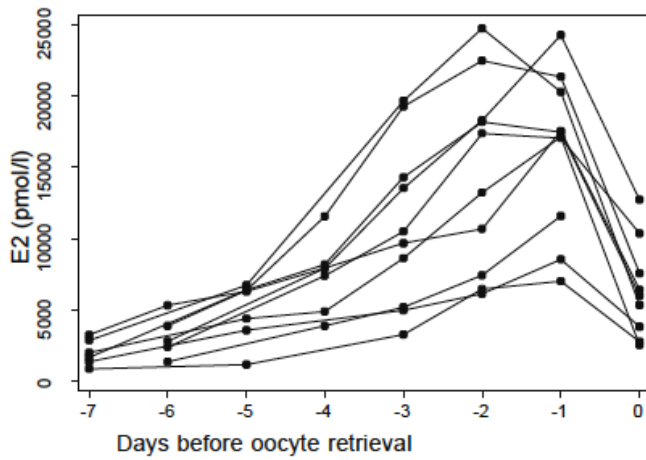


Figure 1. Individual oocyte donor estradiol (E2) and progesterone (P4) values in the week before oocyte retrieval.

Figure 3.5.3. Figure 1 in Chung *et al.* (2012).

Figure 3.5.4 shows the relation between MIB1 for the pregnant women plotted against their E2 on the day of biopsy and for the oocyte donors plotted against their E2 on the day before biopsy, while Figure 3.5.5 shows the relation between MIB1 for the 10 oocyte donors and the 30 pregnant women plotted against their P4 on the day of biopsy. For the pregnant women, there was no relationship between MIB1 and E2 or P4. For the oocyte donors, there was a strong positive relationship between MIB1 and E2 on the day before biopsy – correlation, $r = 0.76$ ($P = 0.010$); while the correlation between MIB1 and E2 on the day of biopsy was much weaker – $r = 0.17$ ($P = 0.65$). For the oocyte donors, there was no relationship between MIB1 and P4 on the day of biopsy or P4 on the day

before biopsy; however, two of the four oocyte donors with low MIB1 values had the lowest P4 values.

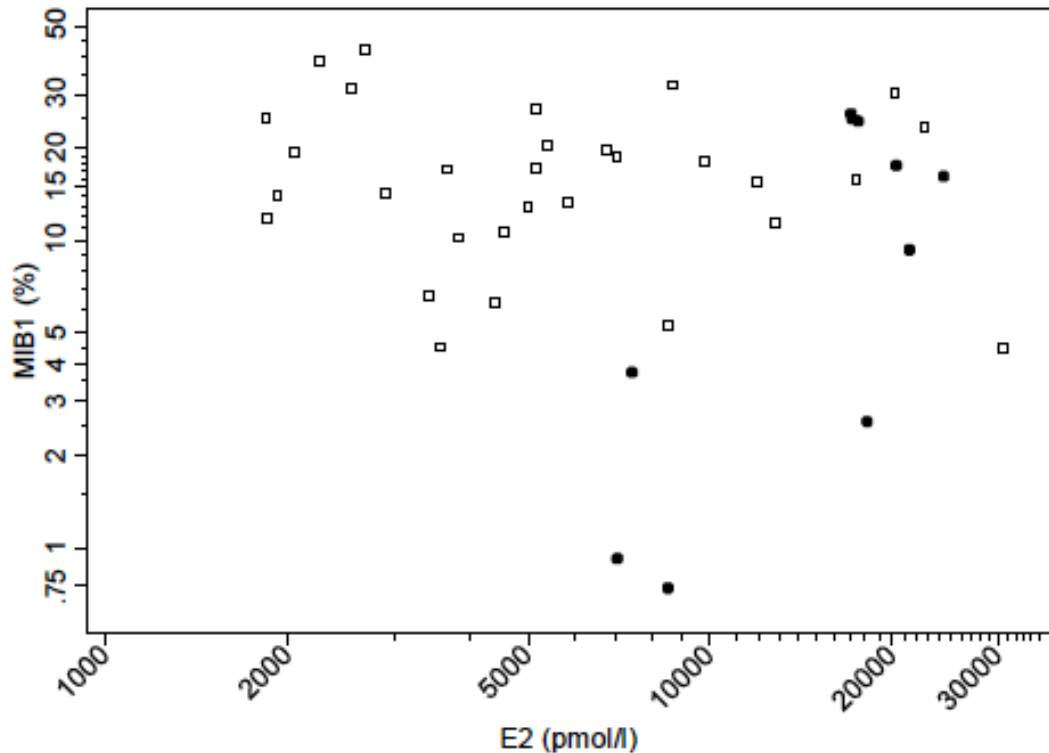


Figure 3. Individual woman TDLU epithelial cell MIB1 values vs estradiol (E2) values - E2 values for oocyte donors on the day before biopsy (•); E2 values for ‘pregnant’ women on the day of biopsy (◻).

Figure 3.5.4. Figure 3 in Chung *et al.* (2012; attached).

The means (and 95% confidence intervals) of the proportion of epithelial cells with positive nuclear staining for MIB1, PRA, PRB and ER α are given in Table 3.5.1. The MIB1 mean value was increased from 1.8% in the cycling women to 7.0% in the oocyte donors ($P = 0.003$) and to 15.4% in the pregnant women.

The PRA mean value was slightly lower in the oocyte donors (17.8%) than in the cycling women (23.5%), but was not as low as in the pregnant women (3.9%). The difference between the oocyte donors and the cycling women was not statistically significant. The PRB mean values were similar in all three groups of women. The ER α mean value was lower in oocyte donors (6.8%) than in cycling women (12.0%).

We previously reported that parous naturally cycling women had significantly lower PRA values than nulliparous naturally cycling women, and lower values of MIB1, PRB, and ER α , but the differences for these factors were not statistically significant. Parity had no effect on MIB1, PRA and ER α in pregnant women, but the PRB mean was marginally statistically significantly greater in the parous group ($P = 0.049$). Eight of the

10 oocyte donors were nulliparous, so that we had no power to investigate the effects of parity in the oocyte donors.

Table 1 Mean (with 95% confidence limits) percentages of Ki67, PRA, PRB, and ER α in oocyte donors, pregnant women, and naturally cycling women

	Group	Mean ^a	lcl ^a	ucl ^a	P value ^b
Ki67	Oocyte donor (N = 10)	7.0	3.0	16.5	
	Pregnant (N = 30)	15.4	12.4	19.1	0.016
	Cycling (N = 26)	1.8	1.2	2.7	0.003
ER α	Oocyte donor	6.8	4.3	9.9	
	Pregnant	11.0	7.9	14.6	0.15
	Cycling	12.0	9.2	15.2	0.034
PRA	Oocyte donor	17.8	13.4	22.9	
	Pregnant	3.9	2.5	5.5	<0.001
	Cycling	23.5	16.2	32.2	0.37
PRB	Oocyte donor	16.9	11.3	23.6	
	Pregnant	12.8	9.4	16.8	0.31
	Cycling	19.2	13.3	26.0	0.67

^a Calculations were made with transformed values—logarithmic for MIB1, and square root for ER α , PRA, and PRB values. lcl and ucl are lower and upper 95% confidence interval values, respectively

^b P values are for comparisons with oocyte donors

Table 3.5.1. Table 1 in Chung *et al.* (2012; attached).

This was the first study to evaluate the immediate effects of short-term exposure to high levels of endogenous estrogen on breast tissue. A large increase in breast-cell proliferation occurred in most of the oocyte donors, similar to the increase seen in pregnant women. In the oocyte donors the increase in MIB1 expression was only definitely seen when their E2 exceeded 10,000 pmol/l and their P4 exceeded 28 nmol/l.

In contrast, the pregnant women demonstrated the same level of breast-cell proliferation over the whole range of observed serum E2 values from ~1,800 pmol/l to ~30,000 pmol/l with no evidence of a dose-response. When we re-plotted Figure 3 using non-SHBGbound E2 rather than E2, a very similar picture was seen. Higher levels of proliferation in pregnant women may be due to their longer exposure to high levels of E2 and to longer exposure to luteal (or higher) levels of P4, it may also be due to their higher ER α expression.

We previously reported that PRA decreased steadily with gestational age in pregnant women (Taylor *et al.*, 2009; attached) and although there was already some decrease early on in pregnancy, PRA only reached very low levels (~1%) after week 12 of gestation.

There was a non-statistically significant 24% reduction of PRA in oocyte donors compared to naturally cycling women, but this was small relative to the reduction seen in pregnant women. We also previously reported that “overall there was little difference in ER α expression between non-pregnant and pregnant subjects”, but the data strongly suggested that “ER α expression is increased early on in pregnancy (<8 weeks gestation) and then declines to lower levels than are seen in non-pregnant subjects”. In contrast, ER α expression in oocyte donors was low.

Based on a strictly limited amount of epidemiological data but considerable data

from rodent experiments, it is possible that a short-term pregnancy and short-term relatively high levels of estrogen may provide some long-term protection against breast cancer. However, the fetoplacental unit in pregnant women is responsible for major endocrinologic changes which are not present in women undergoing ovarian stimulation. Thus, a number of factors in a pregnant woman may contribute to long-term protection against breast cancer. The effects of the high levels of endogenous E2 and P4 achieved during human full-term pregnancy are two-fold: a transient increase in breast cancer risk followed by a significant long-term permanent decrease in risk if the pregnancy occurs prior to around age 32, with the protective effect being greater the earlier the age at which the pregnancy occurs. The mechanism for the protective effect remains unclear, but has been attributed in part to hormonal changes, in particular a reduction in prolactin levels, and may possibly be due to hormone-induced changes in breast function leading to lower breast-cell proliferation and possibly other effects.

Breast-tissue mRNA expression differences between parous and nulliparous rodents have been observed, but whether such changes occur in humans has not been established. There is some evidence that terminated pregnancies may also provide a lesser degree of protection against breast cancer. There are no data available on the effects of a terminated pregnancy on long-term prolactin levels, breast cell proliferation or any other possibly relevant factors.

The same phenomenon of full-term pregnancy-induced protection against mammary carcinogenesis is observed in rats. The protective effect in the rat can also be achieved by administration of exogenous E2 and P4: the serum level of E2 appears to have to be no greater than twice the maximum seen during the estrus cycle and the serum level of P4 appears to have to be no greater than the maximum seen during the estrus cycle. With E2+P4 administration substantial protection could be achieved with as little as 7 days of administration.

There are large differences in the effects of pregnancy in women and in the rat: the ovary is the sole source of serum estrogen and the major source of serum progesterone in pregnancy in the rat, while in women the main source of estrogen and progesterone moves from the ovary to the placenta during the latter part of the first trimester. The serum E2 levels in cycling rats vary from 50 to 250 pmol/l; the maximum value of 250 pmol/l is only exceeded during the third week of pregnancy, when it rises to ~500 pmol/l. Due to the absence of circulating sex-hormone binding globulin (SHBG) in the rat, virtually all of the circulating E2 is free and thus, biologically active. The levels of serum E2 in cycling women are two to three times the levels in the cycling rat, and, contrary to what occurs in the rat, these are greatly increased in pregnancy – they are increased some 5-fold in the first trimester, some 20-fold in the second trimester and some 40-fold in the third trimester compared to the maximum of around 1,100 pmol/l at the pre-ovulatory E2 peak. However, most of the E2 in human pregnancy circulates bound to SHBG. Whether the results in the rat of short-term E2 exposure at only twice the maximum estrus serum E2 level are of relevance to the human situation is, thus, not at all clear.

The serum P4 levels in cycling rats vary from 45 to 160 nmol/l; the levels steadily increase during pregnancy and reach a maximum of 320 nmol/l in the second week, approximately double the maximum seen in the estrus cycle, and then decline in the third week. The levels of serum P4 in cycling women are lower, at 1.5 – 40 nmol/l, than the levels in the cycling rat. Serum P4 levels in women increase steadily during pregnancy –

they are increased some 2-fold in the first trimester, some 4-fold in the second trimester and some 10-fold in the third trimester compared to the maximum of around 40 nmol/l at the luteal-phase serum P4 peak. The maximum seen during pregnancy in women is thus not greatly increased over the maximum level seen in the rat estrus cycle, and the results in the rat of short-term P4 exposure at the maximum estrus cycle serum P4 level could possibly be of more relevance to the human situation.

If short-term high levels of serum E2 do provide long-term protection against breast cancer, we might expect that the breast would change in oocyte donors in a way similar to that seen in pregnant women. The short-term high levels of endogenous E2 did cause a dramatic increase in breast-cell proliferation similar to that associated with pregnancy, but the reduction in PRA was much less than that seen in pregnant women. Studies comparing nulliparous oocyte donors at some time after donation to parous women are needed.

Study of effects of oral contraceptive progestin dose on the breast

We published a manuscript (Hovanessian-Larsen *et al.*, 2012; attached) describing the completely unexpected and most important results obtained from the samples obtained from the completion of Task 2b. Task 2b was a randomized trial comparing the effects on breast tissue of two FDA approved and commonly prescribed oral contraceptives (OCs) – OrthoNovum 1/35® and Ovcon 35®. These two OCs both contain 35 µg of the estrogen, ethinyl-estradiol (EE2), but different doses of the progestin, norethindrone (NET) – OrthoNovum 1/35 contains 1 mg of NET while Ovcon 35 contains 0.4 mg NET. The hypothesis being tested was that Ovcon 35 would be associated with a much lower level of proliferation of TDLU breast epithelial cells than OrthoNovum 1/35 based on the much lower (60% lower) level of progestin in Ovcon 35. We had previously shown based on the results of studies of the increased breast cancer risk from use of menopausal estrogen/progestin therapy (MEPT) that such a difference in dose level (based on the progestin medroxyprogesterone acetate, MPA, used in MEPT in the US) should lead to a close to proportional drop in breast cell proliferation. The 1 mg dose of NET has been equated to an MPA dose of 10 mg (the usual dose of MPA in sequential MEPT) so that this expectation was based on roughly equivalent changes in dose with MEPT (10 mg versus 2.5 mg MPA).

Thirty-three women were randomly assigned 1:1 to the two OCs. All completed the study including contributing a breast-biopsy specimen. Five of the breast-biopsy specimens contained insufficient TDLU epithelial tissue for analysis and one of the remaining women was diagnosed with a follicular cyst. The means (and 95% confidence intervals) of the proportion of epithelial cells with positive nuclear staining for Ki67, PRA, PRB and ER α for the remaining 27 women are given in Table 3.5.2.

Table 1
Ki67, PRA, PRB and ER α percentage associated with two 35-mcg EE2 OCs with different NET doses

Measure	NET dose		p ^a
	1 mg	0.4 mg	
Ki67	7.8 (4.4–13.9)	12.5 (7.0–22.3)	.27
PRA	7.6 (5.3–10.4)	16.7 (8.6–27.3)	.041
PRB	12.0 (8.8–15.8)	23.7 (14.1–35.7)	.030
ER α	9.0 (5.5–13.3)	18.2 (10.0–28.8)	.056

Values shown are means with 95% confidence limits.

^a Two-sided significance level for difference between NET doses.

Table 3.5.2. Table 1 in Hovanessian-Larsen *et al.* (2012; attached).

Completely contrary to expectation, the Ki67 mean value *increased* 60% from 7.8% to 12.5% with the *decrease* in NET dose from 1.0 mg to 0.4 mg. The increases in estrogen and progesterone receptors with this decrease in NET dose were quite striking: the PRA mean value increased 120% from 7.6% to 16.7%, the PRB mean value increased 98% from 12.0% to 23.7%, and the ER α mean value increased 102% from 9.0% to 18.2%.

This approximate doubling of the levels of each of PRA, PRB, and ER α is the first report of an effect of NET dose on PRA, PRB, and ER α expression levels in the breast. These increases in receptor levels is quite sufficient to explain the observed failure to see a decrease in Ki67 with the lower dose of NET, and is likely to be a key part of the explanation why epidemiological studies in general have failed to identify differences in risk of breast cancer by dose of progestin in the OC. Whether this effect of NET dose on receptor levels holds true for other progestins is not known. Increasing progesterone levels after ovulation in the normal menstrual cycle are associated with markedly lower ER expression in almost all studies, but the studies of changes in PR expression over the menstrual cycle are inconsistent.

Studies of ER expression in the breast during an OC cycle have found lower levels in the three weeks on active estrogen-progestin than in the week on placebo, and the levels during OC use are lower than the levels seen during the menstrual cycle. However, studies of PR expression have found higher levels in the three weeks on active estrogen- progestin than in the week on placebo, and the results from the three studies that have investigated how the PR expression levels during OC use compare to the levels seen during the menstrual cycle have produced inconclusive results. There have been no reports on the effects of dose of EE2 or on the effects of the dose and type of progestin in the OC on these findings.

Early studies reported found little difference between OC users and normally cycling women in TDLU breast cell proliferation as measured by thymidine labeling index (TLI). The mean TLIs reported by the two main studies were 0.95% vs 0.84% and 2.9% and 2.9% for OC and natural cycles respectively. More recent studies using Ki67 as the marker of cell proliferation have found some evidence that average proliferation on OCs is greater than over the menstrual cycle – 10.6% vs 9.0%, and 4.8% vs 2.2% respectively.

The Ki67 figure of 7.8% we observed with the much more commonly used 1 mg

NET OC of 7.8% should not be taken as an average figure for the OC cycle since there is clear evidence that proliferation is lower in the placebo week and there is some evidence that proliferation may be at its maximum towards the end of the active pill phase when we took our breast biopsy samples.

The results presented here provide clear evidence that decreasing the dose of the progestin NET in an OC from 1 mg to 0.4 mg increases ER α , PRA and PRB in the breast epithelium. There is indirect evidence strongly suggesting that decreasing the dose of EE2 in an OC will decrease PR, but it may increase ER. An OC with the same NET dose but lower EE2 dose may therefore be associated with a decreased proliferation of breast epithelium. We are currently investigating this possibility in a non-DoD-funded randomized trial similar to the one reported here. Whether it is possible to adjust the doses to achieve an average proliferation rate which is less than that occurring in a normal menstrual cycle is unknown.

Project 4

This project called for the recruitment of 150 elective reduction mammoplasty, mastopexy or breast augmentation patients. The aim is to collect breast tissue from these women and conduct the same types of cellular, hormonal and genetic analyses as is being done in Project 3. In addition, cellular analyses on 100 tissue slides from previous reduction mammoplasties, and 100 autopsy breast tissue samples will be conducted.

Task 1. Months 1-48: Recruit 150 women undergoing elective reduction mammoplasty, mastopexy or breast augmentation to the protocol.

We recruited 34 women undergoing an elective reduction mammoplasty. We were not able to recruit any further patients to the elective reduction mammoplasty, mastopexy or breast augmentation protocols. As we became aware of this we wrote an additional protocol designed to obtain normal breast tissue from volunteers willing to undergo a breast biopsy (Project 3, Task 2d). We recruited 60 women to volunteer for this protocol. IHC for Ki67, PRA, PRB and ER α has been conducted on many of these samples and we will complete this by the end of September.

Task 1a. Months 1-36: Identify and conduct cellular assays on 100 tissue samples from previous reduction mammoplasties.

We consented and obtained detailed questionnaire data on 99 women who had had a previous reduction mammoplasty. IHC for Ki67, PRA, PRB and ER α has been conducted on many of these samples and we will complete this by the end of September.

Task 1b. Months 23-54: Identify and conduct cellular assays on 100 autopsy breast tissue samples.

We obtained 230 such tissue samples. These samples were collected by Dr. Sue Bartow while working at the Office of the New Mexico Medical Investigator between

December 1978 and December 1983; she collected randomly selected breast tissue from autopsied women (Bartow *et al.*, 1997). Dr Bartow kindly made these tissues available to us. With much work on antigen retrieval, we thought we had succeeded in obtaining satisfactory IHC results on these ~30 year old samples, but reproducibility of the IHC results was not obtained and we had to abandon this IHC project.

A secondary aim of this award was to better understand mammographic density as it is the strongest breast cancer risk factor after the major genetic factors of BRCA1/2. These Bartow samples are a very valuable resource in this regard. Samples of this tissue from women without breast cancer were used by Dr. Norman Boyd and colleagues to measure constituents of the tissue (Li *et al.*, 2005). Specifically from tissue slices which had been X-rayed (Faxitron) by Dr. Bartow, Dr. Boyd and colleagues obtained slides and measured the areas of the slide occupied by tissue, by collagen and by glands and epithelial nuclear material. Dr. Boyd and colleagues kindly provided this data to us to allow us to investigate more fully the relationship between Faxitron density, collagen and epithelium. Collagen area % declined from 30.5% in premenopausal women to 12.5% in postmenopausal women. Collagen area % was approximately 80% of the Faxitron density %, while glandular area % was only ~5.9% and ~3.4% of the Faxitron density % in premenopausal and postmenopausal women respectively. In postmenopausal women, epithelial nuclear area % was directly proportional to collagen area %; but, in premenopausal women, the ratio of epithelial nuclear area % to collagen area % declined with increasing collagen area %; but whether this was due to a greater concentration of epithelium per unit collagen in low collagen area % or a greater concentration in fat is not known and we have no knowledge of how this relates to breast cell proliferation. The ratio of epithelium to a fixed collagen area % was much higher in premenopausal than in postmenopausal women, but the relationship of epithelium to collagen was the same in parous and nulliparous women. Thus we conclude that the relationship of mammographic density to breast cancer risk appears likely to be due to a major extent to increased epithelial cell numbers. Additional evidence for this conclusion is that the lower mammographic density in parous compared to nulliparous women is reflected in a similar proportional reduction in breast epithelium, as is the lower mammographic density in postmenopausal women. Much more study of the biological basis of the major breast cancer risks associated with breast densities are needed if we are to exploit this major risk factor in some way to help in developing chemopreventive approaches to breast cancer. A manuscript describing some of these results is in press in the *Annals of Oncology* (attached) and a second manuscript related to this work is in the process of being revised based on reviewer comments (also attached).

Task 2. Months 5-48: Assay tissue samples for hormonal and cellular markers to determine dense and non-dense tissue characteristics, and their association with glandular tissue proliferation.

We assayed the tissue for a series of hormonal and cellular markers. To date, we have characterized ER expression, PRA expression, PRB expression, as well as quantified cell proliferation in the samples collected as part of Tasks 1 and 1a (Taylor *et al.*, 2009).

Task 3. Months 5-48: Assay blood samples for hormone levels.

Blood samples from pregnant women, oocyte donors and premenopausal women in different phases of the menstrual cycle and parity state were assayed for E2 and P4. Analysis of some of these data is presented in Chung *et al.* (2012; attached).

Task 4. Months 37-48: Conduct gene expression arrays on the dense and non-dense tissue samples to determine if the expression profiles differ.

We previously showed (Hawes *et al.*, 2006; attached) as part of this grant that almost all breast epithelial tissue is contained within dense collagen areas. The non-dense tissue samples consist mainly of fat. The amount of breast epithelial tissue in a breast is highly correlated with the amount of mammographic density (collagen). Work done under Task 1b above has shown that in premenopausal women the concentration of epithelium within the dense area is greater in the breasts with lower mammographic density. The question posed here in Task 4 is thus better expressed as “what are the differences in dense tissue epithelium from women with less vs more density?” To do this we need to know the mammographic density in the woman providing the breast tissue sample. We only have this information on the Bartow samples. As we stated above, IHC for Ki67, PRA, PRB and ER α in these ~30 samples was unsuccessful. We carried out laser capture microdissection (LCM) on fresh frozen and more recently collected fixed normal breast tissue samples in an attempt to obtain separate epithelial and stromal cell populations but found that the process of LCM affected the quality of the material to such an extent that even for DNA methylation studies tissue that has been subjected to LCM does not produce high quality data. (We must emphasize that normal breast epithelial tissue is a small proportion of the dense tissue and requires much more laborious and difficult collection than is the case with tumor tissue.) We then performed very labor-intensive microdissection of the intralobular stromal tissue on a limited number of samples and ran them on the Illumina 450K methylation DNA panel. These data did not find, however, any clear profile of DNA methylation markers distinguishing nulliparous from parous women. We concluded that this line of work was unlikely to be productive and did not pursue this further.

Task 5. Months 13-60: Conduct data analysis to compare dense and non-dense tissue characteristics and prepare manuscripts as appropriate.

See Task 1b above.

Key Research Accomplishments – Final Report 2013:

Projects 3 and 4

- Evaluation of tissue samples from reduction mammoplasties resulting in a seminal publication on the relation of mammographic densities to epithelium (Hawes *et al.*, Breast Cancer Research 2006; 8:R24-29).
- Discovery of a sustaining decrease in PRA after pregnancy as a potential marker of the protective effect of pregnancy on breast cancer risk (Taylor *et al.*, Breast Cancer Res Treat 2009; 118:161-168).
- Published a key manuscript describing the completely unexpected lack of decrease, and possible increase, in breast cell proliferation when the dose of the progestin, norethindrone, in oral contraceptives is reduced by 60% and the apparent reason for this being the concomitant increase in estrogen and progesterone receptors (Hovanessian-Larsen *et al.*, Contraception 2012; 86:238-343).
- Published a key manuscript describing the effect of short-term high-dose estrogen exposure on breast cell proliferation, and ER α , PRA and PRB expression compared to naturally cycling women and pregnant women (Chung *et al.*, Breast Cancer Res Treat 2012; 132:653-660).
- Development and initiation of a protocol to allow us to evaluate the appropriateness of a progestin-based breast cancer chemopreventive approach.
- Development and initiation of a protocol to collect interview data and tissue specimens on women having elective reduction mammoplasties.
- Development of a protocol to allow us to evaluate breast cell proliferation in women receiving different progestin-dose oral contraceptives.
- Development of a protocol to allow us to evaluate breast cell proliferation in women receiving micronized progesterone versus placebo to determine the effect of exogenous progesterone on proliferation.
- Development of a protocol to allow us to evaluate the effects of high dose estrogen on breast tissue.
- Development of a protocol to allow us to collect breast tissue from healthy volunteers.
- Contacted and interviewed 99 additional previous reduction mammoplasty subjects to obtain demographic, reproductive, and hormone use data.
- Staining and evaluation of breast epithelial-cell proliferation (Ki67), ER α , PRA, and PRB expression in previously obtained reduction mammoplasty samples and prospectively collected reduction mammoplasty samples.

- Development of a network of collaborators at USC and across the United States to further the work being funded by this grant.

- o At USC we had regular monthly meetings of our working group of investigators with expertise in endocrinology, gynecology, breast cancer pathology, oncology, radiology, epidemiology and molecular biology to review progress of the various projects and specific related tasks and to discuss any data generated from the studies and any new questions that may arise from our studies or published literature.

- o We had fruitful collaborations with Dr. Sue Bartow for studies on breast specimens from autopsies performed in New Mexico. These are the same specimens utilized by Dr. Norman Boyd's group (Li *et al.*, *Cancer Epidemiol Biomarkers Prev* 2005; 14:343-349) and we have analyzed these data further (Pike MC and Pearce CL, Mammographic Density, MRI Background Parenchymal Enhancement and Breast Cancer Risk, *Annals of Oncology*, in press).

- Receipt of grant funding to study the effect of reducing the estrogen dose in an oral contraceptive, while keeping the progestin dose constant, on breast cell proliferation, and ER α , PRA and PRB expression.
- Receipt of grant funding to study the effect of hCG, a known chemopreventive agent against mammary cancer in rodents, on breast tissue in women.
- DNA extraction and successful DNA methylation quality control results from microdissected stromal tissue.

Projects 1 and 2

- Identification of genes expressed in a parity-specific manner in multiple rat strains resulting in a key publication (Blakely *et al.*, *Cancer Res*, 66:6421-6431, 2006; 67:844-846, 2007).
- Treatment of rats with hormonal chemoprevention regimens and determination of effective regimens.
- Evaluation of rat mammary gland morphology.
- Demonstration that low-dose and short-term hormone treatment of rats reduces mammary tumor susceptibility.
- Failure to recapitulate hormone and parity-induced protection against mammary tumorigenesis in mice following extensive attempts in multiple strains of mice, including experiments in which the mice were fed a low phytoestrogen diet.

Reportable Outcomes: Final Report 2013

Publications:

1. Blakely CM, Stoddard AJ, Belka GK, Dugan KD, Notarfrancesco KL, Moody SE, D'Cruz CM, and Chodosh LA. Hormone-induced protection against mammary tumorigenesis is conserved in multiple rat strains and identifies a core gene expression signature induced by pregnancy. *Cancer Research*, 66:6421-6431, 2006; erratum in 67:844-846, 2007.
2. Hawes D, Downey S, Pearce CL, Bartow S, Wan P, Pike MC, Wu AH. Dense breast stromal tissue shows greatly increased concentration of breast epithelium but no increase in its proliferative activity. *Breast Cancer Res* 2006; 8:R24-29.
3. Taylor D, Pearce CL, Hovanessian-Larsen L, Downey S, Spicer DV, Bartow S, Ling C, Pike MC, Wu AH, Hawes D. Progesterone and estrogen receptors in pregnant and premenopausal non-pregnant normal human breast. *Breast Cancer Res Treat* 2009; 118:161-8.
4. Chung K, Hovanessian-Larsen L, Hawes D, Taylor D, Downey S, Spicer DV, Stanczyk FZ, Patel S, Anderson AR, Pike MC, Wu AH, Pearce CL. Breast epithelial cell proliferation is markedly increased with short-term high levels of endogenous estrogen secondary to controlled ovarian hyperstimulation. *Breast Cancer Res Treat* 2012;132 :653-60.
5. Hovanessian-Larsen L, Taylor D, Hawes D, Spicer DV, Press MF, Pike MC, Wu AH, Pearce CL. Oral contraceptive progestin dose: lowering norethindrone dose does not lead to lower breast epithelial-cell proliferation. *Contraception* 2012; 86:238-243.
6. Pike MC and Pearce CL. Mammographic density, MRI background parenchymal enhancement and breast cancer risk. *Annals of Oncology*. In press.
7. Pike MC, Bartow S, Martin L, Hawes D, Pathak D, Boyd NF. The relation of mammographic density to breast collagen and epithelium. In review.

Funding Received:

1. Avon Foundation, Use of hCG and Depo-Provera for Breast Cancer Prevention, MC Pike, Principal Investigator.
2. Whittier Foundation, Oral Contraceptives and Breast Cancer, AH Wu, Principal Investigator.

CONCLUSION:

The successful identification of a set of breast tissue gene expression differences that distinguish parous from nulliparous rats of multiple strains (and confirmed in a strain of mice) is a critical step in the development of a chemoprevention approach to mimic the protective effect of pregnancy. We confirmed a subset of these genetic expression changes in rodents treated with a variety of hormonal chemoprevention regimens, but because of technical problems with microdissection of human tissue we could not test these findings in women.

Our finding that PRA expression is altered during and following pregnancy, precisely as is seen in the rat model of mammary carcinogenesis, provides a potentially important insight into a marker for mimicking the protective effect of a pregnancy on breast cancer risk.

Our finding that breast epithelial tissue in women is overwhelmingly concentrated in mammographically dense areas of the breast (areas of high collagen concentration not seen in rodent breast) provides a deep insight into the reason for increased mammographic density being so closely associated with increased risk of breast cancer – women with increased mammographic density have more breast epithelium. Breast densities are reduced in parous compared to nulliparous women, so that this ties in closely with our work on changes in the breast after pregnancy.

We have demonstrated that oocyte donors undergoing controlled ovarian hyperstimulation have greatly increased levels of estrogen and of breast cell proliferation, both comparable in the majority of donors to the levels seen in the first trimester of pregnancy. This increased cell proliferation is of short duration. Whether their greatly increased estrogen levels are associated with any long-term beneficial effects on the breast, as occurs in rodent models, is not known.

Our completely unexpected finding that a lower progestin dose in oral contraceptives does not lead to lower breast-cell proliferation compared to women on a higher progestin dose pill is a large part of the explanation of why epidemiological studies have failed to identify different risks between different OC formulations. Different effects may be found if the progestin dose is fixed, but the estrogen dose changes, as it appears that this may be the relevant component in oral contraceptives in terms of affecting breast epithelial-cell proliferation. We have obtained funding to test this hypothesis. We have also obtained funding to study the effect of hCG on the breast.

References: Final Report 2013

- Bartow SA, Mettler FA, Black WC. Correlations between radiographic patterns and morphology of the female breast. *Rad Patterns Morph* 13:263-275, 1997.
- Blakely CM, Stoddard AJ, Belka GK, Dugan KD, Notarfrancesco KL, Moody SE, D'Cruz CM, and Chodosh LA. Hormone-induced protection against mammary tumorigenesis is conserved in multiple rat strains and identifies a core gene expression signature induced by pregnancy. *Cancer Research*, 66:6421-6431, 2006; erratum in 67:844-846, 2007.
- Chung K, Hovanessian-Larsen L, Hawes D, Taylor D, Downey S, Spicer DV, Stanczyk FZ, Patel S, Anderson AR, Pike MC, Wu AH, Pearce CL. Breast epithelial cell proliferation is markedly increased with short-term high levels of endogenous estrogen secondary to controlled ovarian hyperstimulation. *Breast Cancer Res Treat* 2012;132 :653-60.
- Hawes D, Downey S, Pearce CL, Bartow S, Wan P, Pike MC, Wu AH. Dense breast stromal tissue shows greatly increased concentration of breast epithelium but no increase in its proliferative activity. *Breast Cancer Res* 2006; 8:R24-29.
- Hovanessian-Larsen L, Taylor D, Hawes D, Spicer DV, Press MF, Pike MC, Wu AH, Pearce CL. Oral contraceptive progestin dose: lowering norethindrone dose does not lead to lower breast epithelial-cell proliferation. *Contraception* 2012; 86:238-243.
- Li T, Sun L, Miller N, Nicklee T, Woo J, Hulse-Smith L, Tsao MS, Khokha R, Martin L, Boyd N. The association of measured breast tissue characteristics with mammographic density and other risk factors for breast cancer. *Cancer Epidemiol Biomarkers Prev* 14:343-349, 2005.
- Taylor D, Pearce CL, Hovanessian-Larsen L, Downey S, Spicer DV, Bartow S, Ling C, Pike MC, Wu AH, Hawes D. Progesterone and estrogen receptors in pregnant and premenopausal non-pregnant normal human breast. *Breast Cancer Res Treat* 2009; 118:161-8.

Personnel – Final Report 2013

University of Southern California – Projects 3 and 4

Malcolm C. Pike
Anna H. Wu
C. Leigh Pearce
Debra Hawes
Michael F. Press
Sue Ellen Martin
Frank Stanczyk
Jonathan Buckley
Lilly Chang
Alex Trana
Angela Umali
Peggy Wan
Lillian Young
Serina Ovalle
Yongtian Li
Randall Widelitz
Anna Rebecca Gallardo
Fabiola Enriquez
Heidi St. Royal
Linda Hovannesian-Larsen
Frank Stanczyk
Valerie Mira
David Ruble
Leticia Vasquez-Caldera
John Casagrande
Douglas Stram

University of Pennsylvania – Projects 1 and 2

Lewis H. Chodosh
Chien-Chung Chen
Celina D'Cruz
Congzhou Liu
Patrick Taulman
Jinling Wu
Dhruv Pant
Adanma Ezidinma
George Belka
Kate Dugan
Raina Fitzgerald-Anderson
Zhandong Liu

Kathy Notarfrancesco
Tien-chi Pan
Barbara Sheilds
Judith Smith
Alex Stoddard

Hormone-Induced Protection against Mammary Tumorigenesis Is Conserved in Multiple Rat Strains and Identifies a Core Gene Expression Signature Induced by Pregnancy

Collin M. Blakely, Alexander J. Stoddard, George K. Belka, Katherine D. Dugan, Kathleen L. Notarfrancesco, Susan E. Moody, Celina M. D'Cruz, and Lewis A. Chodosh

Departments of Cancer Biology, Cell and Developmental Biology, and Medicine, and The Abramson Family Cancer Research Institute, University of Pennsylvania School of Medicine, Philadelphia, Pennsylvania

Abstract

Women who have their first child early in life have a substantially lower lifetime risk of breast cancer. The mechanism for this is unknown. Similar to humans, rats exhibit parity-induced protection against mammary tumorigenesis. To explore the basis for this phenomenon, we identified persistent pregnancy-induced changes in mammary gene expression that are tightly associated with protection against tumorigenesis in multiple inbred rat strains. Four inbred rat strains that exhibit marked differences in their intrinsic susceptibilities to carcinogen-induced mammary tumorigenesis were each shown to display significant protection against methylnitrosourea-induced mammary tumorigenesis following treatment with pregnancy levels of estradiol and progesterone. Microarray expression profiling of parous and nulliparous mammary tissue from these four strains yielded a common 70-gene signature. Examination of the genes constituting this signature implicated alterations in transforming growth factor- β signaling, the extracellular matrix, amphiregulin expression, and the growth hormone/insulin-like growth factor I axis in pregnancy-induced alterations in breast cancer risk. Notably, related molecular changes have been associated with decreased mammographic density, which itself is strongly associated with decreased breast cancer risk. Our findings show that hormone-induced protection against mammary tumorigenesis is widely conserved among divergent rat strains and define a gene expression signature that is tightly correlated with reduced mammary tumor susceptibility as a consequence of a normal developmental event. Given the conservation of this signature, these pathways may contribute to pregnancy-induced protection against breast cancer. (Cancer Res 2006; 66(12): 6421-31)

Introduction

Epidemiologic studies clearly show that a woman's risk of developing breast cancer is influenced by reproductive endocrine events (1). For example, early age at first full-term pregnancy, as well as increasing parity and duration of lactation, have each been shown to reduce breast cancer risk (2, 3). In particular, women who have their first child before the age of 20 have up to a

50% reduction in lifetime breast cancer risk compared with their nulliparous counterparts (2). Notably, the protective effects of an early full-term pregnancy have been observed in multiple ethnic groups and geographic locations, suggesting that parity-induced protection results from intrinsic biological changes in the breast rather than specific socioeconomic or environmental factors. At present, however, the biological mechanisms underlying this phenomenon are unknown.

Several models to explain the protective effects of parity have been proposed. For instance, parity has been hypothesized to induce the terminal differentiation of a subpopulation of mammary epithelial cells, thereby decreasing their susceptibility to oncogenesis (4). Related to this, parity has been suggested to induce changes in cell fate within the mammary gland, resulting in a population of mammary epithelial cells that are more resistant to oncogenic stimuli by virtue of decreased local growth factor expression and/or increased transforming growth factor (Tgf)- β 3 and p53 activity (5, 6). Others have suggested that the process of involution that follows pregnancy and lactation acts to eliminate premalignant cells or cells that are particularly susceptible to oncogenic transformation (5). Conversely, parity-induced decreases in breast cancer susceptibility could also be due to persistent changes in circulating hormones or growth factors rather than local effects on the mammary gland (7). At present, however, only limited cellular or molecular evidence exists to support any of these models.

Similar to humans, both rats and mice exhibit parity-induced protection against mammary tumorigenesis. Administration of the chemical carcinogens, 7,12-dimethylbenzanthracene or methylnitrosourea, to nulliparous rats results in the development of hormone-dependent mammary adenocarcinomas that are histologically similar to human breast cancers (8). In outbred Sprague-Dawley, and inbred Lewis and Wistar-Furth rats, a full-term pregnancy either shortly before or after carcinogen exposure results in a high degree of protection against mammary carcinogenesis (7, 9, 10). Similarly, treatment of rats with pregnancy-related hormones, such as 17- β -estradiol (E) and progesterone (P), can mimic the protective effects of pregnancy in rat mammary carcinogenesis models (11, 12). This suggests that the mechanisms of parity-induced protection and estradiol and progesterone-induced protection may be similar. Using analogous approaches, Medina and colleagues have shown parity-induced as well as hormone-induced protection against 7,12-dimethylbenzanthracene-initiated carcinogenesis in mice (13, 14). As such, rodent models recapitulate the ability of reproductive endocrine events to modulate breast cancer risk as observed in humans. This, in turn, permits the mechanisms of parity-induced protection to be studied within defined genetic and reproductive contexts.

Requests for reprints: Lewis A. Chodosh, Department of Cancer Biology, University of Pennsylvania School of Medicine, 612 Biomedical Research Building II/III, 421 Curie Boulevard, Philadelphia, PA 19104-6160. Phone: 215-898-1321; Fax: 215-573-6725; E-mail: chodosh@mail.med.upenn.edu.

©2006 American Association for Cancer Research.
doi:10.1158/0008-5472.CAN-05-4235

Previously, analyses of gene expression changes that occur in rodent models in response to parity, or hormonal treatments that mimic parity, have been used to suggest potential cellular and molecular mechanisms for pregnancy-induced protection against breast cancer (6, 15). Rosen and colleagues used subtractive hybridization analysis to identify genes in the mammary glands of Wistar-Furth rats that were persistently up-regulated 4 weeks posttreatment with estradiol and progesterone (15). Estradiol and progesterone treatment was found to increase the mRNA expression of a wide range of genes, including those involved in differentiation, cell growth, and chromatin remodeling. Similarly, we used microarray expression profiling to assess global gene expression changes induced by parity in the mammary glands of FVB mice (6). This analysis revealed parity-induced increases in epithelial differentiation markers, *Tgfb3* and its downstream targets, and cellular markers reflecting the influx of macrophages and lymphocytes into the parous gland. We also found that parity resulted in persistent decreases in the expression of a number of growth factor-encoding genes, including amphiregulin (*Areg*) and insulin-like growth factor (*Igf-I*). Together, these studies provided initial insights into cellular and molecular mechanisms that could contribute to parity-induced protection.

Notably, early first full-term pregnancy in humans primarily decreases the incidence of estrogen receptor (ER)-positive breast cancers (16). Because rats are more similar to humans than are mice with respect to the incidence of ER-positive mammary tumors (17), in the present study we used microarray expression profiling to identify persistent gene expression changes in the mammary glands of this rodent species to explore potential mechanisms of parity-induced protection. To date, a comprehensive analysis of parity-induced up-regulated and down-regulated gene expression changes in the rat has not been performed.

A major challenge posed by global gene expression surveys is the large number of differentially expressed genes that are typically identified, only a few of which may contribute causally to the phenomenon under study. Consequently, we considered approaches to identifying parity-induced changes in the rat mammary gland that would permit the resulting list of expressed genes to be narrowed to those most robustly associated with parity-induced protection against mammary tumorigenesis. Given the marked genetic and biological heterogeneity between different inbred rat strains, we reasoned that identifying expression changes that are conserved across multiple strains exhibiting hormone-induced protection against mammary tumorigenesis would facilitate the identification of a core set of genes associated with parity-induced protection against breast cancer.

To achieve this goal, we focused on gene expression changes that are conserved among different strains of rats that exhibit hormone-induced protection against mammary tumorigenesis. We first identified four genetically distinct inbred rat strains that exhibit hormone-induced protection against methylnitrosourea-induced mammary tumorigenesis independent of their inherent susceptibility to this carcinogen. We then used oligonucleotide microarrays to identify a core 70-gene expression signature that closely reflects parity-induced changes in the mammary gland that were conserved among each of these strains. The results of this analysis extend prior observations with respect to parity-induced changes in the growth hormone/*Igf-I* axis, identify novel parity-induced changes associated with the extracellular matrix (ECM), and implicate a core set of pathways in pregnancy-induced protection against breast cancer.

Materials and Methods

Animals and tissues. Lewis, Wistar-Furth, Fischer 344, and Copenhagen rats (Harlan, Indianapolis, IN) were housed under 12-hour light/12-hour dark cycles with access to food and water ad libitum. Animal care was performed according to institutional guidelines. To generate parous (G1P1) rats, 9-week-old females were mated and allowed to lactate for 21 days after parturition. After 28 days of postlactational involution, rats were sacrificed by carbon dioxide asphyxiation and the abdominal mammary glands were harvested and snap-frozen following lymph node removal, or whole-mounted and fixed in 4% paraformaldehyde. Whole-mounted glands were stained with carmine alum as previously described (6). For histologic analysis of whole mammary glands and tumors, paraffin-embedded tissues were sectioned and stained with H&E or Mason's trichrome as previously described (6). Tissues were harvested from age-matched nulliparous (G0P0) animals in an identical manner.

Carcinogen and hormone treatments. Twenty-five to 30 nulliparous female Lewis, Fischer 344, Wistar-Furth, and Copenhagen rats were weighed and treated at 7 weeks of age with methylnitrosourea (Sigma-Aldrich, St. Louis, MO) at a dose of 50 mg/kg by a single i.p. injection. At 9 weeks of age, animals from each strain were assigned to one of two groups and treated with hormone pellets (Innovative Research, Sarasota, FL) by s.c. implantation. Group 1 received pellets containing 35 mg of 17- β -estradiol + 35 mg of progesterone, whereas group 2 received pellets containing placebo. Pellets were removed after 21 days of treatment. No signs of toxicity were observed. The development of mammary tumors was assessed by weekly palpation. Animals were sacrificed at a predetermined tumor burden, or at 60 weeks postmethylnitrosourea. At sacrifice, all mammary glands were assessed for tumors, which were fixed in 4% paraformaldehyde and embedded in paraffin. Tumor samples from each strain were confirmed as carcinomas by histologic evaluation. Statistical differences in tumor-free survival between experimental groups were determined by log rank tests and by the generation of hazard ratios (HR) based on the slope of the survival curves using GraphPad Prism 4.0 software.

Microarray analysis. RNA was isolated from snap-frozen abdominal mammary glands by the guanidine thiocyanate/cesium chloride method as previously described (6). Ten micrograms of total RNA from individual Wistar-Furth (six G0P0 and five G1P1), Fischer 344 (eight G0P0 and six G1P1), and Copenhagen (six G0P0 and five G1P1) rats was used to generate cDNA and biotinylated cRNA as previously described (6). For Lewis rats, three G0P0 and three G1P1 samples were analyzed, each of which was comprised of 10 μ g of pooled RNA from three animals. To permit the identification of epithelial as well as stromal gene expression changes, intact mammary glands (with lymph nodes removed) were used. Samples were hybridized to high-density oligonucleotide microarrays (RGU34A) containing ~8,800 probe sets representing ~4,700 genes and expressed sequence tags. Affymetrix comparative algorithms (MAS 5.0) and Chipstat were used to identify genes that were differentially expressed between nulliparous and parous samples (18). Robust Multichip Average signal values were generated using Bioconductor (19).

Genes were selected for further analysis whose expression changed significantly by the above analysis in three out of four strains. Significance was assessed by randomly generating eight lists equal in size to the up-regulated and down-regulated lists for each strain from the population of nonredundant genes called present on the chip in at least one sample (2,428 genes). One million random draw trials were performed to calculate a nominal *P* value for combined list length and to estimate the false discovery rate (FDR) using the median list size occurring by chance.

Hierarchical clustering was done using R statistical software¹ and as described (20). Mouse genes were identified using the Homologene database (National Center for Biotechnology Information).

Quantitative real-time PCR. Five micrograms of DNase-treated RNA were used to generate cDNA by standard methods. *Csn2*, *Mmp12*, *Tgfb3*,

¹ <http://www.R-project.org>.

Igf1p5, *Areg*, *Igf-I*, *Ghr*, *Serpinh1*, and *Sparc* were selected for confirmation by quantitative real-time PCR (QRT-PCR) using TaqMan assays (Applied Biosystems, Foster City, CA). *B2m* was used as a control (21, 22). Reactions were performed in duplicate in 384-well microtiter plates in an ABI Prism Sequence Detection System according to standard methods (Applied Biosystems). One-tailed *t* tests were performed to determine statistical significance using Prism 4.0 software.

Results

Hormone-induced protection in inbred rat strains. To determine whether hormone-induced protection against mammary tumorigenesis is a feature unique to carcinogen-sensitive strains, we compared the extent of protection induced by hormones in four different rat strains: Lewis, Wistar-Furth, Fischer 344, and Copenhagen. Two of these strains (Lewis and Wistar-Furth) have been reported to exhibit hormone-induced protection (9, 12). However, it has not been determined whether carcinogen-resistant strains of rats, such as Copenhagen (23), also exhibit protection. Female rats from each strain were treated with a single dose of methylnitrosourea at 7 weeks of age, followed by s.c. implantation of either placebo or hormone pellets (35 mg of estradiol + 35 mg of progesterone) at 9 weeks of age. Among the placebo-treated groups, Lewis rats exhibited the highest susceptibility to methylnitrosourea-induced mammary tumorigenesis with 100% penetrance and a median tumor latency of 13 weeks (Fig. 1A). Fischer 344 and Wistar-Furth rats displayed intermediate carcinogen sensitivity with latencies of 24 and 36 weeks, respectively. In contrast, Copenhagen rats exhibited a high degree of resistance to methylnitrosourea-induced mammary tumorigenesis with only 5 of 12 animals developing mammary tumors, with an average latency of 51 weeks.

Surprisingly, despite the wide variance in carcinogen sensitivity of nulliparous rats from these four strains, estradiol and progesterone treatment induced a significant ($P < 0.05$) degree of protection against mammary tumorigenesis in each strain (Fig. 1B). For example, whereas Lewis and Copenhagen strains differed markedly in their sensitivity to methylnitrosourea, they exhibited strikingly similar degrees of hormone-induced protection with HRs of 0.19 [95% confidence interval (CI), 0.05-0.40] and 0.16 (95% CI, 0.02-0.63), respectively. The Wistar-Furth (HR, 0.31; 95% CI, 0.09-0.90) and Fischer 344 (HR, 0.38; 95% CI, 0.10-0.71) strains exhibited lesser, but significant degrees of protection. These experiments show that hormone treatments that mimic pregnancy confer protection against mammary tumorigenesis in each strain irrespective of the intrinsic carcinogen susceptibility of nulliparous animals from that strain.

Morphologic changes induced by parity in the rat mammary gland. Parity-induced changes in breast cancer susceptibility have been reported to be accompanied by persistent changes in the structure of the mammary gland in humans, as well as in rats and mice (4, 6). Consistent with this, carmine-stained whole-mount analysis of nulliparous and parous mammary glands from each of the four rat strains revealed that the architecture of the parous mammary epithelial tree was more complex than that of age-matched nulliparous animals, with a higher degree of ductal side-branching (Fig. 1C). These effects were observed in each of the four strains analyzed, suggesting that changes in the structural and cellular composition of the mammary gland may occur as a consequence of parity.

Microarray analysis of parity-induced changes in the rat mammary gland. The similar morphologic changes induced by parity suggested that the hormone-induced protection against

mammary tumorigenesis that we observed in different rat strains might be accompanied by common molecular alterations. To identify these changes, we first performed oligonucleotide microarray expression profiling on pooled samples from nulliparous and parous Lewis rats. Genes whose expression changes were considered to be statistically significant using established algorithms, and whose expression changed by at least 1.2-fold as a result of parity, were selected for further analysis (18). This combined analytic approach has previously been shown to be capable of identifying differentially expressed genes with high sensitivity and specificity (18). Gene expression analysis performed in this manner identified 75 up-regulated and 148 down-regulated genes in parous compared with nulliparous mammary glands. Examination of this list of differentially expressed genes confirmed our previous findings in mice that parity results in the persistent up-regulation of *Tgfb3*, as well as differentiation and immune markers, as well as the persistent down-regulation of growth factor encoding genes, such as *Areg* and *Igf-I* (ref. 6; data not shown).

To narrow the list of candidate genes whose regulation might contribute to the protected state associated with parity, we attempted to identify parity-induced gene expression changes that were conserved across multiple rat strains. To this end, total RNA was isolated from the mammary glands of nulliparous and parous Wistar-Furth, Fischer 344, and Copenhagen rats, and analyzed on RGU34A arrays in a manner analogous to that employed for Lewis rats. This led to the identification of 68, 64, and 92 parity up-regulated genes and 132, 209, and 149 parity down-regulated genes in Wistar-Furth, Fischer 344, and Copenhagen rats, respectively.

Unsupervised hierarchical clustering performed using the expression profiles of 1,954 globally varying genes across the nulliparous and parous data sets representing the four rat strains revealed that samples clustered primarily based on strain without regard to parity status (Fig. 2A). This suggested that the principal source of global variation in gene expression across these data sets was due to genetic differences between strains rather than reproductive history. This observation suggested that determining which parity-induced gene expression changes were conserved among these highly divergent rat strains could represent a powerful approach to defining a parity-related gene expression signature correlated with hormone-induced protection against mammary tumorigenesis.

To identify parity-induced gene expression changes that were conserved across strains, we selected genes that exhibited ≥ 1.2 -fold change in at least three of the four strains analyzed. This led to the identification of 24 up-regulated (Table 1) and 46 down-regulated genes (Table 2). Based on the number of parity-induced gene expression changes observed for each strain, an overlap of this size is highly unlikely by chance (up-regulated: $P < 1 \times 10^{-6}$, FDR < 1%; down-regulated: $P < 1 \times 10^{-6}$, FDR = 4%). As such, this approach led to the identification of 70 genes whose expression is persistently altered by parity across multiple strains of rats that exhibit hormone-induced protection against mammary tumorigenesis.

A gene expression signature distinguishes parous and nulliparous rats and mice. To confirm the validity of the 70-gene parity-related expression signature derived from the above studies, we performed oligonucleotide microarray analysis on samples from nulliparous and parous Lewis rats that were generated independently from those used to derive this signature. Hierarchical clustering analysis of these independent samples using the 70-gene signature revealed that the expression profiles of these genes were sufficient to accurately distinguish parous from nulliparous Lewis rat samples in a blinded manner (Fig. 2B).

To determine whether this parity-related signature could distinguish between nulliparous and parous mammary glands from multiple strains of rats, Lewis, Wistar-Furth, Fischer 344, and Copenhagen microarray data sets were clustered in an unsupervised manner based solely on the expression of the 70 genes comprising the parity signature (Fig. 2C). In each of the four rat strains examined, the 70-gene signature was sufficient

to distinguish parous from nulliparous rats (Fig. 2C). Thus, this signature reflects parity-induced gene expression changes that are highly conserved among four genetically divergent rat strains.

Early full-term pregnancy has been reported to result in protection against mammary tumorigenesis in mice, as it does in humans and rats (13). Accordingly, we mapped the 70 genes

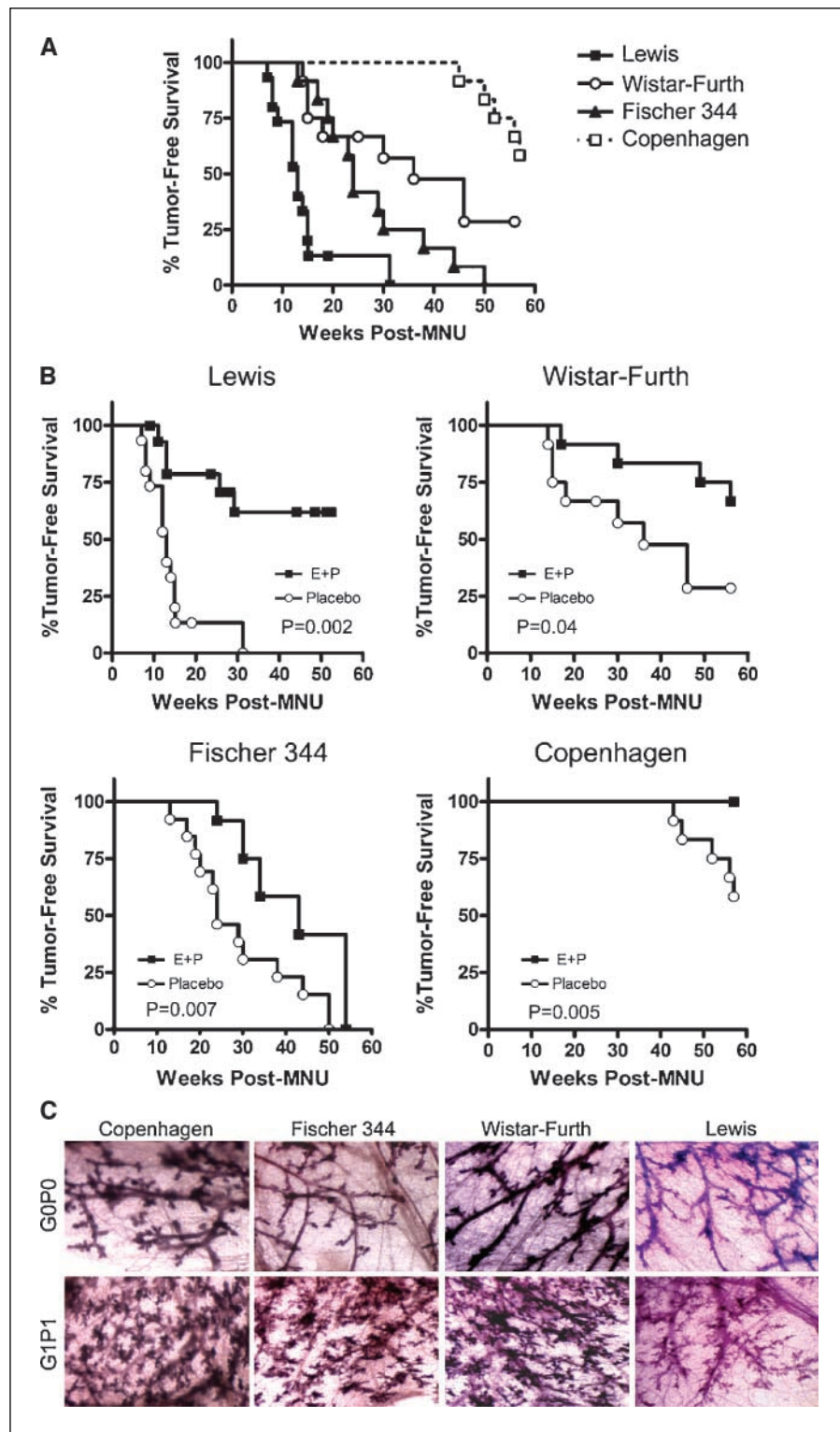


Figure 1. Hormone-induced protection against mammary tumorigenesis is conserved among multiple rat strains. **A**, Kaplan-Meier curves plotting the time to the formation of a first mammary tumor in placebo-treated groups for Lewis ($n = 15$), Wistar-Furth ($n = 12$), Fischer 344 ($n = 13$), and Copenhagen ($n = 12$) rats treated with methylnitrosourea (MNU) at 7 weeks of age. Significant differences in tumor incidence were identified between Lewis and Wistar-Furth ($P = 0.0003$), Lewis and Fischer 344 ($P = 0.0005$), Lewis and Copenhagen ($P = 0.0001$), Wistar-Furth and Copenhagen ($P = 0.024$), and Fischer 344 and Copenhagen ($P = 0.0001$) as determined by a log rank test. Wistar-Furth and Fischer 344 were not significantly different ($P = 0.14$). **B**, mammary tumor incidence for placebo and estradiol and progesterone-treated rats is plotted for each strain. Cohort sizes for estradiol and progesterone-treated animals were: Lewis ($n = 16$), Wistar-Furth ($n = 12$), Fischer 344 ($n = 12$), and Copenhagen ($n = 12$). Each strain exhibited significantly decreased tumor incidence in estradiol and progesterone-treated compared with placebo-treated cohorts. **C**, carmine-stained whole mounts of abdominal mammary glands from nulliparous (G0P0) and parous (G1P1) rats from each strain (original magnification, $\times 50$). Samples are representative of three animals per group.

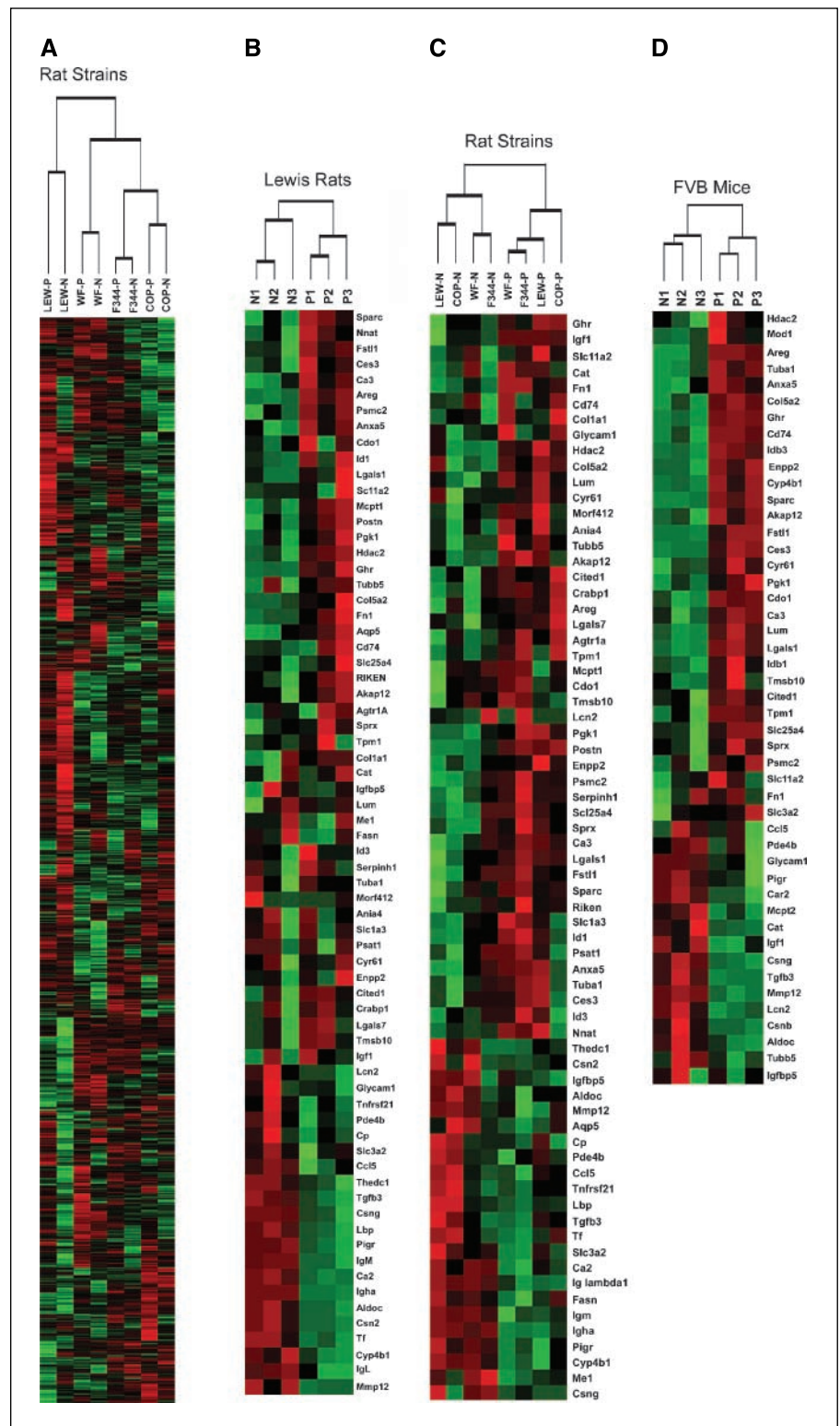


Figure 2. A parity-related gene expression signature distinguishes between nulliparous and parous rats and mice. Unsupervised hierarchical clustering analysis. Nulliparous (*N*), parous (*P*), Lewis (*LEW*), Fischer 344 (*F344*), Wistar-Furth (*WF*), and Copenhagen (*COP*). **A**, nulliparous and parous samples from each strain were clustered based on the median expression values of ~1,900 genes exhibiting global variation in gene expression across the data sets. **B**, six independent Lewis samples [three nulliparous (N1-N3) and three parous (P1-P3)] were clustered based solely on the expression of genes in the 70-gene parity signature. **C**, clustering analysis based solely on the expression of the 70-gene parity signature was performed on nulliparous and parous samples from Lewis, Wistar-Furth, Fischer, and Copenhagen rats. **D**, the 70-gene rat parity signature was mapped to the mouse genome using Homologene, yielding 47 mouse genes. Six FVB mouse samples [three nulliparous (N1-N3) and three parous (P1-P3)] were clustered based on the expression profiles of these 47 genes.

constituting the rat parity signature to the mouse genome, and assessed their expression profiles in nulliparous and parous FVB mouse mammary samples. Of the 70 genes that were mapped, 47 were represented on Affymetrix MGU74Av2 microarrays. These 47 genes were sufficient to distinguish nulliparous from parous samples in a blinded manner (Fig. 2D). Thus, a parity-related gene

expression signature generated in the rat is able to predict reproductive history in the mouse, suggesting that the persistent molecular alterations that occur in response to parity are conserved across rodent species.

Among the 70 genes that we identified as being consistently regulated by parity, at least five categories were evident.

Table 1. Genes up-regulated in parous rats

Gene name	Symbol	Gene ID	Function	Category	Fold-change G1P1 versus G0P0				
					Lewis	WF	F344	Cop	Median
Immunoglobulin heavy chain	<i>Igha</i>	314487	Immunoglobulin	Immune	39.4	25.4	4.5	6.9	25.4
Casein β	<i>Csn2</i>	29173	Milk protein	Differentiation	8.0	5.2	1.9	1.5	5.2
IgM light chain		287965	Immunoglobulin	Immune	2.5	3.8	1.8	1.6	2.5
Matrix metalloproteinase 12	<i>Mmp12</i>	117033	Proteolysis	ECM/Immune	2.6	1.4	2.0	1.3	2.0
Casein γ	<i>Csng</i>	114595	Milk protein	Differentiation	3.1	1.9	1.2	0.9	1.9
Fatty acid synthase	<i>Fasn</i>	50671	Fatty acid biosynthesis	Metabolism/ differentiation	2.0	1.6	1.7	0.9	1.7
Cytochrome P450, family 4, subfamily b,1	<i>Cyp4b1</i>	24307	Monooxygenase activity	Metabolism	1.6	1.5	1.2	1.2	1.5
Carbonic anhydrase 2	<i>Ca2</i>	54231	Carbon dioxide hydration	Metabolism	1.5	1.5	1.4	1.1	1.5
Ig lambda-1 chain C region		363828	Immunoglobulin	Immune	1.5	1.4	1.4	1.3	1.4
Malic enzyme 1	<i>Me1</i>	24552	Pyruvate synthesis	Metabolism	1.3	1.4	1.4	1.1	1.4
Insulin-like growth factor binding protein 5	<i>Igfbp5</i>	25285	Igf-I-binding	Growth factor/ ECM	2.4	1.4	0.9	2.7	1.4
Lipopolysaccharide binding protein	<i>Lbp</i>	29469	Antibacterial	Immune	2.1	1.3	1.4	2.0	1.4
Polymeric immunoglobulin receptor	<i>Pigr</i>	25046	Trancytosis	Immune	1.7	1.4	1.2	1.1	1.4
Transforming growth factor, β 3	<i>Tgfb3</i>	25717	Cell growth/ proliferation	Tgf- β	1.5	1.3	1.2	1.4	1.3
Aquaporin 5	<i>Aqp5</i>	25241	Water transport	Transporter	1.3	1.7	1.2	1.5	1.3
Phosphodiesterase 4B	<i>Pde4b</i>	24626	Cyclic AMP phosphodiesterase	Signal transduction	1.3	1.4	1.0	1.4	1.3
Thioesterase domain containing 1	<i>Thecd1</i>	64669	Fatty acid biosynthesis	Metabolism/ differentiation	1.9	1.2	1.3	1.5	1.3
Transferrin	<i>Tf</i>	24825	Iron transport	Transport/ differentiation	1.4	1.2	1.3	1.5	1.3
Ceruloplasmin	<i>Cp</i>	24268	Copper transport	Transport/ differentiation	1.3	1.0	1.2	2.2	1.2
Similar to death receptor 6	<i>Tnfrsf21</i>	316256	Apoptosis	Signal transduction	1.3	1.0	1.2	1.3	1.2
Aldolase C, fructose-biphosphate	<i>Aldoc</i>	24191	Fructose metabolism	Metabolism	1.2	1.2	1.1	1.3	1.2
Lipocalin 2	<i>Lcn2</i>	170496	Iron binding/antibacterial	Immune	1.3	1.1	1.2	1.4	1.2
Solute carrier family 3, member 2	<i>Slc3a2</i>	50567	Amino acid transporter	Transporter	1.2	1.1	1.2	1.3	1.2

NOTE: Genes identified as up-regulated by at least 1.2-fold in three out of four rat strains as a result of parity are reported from the highest to lowest median fold change. Gene names and symbols are reported based on the Rat Genome Database, and Gene ID according to Entrez Gene. Gene functions and categories are based on Gene Ontology.

Abbreviations: WF, Wistar-Furth; F344, Fischer 344; Cop, Copenhagen.

These included the previously identified differentiation, immune, Tgf- β , and growth factor categories (6), as well as an additional category of genes that are involved in ECM structure and function (Tables 1 and 2). We previously showed that clustering based on genes in each of the first four categories was sufficient to distinguish between nulliparous and parous rats (6). In an analogous manner, we tested whether unsupervised clustering based solely on ECM-related genes would be sufficient to differentiate between nulliparous and parous rat or mouse samples. In each case, ECM-related gene expression patterns alone were sufficient to distinguish between nulliparous and parous mammary samples from the four different rat strains (Fig. 3A), from independent mammary samples derived

from nulliparous and parous Lewis rats (Fig. 3B), and from mammary samples derived from FVB mice (Fig. 3C). This indicates that differential expression of a subset of genes involved in ECM structure and function represents a conserved feature of parity-induced changes in the rodent mammary gland.

Parity up-regulates *Tgfb3* and expression of differentiation and immune markers. Our previous analysis of parity-induced gene expression changes in FVB mice was consistent with the parity-induced up-regulation of Tgf- β 3 activity. Similarly, in the current study, we found that *Tgfb3* expression was up-regulated by parity in each of the four rat strains examined (Table 1). This finding was confirmed by QRT-PCR

Table 2. Genes down-regulated in parous rats

Gene name	Symbol	Gene ID	Function	Category	Fold-change G1P1 versus G0P0				
					Lewis	WF	F344	Cop	Median
Periostin	<i>Postn</i>	361945	Transcription factor	Differentiation	1.9	2.1	1.8	2.2	2.0
Amphiregulin	<i>Areg</i>	29183	Epidermal growth factor receptor ligand	Growth factor	3.5	2.1	1.7	1.9	2.0
Cellular retinoic acid binding protein I	<i>Crabp1</i>	25061	Retinoic acid receptor signaling	Signal transduction	1.8	2.1	1.3	1.5	1.7
Insulin-like growth factor 1	<i>Igf-1</i>	24482	Cell proliferation/survival	Growth factor	1.7	1.2	1.5	1.5	1.5
Fibronectin 1	<i>Fn1</i>	25661	Integrin signaling	ECM	1.4	1.3	1.5	1.6	1.5
A kinase (PRKA) anchor protein (gravin) 12	<i>Akap12</i>	83425	Scaffolding protein	Signal transduction	1.2	1.6	1.6	1.3	1.4
Neuronatin	<i>Nnat</i>	94270	Protein transport		2.0	1.4	1.5	0.9	1.4
Glycosylation dependent cell adhesion molecule 1	<i>Glycam1</i>	25258	Selectin ligand	Differentiation	0.5	2.2	1.2	1.7	1.4
Secreted acidic cysteine rich glycoprotein	<i>Sparc</i>	24791	ECM Formation	ECM	1.6	1.1	1.4	1.4	1.4
Ectonucleotide pyrophosphatase/phosphodiesterase 2	<i>Enpp2</i>	84050	Lysophospholipase	Cell motility	2.1	1.4	1.4	1.0	1.4
Lectin, galactose binding, soluble 1	<i>Lgals1</i>	56646	Integrin signaling	ECM	1.5	1.2	1.4	1.4	1.4
Inhibitor of DNA binding 1, helix-loop-helix protein	<i>Id1</i>	25261	Transcriptional repression	Tgf- β	1.4	1.4	1.4	1.1	1.4
Follistatin-like 1	<i>Fstl1</i>	79210			1.5	1.7	1.2	1.2	1.4
Phosphoserine aminotransferase 1	<i>Psat1</i>	293820	Serine biosynthesis	Metabolism	1.4	1.2	1.5	1.3	1.4
Lumican	<i>Lum</i>	81682	Proteoglycan	ECM	1.3	1.5	1.1	1.4	1.3
Melanocyte-specific gene 1 protein	<i>Cited1</i>	64466	Transcription factor	Signal transduction	1.4	1.9	1.2	1.3	1.3
Serine proteinase inhibitor, clade H, member 1	<i>Serpinh1</i>	29345	Procollagen binding	ECM	1.4	1.3	1.3	1.4	1.3
Sushi-repeat-containing protein	<i>Sprx</i>	64316			1.3	1.3	1.3	1.5	1.3
Carboxylesterase 3	<i>Ces3</i>	113902	Fatty acid metabolism	Metabolism	1.8	1.1	1.3	1.4	1.3
Cysteine rich protein 61	<i>Cyr61</i>	83476	Integrin signaling	ECM	1.1	1.3	1.3	1.6	1.3
Solute carrier family 1, member 3	<i>Slc1a3</i>	29483	Amino acid transporter	Transporter	1.4	1.3	1.3	1.1	1.3
Similar to RIKEN cDNA 6330406I15	<i>RDG1307396</i>	360757			1.6	1.2	1.3	1.3	1.3
Catalase	<i>Cat</i>	24248	Hydrogen peroxide reductase	ROS	1.7	1.0	1.4	1.2	1.3
Tropomyosin 1, α	<i>Tpm1</i>	24851	Actin binding		1.1	1.3	1.3	1.3	1.3
Activity and neurotransmitter-induced early gene protein 4	<i>Ania4</i>	360341	CAM kinase	Kinase	1.5	1.2	1.2	1.3	1.3
Solute carrier family 11, member 2	<i>Slc11a2</i>	25715	Divalent metal ion transporter	Transporter	1.4	1.0	1.3	1.2	1.3
Inhibitor of DNA binding 3, helix-loop-helix protein	<i>Id3</i>	25585	Transcriptional repression	Tgf- β	1.5	1.2	1.3	0.9	1.3
Solute carrier family 25 member 4	<i>Slc25a4</i>	85333	Nucleotide translocator	Transporter	1.3	1.3	1.2	1.3	1.3
Growth hormone receptor	<i>Ghr</i>	25235	Growth hormone signaling	Growth factor	2.1	1.1	1.2	1.3	1.3
Phosphoglycerate kinase 1	<i>Pgk1</i>	24644	Phosphoprotein glycolysis	Metabolism	1.6	1.2	1.3	1.2	1.3

(Continued on the following page)

Table 2. Genes down-regulated in parous rats (Cont'd)

Gene name	Symbol	Gene ID	Function	Category	Fold-change G1P1 versus G0P0				
					Lewis	WF	F344	Cop	Median
Cytosolic cysteine dioxygenase 1	<i>Cdo1</i>	81718	Cysteine metabolism	Metabolism	1.5	1.2	1.2	1.3	1.3
Mast cell protease 1	<i>Mcpt1</i>	29265	Proteolysis	ECM	1.6	1.3	1.2	1.2	1.2
Collagen, type V, $\alpha 2$	<i>Col5a2</i>	85250	ECM structural protein	ECM	1.0	1.2	1.3	1.5	1.2
Carbonic anhydrase 3	<i>Ca3</i>	54232	Carbon metabolism	Metabolism	1.8	1.2	1.1	1.3	1.2
Tubulin, $\alpha 1$	<i>Tuba1</i>	64158	Microtubule component	Cell structure	1.5	1.2	1.2	1.2	1.2
Angiotensin II receptor, type 1	<i>Agtr1A</i>	24180	Angiotensin receptor	Signal transduction	1.3	1.2	1.2	1.3	1.2
Collagen, type I, $\alpha 1$	<i>Col1a1</i>	29393	ECM structural protein	ECM	1.1	1.2	1.2	1.8	1.2
Annexin A5	<i>Anxa5</i>	25673	Calcium ion binding		1.6	1.2	1.2	1.2	1.2
Thymosin, $\beta 10$	<i>Tmsb10</i>	50665	Actin binding		1.3	1.2	1.2	1.0	1.2
Tubulin, $\beta 5$	<i>Tubb5</i>	29214	Microtubule component	Cell structure	1.1	1.3	1.2	1.2	1.2
Histone deacetylase 2	<i>Hdac2</i>	84577	Chromatin rearrangement		1.2	1.2	1.3	1.1	1.2
Lectin, galactose binding, soluble 7	<i>Lgals7</i>	29518	Galactose binding		1.1	1.8	1.2	1.2	1.2
CD74 antigen	<i>Cd74</i>	25599		Immune	1.2	1.2	1.0	1.3	1.2
Proteasome 26S subunit, ATPase 2	<i>Psmc2</i>	25581	Protein degradation		1.3	1.1	1.2	1.1	1.2
MORF-related gene X	<i>Morf412</i>	317413			1.4	1.2	1.1	1.2	1.2

NOTE: Genes identified as down-regulated by at least 1.2-fold in three out of four rat strains as a result of parity are reported from the highest to lowest median fold change. Gene names and symbols are reported based on the Rat Genome Database, and Gene ID according to Entrez Gene. Gene functions and categories are based on Gene Ontology.

Abbreviations: WF, Wistar-Furth; F344, Fischer 344; Cop, Copenhagen.

analysis of independent parous and nulliparous Lewis rat samples (Fig. 4A).

Also consistent with our prior observations, parity resulted in a persistent increase in the expression of genes involved in mammary differentiation, including the milk proteins β -casein and γ -casein, and the metal ion transporters ceruloplasmin and transferrin (ref. 6; Table 1; Fig. 4A).

As we have previously shown in the mouse, the 70-gene rat parity-related gene expression signature reflected the increased presence of immune cells in the parous mammary gland. In particular, increased expression of multiple immunoglobulin heavy and light chain genes in the parous gland suggested an increase in the population of plasma cells, whereas up-regulation of *Mmp12* and *Tnfrsf21* was consistent with increased numbers of macrophages and T cells (Table 1; Fig. 4A). Similarly, increased antibacterial and antiviral activity was suggested by the up-regulation of *Lbp*, *Lcn2*, and *Ccl5* (refs. 24–26; Table 1).

Parity results in down-regulation of amphiregulin and the growth hormone/Igf-I axis. Previous gene expression profiling of mouse mammary development revealed that parity results in a persistent decrease in the expression of several growth factor-encoding genes, including *Areg* and *Igf-I* (6). The present study confirmed that decreased expression of *Areg* and *Igf-I* are consistent features of the parous state in rats (Table 2; Fig. 4B). Additional evidence supporting parity-induced down-regulation of the growth hormone/Igf-I axis in the mammary glands of multiple rat strains was suggested by a decrease in growth hormone receptor (*Ghr*) expression (Table 2; Fig. 4B) as well as an increase in

Igfbp5 expression (Table 1; Fig. 4A), which functions to sequester local Igf-I in the ECM (27).

Parity regulates ECM gene expression. Mammary epithelial-ECM interactions play an important role in both normal mammary gland development and tumorigenesis (28). Moreover, persistent changes in the structure and function of the ECM have been shown in the mammary glands of parous rats (29). In the present study, microarray expression profiling suggested that a principal effect of parity in the rodent mammary gland is alteration of ECM gene expression. Thirteen of the 70 genes constituting the parity signature encode ECM structural components or proteins that regulate ECM formation or signaling (Tables 1 and 2). Notably, the majority of ECM-related gene expression changes induced by parity represented decreases in expression, including the ECM structural components, fibronectin 1, lumican, and collagen type I and collagen type V (Table 2). Parity-induced decreases in the expression of genes that regulate ECM formation or cellular interactions were also observed, including, *Sparc*, *Lgals1*, *Lgals7*, *Serpinh1*, *Cyr61*, and *Mcpt1* (Table 2; Fig. 4B).

To determine whether these parity-induced ECM-related gene expression changes were accompanied by differences in ECM structure, we stained histologic sections with Mason's trichrome to evaluate total collagen content. Although proximal epithelial structures seemed similar with respect to periductal trichrome staining (data not shown), a significant decrease in the extent of trichrome staining surrounding distal ducts was observed in the parous gland (Fig. 4C). These results provide further evidence that parity results in structural changes in the ECM.

Discussion

Women who have their first child early in life have a substantially reduced lifetime risk of breast cancer, an effect that is largely restricted to ER-positive tumors. Similar to humans, rats frequently develop ER-positive breast cancers and exhibit parity-induced protection against mammary tumorigenesis. In the current study, we set out to identify persistent parity-induced changes in gene expression that are conserved among multiple rat strains that exhibit hormone-induced protection against mammary tumorigenesis. We found that four genetically diverse inbred rat strains exhibit hormone-induced protection against mammary tumorigenesis and share a 70-gene pregnancy-induced expression signature. Our findings constitute the first global survey of parity-induced changes in gene expression in the rat—which represents the principal model for studying this phenomenon—as well as the first study to show conservation of parity-induced gene expression changes in multiple inbred rat strains that exhibit hormone-induced protection. Beyond suggesting that parity-induced protection is as robust and widely conserved a phenomenon in rats as it is in humans, our findings provide new insights into potential mechanisms by which early first-full term pregnancy decreases breast cancer risk.

These current studies extend our previous observations that parity results in persistently increased mammary expression of *Tgfb3* to include multiple additional strains of rats. Notably, loss of Tgf- β signaling in stromal fibroblasts promotes the growth and invasion of mammary carcinomas (30). Tgf- β may also have direct effects on mammary epithelial cells, resulting in the inhibition of mammary tumorigenesis (31). The sum of these effects is predicted to decrease the susceptibility of the parous gland to oncogenic transformation.

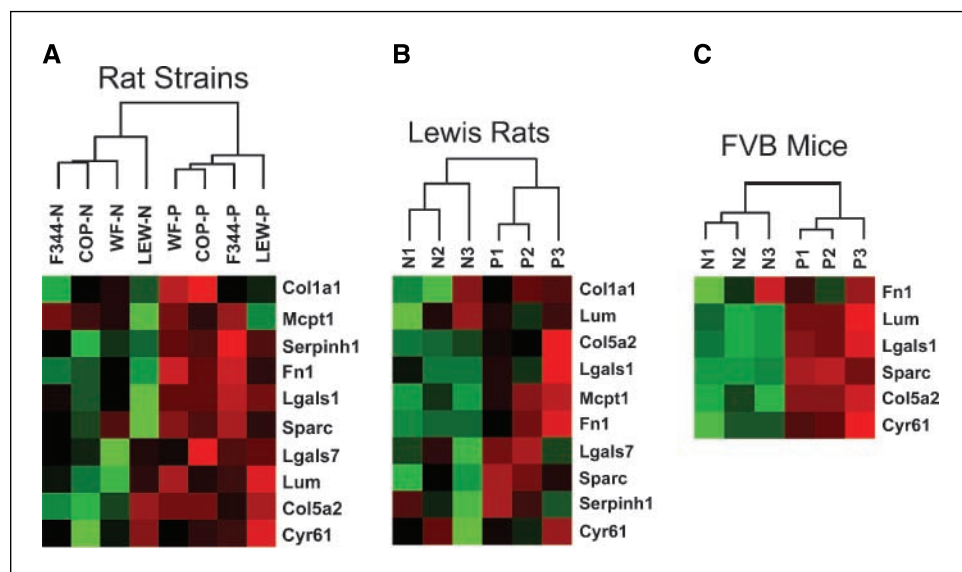
One of the most consistent and robust parity-induced changes in gene expression that we have observed in the rodent mammary gland is down-regulation of the epidermal growth factor receptor ligand, *Areg*. AREG is overexpressed in a high proportion of human breast cancers and correlates with large tumor size and nodal involvement (32). Studies in genetically engineered mice and mammary epithelial cell lines suggest an important role

for AREG in driving mammary epithelial proliferation, whereas recent evidence indicates that this growth factor may alter the ECM by the regulation of protease expression and secretion, including matrix metalloproteinase-2, matrix metalloproteinase-9, urokinase-type plasminogen activator, and plasminogen activator inhibitor-1 (33). Thus, parity-mediated down-regulation of *Areg* may not only inhibit epithelial proliferation, but may also hinder the invasive abilities of transformed cells in the mammary gland.

In addition to the down-regulation of *Areg*, we have confirmed that parity also results in the persistent down-regulation of *Igf-I*. Notably, a strong positive correlation exists between serum IGF-I levels and breast cancer risk in premenopausal women (34). Local and serum levels of IGF-I are regulated by growth hormone through its interaction with growth hormone receptor (35). Additional findings indicate that parity results in a persistent decrease in circulating growth hormone levels in rats (7); moreover, treatment of parous rats with Igf-I results in an increase in carcinogen-induced mammary tumorigenesis to levels similar to those observed in nulliparous controls (36). Consistent with this, spontaneous dwarf rats, which lack functional growth hormone, are highly resistant to carcinogen-induced mammary tumorigenesis (37).

Additional evidence for down-regulation of the growth hormone/Igf-I axis within the parous mammary gland was suggested in the present study by increases in *Igfbp5* expression and decreases in *Ghr* expression. As such, our findings suggest that—in addition to reducing circulating levels of growth hormone—parity may modulate local expression and activity of Igf-I within the mammary gland. Whereas Igf-I acts directly on mammary epithelial cells to promote proliferation and inhibit apoptosis (38), Igf-I in the mammary gland is likely produced in the stromal compartment in response to Ghr signaling (39). Local regulation of Igf-I activity also occurs through interactions with Igf-I binding proteins, such as *Igfbp5*, which binds and sequesters Igf-I in the ECM (40). As such, parity-induced down-regulation of Ghr and Igf-I expression in the mammary gland, coupled with up-regulation of *Igfbp5* expression, would be predicted to result in decreased Igf-I activity. This represents a

Figure 3. ECM gene expression distinguishes between nulliparous and parous rats and mice. Unsupervised hierarchical clustering analysis. A, a subset of parity-regulated genes involved in ECM structure and regulation was used to cluster nulliparous and parous mammary samples from Lewis (*LEW*), Wistar-Furth (*WF*), Fischer (*F344*), and Copenhagen (*COP*) rats. B, six independent Lewis samples [three nulliparous (N1-N3) and three parous (P1-P3) samples] were clustered based on the expression of ECM-related genes. C, six FVB mouse samples [three nulliparous (N1-N3) and three parous (P1-P3)] were clustered based on the expression of ECM-related genes identified in the rat parity signature that were mapped to the mouse genome.



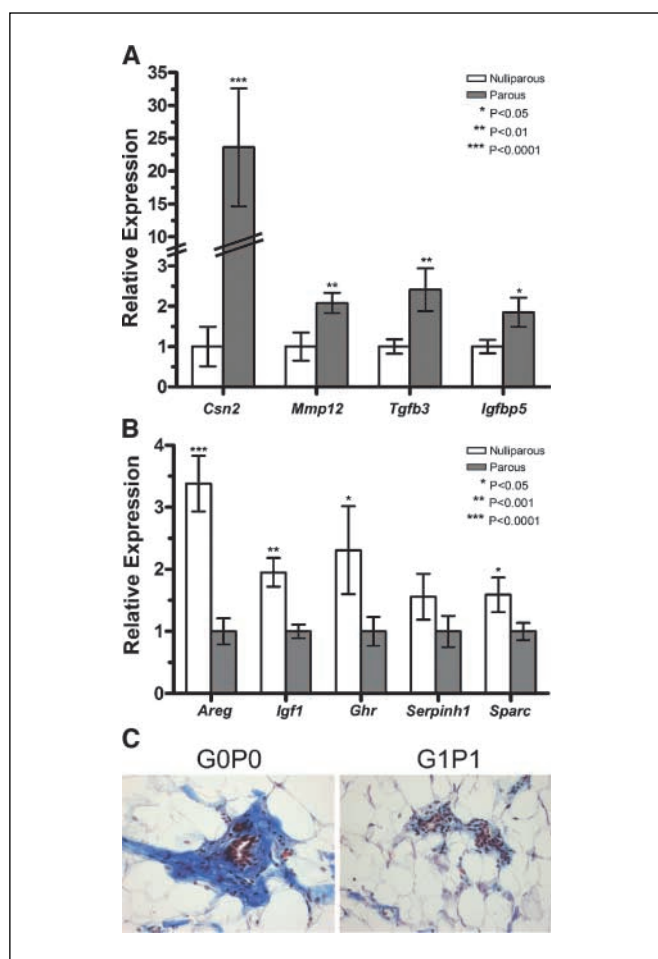


Figure 4. Confirmation of gene expression changes. *A* and *B*, TaqMan QRT-PCR was performed on cDNAs generated from 21 nulliparous and 21 parous Lewis rat mammary samples. Each reaction was performed in duplicate. Expression values for each gene were normalized to *B2m*. *A*, relative expression of parity up-regulated genes. *White columns*, mean expression in nulliparous samples normalized to 1.0 for each gene; *gray columns*, mean expression of each gene in parous relative to nulliparous samples; *bars*, \pm SE. *B*, relative expression of parity down-regulated genes. *White columns*, mean expression of each gene in nulliparous relative to parous samples; *gray columns*, mean expression in parous samples normalized to 1.0 for each gene; *bars*, \pm SE. *P* values were generated using a one-tailed, unpaired Student's *t* test. *C*, Mason's trichrome staining. Abdominal mammary glands from nulliparous and parous Lewis rats were stained with Mason's trichrome to assess total collagen present in the ECM surrounding epithelial structures. Images are representative of distal structures in the mammary glands of three nulliparous and three parous Lewis rats (original magnification, \times 200).

plausible mechanism by which parity may confer protection against breast cancer.

The functional unit of the mammary gland consists of a complex stroma that surrounds the epithelial compartment. Stromal-epithelial interactions play a prominent role, not only in mammary development, but also in tumorigenesis (28). Fibroblasts represent the most prominent cell type of the periductal stroma and, in addition to secreting growth factors that activate epithelial receptors, they are the primary synthesizers of ECM constituents such as fibronectin, collagen, and proteoglycans. Accumulating evidence indicates that stromal constituents, including fibroblasts and ECM structural components, could have differential effects on epithelial cells depending on the

source of the tissue from which they are isolated (41). Consistent with this, Schedin et al. have shown that the ability of mammary epithelial cells to form ductal structures in culture is markedly influenced by the developmental context of the ECM in which they are cultured (29). Further support for the role of ECM regulation in parity-induced protection against breast cancer comes from our observation that parous mammary glands exhibit decreased trichrome staining as well as persistent down-regulation of ECM structural and regulatory genes. Because cross-talk between epithelial and stroma cells occurs through local growth factors and their receptors (42), it is possible that parity-induced down-regulation of *Areg* and *Igf-1* in combination with up-regulation of *Tgfb3* may alter stromal-epithelial interactions in such a way as to decrease susceptibility to mammary carcinogenesis.

Finally, it is interesting to speculate that parity-induced changes in the ECM may be related to measures of breast cancer risk associated with mammographic breast density. Increased mammographic density has been consistently shown to correlate with high breast cancer risk (43). Mammographic density has also been reported to be negatively correlated with parity (44). Although breast density was initially believed to reflect the epithelial content of the breast, current evidence suggests that ECM composition—in particular collagen and proteoglycans such as lumican—may be the primary determinant of mammographic density (44, 45). Intriguingly, recent studies have implicated the ratio of serum IGF-I to IGF-BP3 as a major determinant of mammographic density (46). Consistent with this, Guo et al. found increased IGF-I tissue staining in samples from women with increased breast density (45). Our findings support the hypothesis that parity decreases Igf-I expression and activity and diminishes the expression of selected ECM structural components. Together, these changes may lead to decreases in both mammographic breast density and breast cancer risk. Validation of this hypothesis will require confirmation that parity alters local IGF-I levels and mammographic breast density in women, and that modulation of Igf-I in rodent models will alter breast density as well as pregnancy-induced protection against breast cancer.

In summary, the results presented in this study extend previous observations that parity results in local changes in growth factor gene expression in the mammary gland. We hypothesize that the evolutionarily conserved parity-induced alterations in gene expression identified in this study result in the modification of the extracellular environment and changes in stromal-epithelial interactions. We hypothesize that the ultimate effect of these changes is to create a tumor suppressive state, thereby providing a potential mechanism to explain parity-induced protection against mammary tumorigenesis. Whether analogous parity-induced changes occur in the human breast remains an important yet unresolved question.

Acknowledgments

Received 11/29/2005; revised 3/28/2006; accepted 4/24/2006.

Grant support: CA92910 from the National Cancer Institute, grants W81XWH-05-1-0405, W81XWH-05-1-0390, DAMD17-03-1-0345 (C.M. Blakely), and DAMD17-00-1-0401 (S.E. Moody) from the U.S. Army Breast Cancer Research Program, and grants from the Breast Cancer Research Foundation and the Emerald Foundation.

The costs of publication of this article were defrayed in part by the payment of page charges. This article must therefore be hereby marked *advertisement* in accordance with 18 U.S.C. Section 1734 solely to indicate this fact.

The authors thank the members of the Chodosh Laboratory for helpful discussions and critical reading of the manuscript.

References

1. Chodosh LA, D'Cruz CM, Gardner HP, et al. Mammary gland development, reproductive history, and breast cancer risk. *Cancer Res* 1999;59:1765-71.
2. MacMahon B, Cole P, Lin TM, et al. Age at first birth and breast cancer risk. *Bull World Health Organ* 1970;43:209-21.
3. Layde PM, Webster LA, Baughman AL, Wingo PA, Rubin GL, Ory HW. The independent associations of parity, age at first full term pregnancy, and duration of breastfeeding with the risk of breast cancer. *Cancer and Steroid Hormone Study Group. J Clin Epidemiol* 1989;42:963-73.
4. Russo J, Moral R, Balogh GA, Mailo D, Russo IH. The protective role of pregnancy in breast cancer. *Breast Cancer Res* 2005;7:131-42.
5. Sivaraman L, Medina D. Hormone-induced protection against breast cancer. *J Mammary Gland Biol Neoplasia* 2002;7:77-92.
6. D'Cruz CM, Moody SE, Master SR, et al. Persistent parity-induced changes in growth factors, TGF- β 3, and differentiation in the rodent mammary gland. *Mol Endocrinol* 2002;16:2034-51.
7. Thordarson G, Jin E, Guzman RC, Swanson SM, Nandi S, Talamantes F. Refractoriness to mammary tumorigenesis in parous rats: is it caused by persistent changes in the hormonal environment or permanent biochemical alterations in the mammary epithelia? *Carcinogenesis* 1995;16:2847-53.
8. Russo J, Gusterson BA, Rogers AE, Russo IH, Wellings SR, van Zwieten MJ. Comparative study of human and rat mammary tumorigenesis. *Lab Invest* 1990;62:244-78.
9. Sivaraman L, Stephens LC, Markaverich BM, et al. Hormone-induced refractoriness to mammary carcinogenesis in Wistar-Furth rats. *Carcinogenesis* 1998;19:1573-81.
10. Yang J, Yoshizawa K, Nandi S, Tsubura A. Protective effects of pregnancy and lactation against *N*-methyl-*N*-nitrosourea-induced mammary carcinomas in female Lewis rats. *Carcinogenesis* 1999;20:623-8.
11. Rajkumar L, Guzman RC, Yang J, Thordarson G, Talamantes F, Nandi S. Short-term exposure to pregnancy levels of estrogen prevents mammary carcinogenesis. *Proc Natl Acad Sci U S A* 2001;98:11755-9.
12. Guzman RC, Yang J, Rajkumar L, Thordarson G, Chen X, Nandi S. Hormonal prevention of breast cancer: mimicking the protective effect of pregnancy. *Proc Natl Acad Sci U S A* 1999;96:2520-5.
13. Medina D, Smith GH. Chemical carcinogen-induced tumorigenesis in parous, involuted mouse mammary glands. *J Natl Cancer Inst* 1999;91:967-69.
14. Medina D, Kittrell FS. p53 function is required for hormone-mediated protection of mouse mammary tumorigenesis. *Cancer Res* 2003;63:6140-3.
15. Ginger MR, Gonzalez-Rimbau MF, Gay JP, Rosen JM. Persistent changes in gene expression induced by estrogen and progesterone in the rat mammary gland. *Mol Endocrinol* 2001;15:1993-2009.
16. Colditz GA, Rosner BA, Chen WY, Holmes MD, Hankinson SE. Risk factors for breast cancer according to estrogen and progesterone receptor status. *J Natl Cancer Inst* 2004;96:218-28.
17. Turcot-Lemay L, Kelly PA. Response to ovariectomy of *N*-methyl-*N*-nitrosourea-induced mammary tumors in the rat. *J Natl Cancer Inst* 1981;66:97-102.
18. Master SR, Stoddard AJ, Bailey LC, Pan TC, Dugan KD, Chodosh LA. Genomic analysis of early murine mammary gland development using novel probe-level algorithms. *Genome Biol* 2005;6:R20.
19. Gentleman RC, Carey VJ, Bates DM, et al. Bioconductor: open software development for computational biology and bioinformatics. *Genome Biol* 2004;5:R80.
20. Phang TL, Neville MC, Rudolph M, Hunter L. Trajectory clustering: a non-parametric method for grouping gene expression time courses, with applications to mammary development. *Pac Symp Biocomput* 2003;351-62.
21. Waha A, Sturte C, Kessler A, et al. Expression of the ATM gene is significantly reduced in sporadic breast carcinomas. *Int J Cancer* 1998;78:306-9.
22. Ito K, Fujimori M, Nakata S, et al. Clinical significance of the increased multidrug resistance-associated protein (MRP) gene expression in patients with primary breast cancer. *Oncol Res* 1998;10:99-109.
23. Gould MN, Zhang R. Genetic regulation of mammary carcinogenesis in the rat by susceptibility and suppressor genes. *Environ Health Perspect* 1991;93:161-7.
24. Flo TH, Smith KD, Sato S, et al. Lipocalin 2 mediates an innate immune response to bacterial infection by sequestering iron. *Nature* 2004;432:917-21.
25. Elliott MB, Tebbey PW, Pryharski KS, Scheuer CA, Laughlin TS, Hancock GE. Inhibition of respiratory syncytial virus infection with the CC chemokine RANTES (CCL5). *J Med Virol* 2004;73:300-8.
26. Branger J, Florquin S, Knapp S, et al. LPS-binding protein-deficient mice have an impaired defense against Gram-negative but not Gram-positive pneumonia. *Int Immunol* 2004;16:1605-11.
27. Flint DJ, Beattie J, Allan GJ. Modulation of the actions of IGFs by IGFBP-5 in the mammary gland. *Horm Metab Res* 2003;35:809-15.
28. Tlsty TD, Hein PW. Know thy neighbor: stromal cells can contribute oncogenic signals. *Curr Opin Genet Dev* 2001;11:54-9.
29. Schedin P, Mitrenga T, McDaniel S, Kaeck M. Mammary ECM composition and function are altered by reproductive state. *Mol Carcinog* 2004;41:207-20.
30. Cheng N, Bhowmick NA, Chytil A, et al. Loss of TGF- β type II receptor in fibroblasts promotes mammary carcinoma growth and invasion through upregulation of TGF- α , MSP- and HGF-mediated signaling networks. *Oncogene* 2005;24:5053-68.
31. Pierce DF, Jr., Gorska AE, Chytil A, et al. Mammary tumor suppression by transforming growth factor β 1 transgene expression. *Proc Natl Acad Sci U S A* 1995;92:4254-8.
32. Ma L, de Roquancourt A, Bertheau P, et al. Expression of amphiregulin and epidermal growth factor receptor in human breast cancer: analysis of autocrine and stromal-epithelial interactions. *J Pathol* 2001;194:413-9.
33. Menashi S, Serova M, Ma L, Vignot S, Mourah S, Calvo F. Regulation of extracellular matrix metalloproteinase inducer and matrix metalloproteinase expression by amphiregulin in transformed human breast epithelial cells. *Cancer Res* 2003;63:7575-80.
34. Schernhammer ES, Holly JM, Pollak MN, Hankinson SE. Circulating levels of insulin-like growth factors, their binding proteins, and breast cancer risk. *Cancer Epidemiol Biomarkers Prev* 2005;14:699-704.
35. Laban C, Bustin SA, Jenkins PJ. The GH-IGF-I axis and breast cancer. *Trends Endocrinol Metab* 2003;14:28-34.
36. Thordarson G, Slusher N, Leong H, et al. Insulin-like growth factor (IGF)-I obliterates the pregnancy-associated protection against mammary carcinogenesis in rats: evidence that IGF-I enhances cancer progression through estrogen receptor- α activation via the mitogen-activated protein kinase pathway. *Breast Cancer Res* 2004;6:R423-36.
37. Thordarson G, Semaan S, Low C, et al. Mammary tumorigenesis in growth hormone deficient spontaneous dwarf rats: effects of hormonal treatments. *Breast Cancer Res Treat* 2004;87:277-90.
38. Hadsell DL, Bonnette SG. IGF and insulin action in the mammary gland: lessons from transgenic and knockout models. *J Mammary Gland Biol Neoplasia* 2000;5:19-30.
39. Gallego MI, Binart N, Robinson GW, et al. Prolactin, growth hormone, and epidermal growth factor activate Stat5 in different compartments of mammary tissue and exert different and overlapping developmental effects. *Dev Biol* 2001;229:163-75.
40. Marshman E, Green KA, Flint DJ, White A, Streuli CH, Westwood M. Insulin-like growth factor binding protein 5 and apoptosis in mammary epithelial cells. *J Cell Sci* 2003;116:675-82.
41. Barcellos-Hoff MH, Ravani SA. Irradiated mammary gland stroma promotes the expression of tumorigenic potential by unirradiated epithelial cells. *Cancer Res* 2000;60:1254-60.
42. Bhowmick NA, Neilson EG, Moses HL. Stromal fibroblasts in cancer initiation and progression. *Nature* 2004;432:332-7.
43. Tice JA, Cummings SR, Ziv E, Kerlikowske K. Mammographic breast density and the Gail model for breast cancer risk prediction in a screening population. *Breast Cancer Res Treat* 2005;94:115-22.
44. Li T, Sun L, Miller N, et al. The association of measured breast tissue characteristics with mammographic density and other risk factors for breast cancer. *Cancer Epidemiol Biomarkers Prev* 2005;14:343-9.
45. Guo YP, Martin LJ, Hanna W, et al. Growth factors and stromal matrix proteins associated with mammographic densities. *Cancer Epidemiol Biomarkers Prev* 2001;10:243-8.
46. Diorio C, Pollak M, Byrne C, et al. Insulin-like growth factor-I, IGF-binding protein-3, and mammographic breast density. *Cancer Epidemiol Biomarkers Prev* 2005;14:1065-73.

Correction: Pregnancy-Induced Protection against Mammary Tumorigenesis

In the article on pregnancy-induced protection against mammary tumorigenesis in the June 15, 2006 issue of *Cancer Research* (1), the parity status of six of the 43 arrays used to derive the 70-gene expression signature was misclassified through an error in data entry. These arrays represented six of the 14 arrays run for Fischer 344 rats. The remaining 37 arrays for the Lewis, Wistar-Furth, Copenhagen, and Fischer 344 mammary samples were properly classified, as were the independent Lewis rat and FVB mouse samples used to validate the findings. This misclassification both obscured genuine parity-induced changes in the Fischer 344 strain and added biological noise due to genes that were covarying but unrelated to parity. As a consequence, after correcting the parity status for the six Fischer 344 arrays and applying the same analytical criteria described in the article, the authors found that the core parity-induced gene expression signature was reduced from 70 to 47 genes. Similar to the original 70-gene signature, this 47-gene signature is sufficient to distinguish between independent nulliparous and parous samples from all rat and mouse strains

analyzed in the article. Corrected versions of Tables 1 and 2 appear below.

Each of the five originally identified functional gene categories (Tgf- β 3, differentiation, immune markers, growth hormone/Igf-1 axis, and extracellular matrix components) are retained within this signature. Genes lost from the original 70-gene signature remain significantly altered in two of the four rat strains and are still plausible candidates for contributing to parity-induced protection against mammary tumorigenesis. Notably, a role for downregulation of *Ghr*, which is not included in the corrected signature, in parity-induced protection is still supported by the FVB mouse data and the QRT-PCR analysis of independent Lewis rat samples presented in the article. Also consistent with a role for the GH/Igf-1 pathway in parity-induced protection, *Igf-1* remains downregulated — and *Igfbp5* remains upregulated — on the corrected list of genes.

Overall, despite the reassignment of six samples, the conclusions of the article remain unaltered. Moreover, as a primary goal of the original article was to narrow down the list of genes to those most robustly associated with parity-induced protection, the corrected signature accomplishes this and provides an even

Table 1. Genes up-regulated in parous rats

Gene name	Symbol	Gene ID	Function	Category	Fold-change G1P1 versus G0P0				
					Lewis	WF	F344	Cop	Median
Immunoglobulin heavy chain	<i>Igha</i>	314487	Immunoglobulin	Immune	39.4	25.4	12.4	6.9	18.9
Casein beta	<i>Csn2</i>	29173	Milk protein	Differentiation	8.0	5.2	1.6	1.5	3.4
IgM light chain		287965	Immunoglobulin	Immune	2.5	3.8	2.0	1.6	2.2
Insulin-like growth factor binding protein 5	<i>Igfbp5</i>	25285	Igf1-binding	Growth factor/ECM	2.4	1.4	1.1	2.7	1.9
Casein gamma	<i>Csng</i>	114595	Milk protein	Differentiation	3.1	1.9	1.8	0.9	1.9
Lipopolysaccharide binding protein	<i>Lbp</i>	29469	Antibacterial	Immune	2.1	1.3	1.0	2.0	1.7
Matrix metalloproteinase 12	<i>Mmp12</i>	117033	Proteolysis	ECM/Immune	2.6	1.4	1.6	1.3	1.5
Carbonic anhydrase 2	<i>Ca2</i>	54231	Carbon metabolism	Metabolism	1.5	1.5	1.5	1.1	1.5
Fatty acid synthase	<i>Fasn</i>	50671	Fatty acid biosynthesis	Metabolism/Differentiation	2.0	1.6	1.3	0.9	1.5
Cytochrome P450, family 4, subfamily b,1	<i>Cyp4b1</i>	24307	Monoxygenase activity	Metabolism	1.6	1.5	1.4	1.2	1.4
Transforming growth factor, beta 3	<i>Tgfb3</i>	25717	Cell growth/proliferation	Tgf- β	1.5	1.3	0.9	1.4	1.4
Thioesterase domain containing 1	<i>Thedc1</i>	64669	Fatty acid biosynthesis	Metabolism/Differentiation	1.9	1.2	0.8	1.5	1.3
Malic enzyme 1	<i>Me1</i>	24552	Pyruvate synthesis	Metabolism	1.3	1.4	1.4	1.1	1.3
Phosphodiesterase 4B	<i>Pde4b</i>	24626	cAMP phosphodiesterase	Signal transduction	1.3	1.4	0.8	1.4	1.3
Polymeric immunoglobulin receptor	<i>Pigr</i>	25046	Trancytosis	Immune	1.7	1.4	1.2	1.1	1.3
Kruppel-like factor 9	<i>Klf9</i>	117560	Transcription Factor	Signal transduction	1.3	1.4	1.2	1.1	1.3
Matrix metalloproteinase 11	<i>Mmp11</i>	25481	Proteolysis	ECM	1.2	1.2	1.2	1.2	1.2

NOTE: Genes identified as up-regulated by at least 1.2-fold in three out of four rat strains as a result of parity are reported from highest to lowest median fold-change. Gene names and symbols are reported based on the Rat Genome Database, and Gene ID according to Entrez Gene. Gene functions and categories are based upon GeneOntology.

Abbreviations: WF, Wistar-Furth; F344, Fischer 344; Cop, Copenhagen.

smaller overlap of evolutionarily conserved gene expression changes associated with parity-induced protection against mammary tumorigenesis.

1. Blakely CM, Stoddard AJ, Belka GK, Dugan KD, Notarfrancesco KL, Moody SE, D'Cruz CM, Chodosh LA. Hormone-induced protection against mammary tumorigenesis is conserved in multiple rat strains and identifies a core gene expression signature induced by pregnancy. *Cancer Res* 2006;66:6421-31.

Table 2. Genes down-regulated in parous rats

Gene name	Symbol	Gene ID	Function	Category	Fold-change G0P0 versus G1P1				
					Lewis	WF	F344	Cop	Median
Periostin	<i>Postn</i>	361945	Cell adhesion	ECM	1.9	2.1	1.6	2.2	2.0
Amphiregulin	<i>Areg</i>	29183	Epidermal growth factor receptor ligand	Growth factor	3.5	2.1	1.9	1.9	2.0
Cellular retinoic acid binding protein I	<i>Crabp1</i>	25061	Retinoic acid receptor signaling	Signal transduction	1.8	2.1	1.3	1.5	1.7
Glycosylation dependent cell adhesion molecule 1	<i>Glycam1</i>	25258	Selectin ligand	Differentiation	0.5	2.2	1.3	1.7	1.5
Secreted acidic cysteine rich glycoprotein	<i>Sparc</i>	24791	ECM Formation	ECM	1.9	1.3	1.1	1.7	1.5
Lumican	<i>Lum</i>	81682	Proteoglycan	ECM	1.3	1.5	1.5	1.4	1.5
3-hydroxy-3-methylglutaryl-Coenzyme A synthase 2	<i>Hmgcs2</i>	24450	Cholesterol/ketone body biosynthesis	Metabolism	2.9	1.3	1.6	1.0	1.5
Fibronectin 1	<i fn1<="" i=""></i>	25661	Integrin signaling	ECM	1.4	1.3	1.3	1.6	1.4
Cbp/p300-interacting transactivator with Glu/Asp-rich carboxy-terminal domain 1	<i>Cited1</i>	64466	Transcription factor	Signal transduction	1.4	1.9	1.3	1.3	1.4
Ectonucleotide pyrophosphatase/phosphodiesterase 2	<i>Enpp2</i>	84050	Lysophospholipase	Cell motility	1.7	1.4	0.8	1.3	1.4
Insulin-like growth factor 1	<i>Igf1</i>	24482	Cell proliferation/survival	Growth factor	1.7	1.2	1.1	1.5	1.3
Sushi-repeat-containing protein	<i>Sprx</i>	64316			1.3	1.3	1.1	1.5	1.3
Lectin, galactose binding, soluble 1	<i>Lgals1</i>	56646	Integrin signaling	ECM	1.5	1.2	0.8	1.4	1.3
A kinase (PRKA) anchor protein (gravin) 12	<i>Akap12</i>	83425	Scaffolding protein	Signal transduction	1.2	1.6	1.2	1.3	1.3
Lectin, galactose binding, soluble 7	<i>Lgals7</i>	29518	Galactose binding		1.1	1.8	1.4	1.2	1.3
Tropomyosin 1, alpha	<i>Tpm1</i>	24851	Actin binding		1.1	1.3	1.3	1.3	1.3
Activity and neurotransmitter induced early gene protein 4	<i>Ania4</i>	360341	CAM kinase	Kinase	1.5	1.2	1.0	1.3	1.3
Cytosolic cysteine dioxygenase 1	<i>Cdo1</i>	81718	Cysteine metabolism	Metabolism	1.5	1.2	0.8	1.3	1.3
Carbonic anhydrase 3	<i>Ca3</i>	54232	Carbon metabolism	Metabolism	1.8	1.2	0.8	1.3	1.2
CD74 antigen	<i>Cd74</i>	25599		Immune	1.2	1.2	1.3	1.3	1.2
Tubulin, alpha 1	<i>Tuba1</i>	64158	Microtubule component	Cell structure	1.5	1.2	0.9	1.2	1.2
Similar to RIKEN cDNA 6330406I15	<i>RGD1307396</i>	360757			1.6	1.2	1.0	1.3	1.2
Collagen, type 1, alpha 1	<i>Colla1</i>	29393	ECM structural protein	ECM	0.9	1.2	1.2	1.6	1.2
Phosphoglycerate kinase 1	<i>Pgk1</i>	24644	Phosphoprotein glycolysis	Metabolism	1.6	1.2	0.9	1.2	1.2
Annexin A5	<i>Anxa5</i>	25673	Calcium ion binding		1.6	1.2	0.8	1.2	1.2
Prohibitin	<i>Phb</i>	25344	Regulation of cell cycle	Signal transduction	1.3	1.2	1.2	1.1	1.2
Valosin-containing protein	<i>Vcp</i>	116643	Endoplasmic reticulum protein catabolism		1.2	1.2	1.2	1.2	1.2
Tropomyosin 4	<i>Tpm4</i>	24852	Actin binding		1.1	1.3	1.2	1.2	1.2
Tubulin, beta 5	<i>Tubb5</i>	29214	Microtubule component	Cell structure	1.1	1.3	1.2	1.2	1.2
MORF-related gene X	<i>Morf412</i>	317413			1.4	1.2	1.0	1.2	1.2

NOTE: Genes identified as down-regulated by at least 1.2-fold in three out of four rat strains as a result of parity are reported from highest to lowest median fold-change. Gene names and symbols are reported based on the Rat Genome Database, and Gene ID according to Entrez Gene. Gene functions and categories are based upon GeneOntology.
Abbreviations: WF, Wistar-Furth; F344, Fischer 344; Cop, Copenhagen.

Research article

Open Access

Dense breast stromal tissue shows greatly increased concentration of breast epithelium but no increase in its proliferative activityDebra Hawes¹, Susan Downey², Celeste Leigh Pearce³, Sue Bartow⁴, Peggy Wan³, Malcolm C Pike³ and Anna H Wu³¹Department of Pathology, Keck School of Medicine, University of Southern California, 2011 Zonal Avenue, Los Angeles, CA 90089, USA²Department of Surgery, Keck School of Medicine, University of Southern California, 1510 San Pablo Street, Los Angeles, CA 90033, USA³Department of Preventive Medicine, Keck School of Medicine, University of Southern California/Norris Comprehensive Cancer Center, 1441 Eastlake Avenue, Los Angeles, CA 90033, USA⁴107 Stark Mesa, Carbondale, CO 81623, USACorresponding author: Malcolm C Pike, mcpike@usc.edu

Received: 2 Feb 2006 Revisions requested: 21 Feb 2006 Revisions received: 8 Mar 2006 Accepted: 30 Mar 2006 Published: 28 Apr 2006

Breast Cancer Research 2006, **8**:R24 (doi:10.1186/bcr1408)This article is online at: <http://breast-cancer-research.com/content/8/2/R24>© 2006 Hawes *et al.*; licensee BioMed Central Ltd.This is an open access article distributed under the terms of the Creative Commons Attribution License (<http://creativecommons.org/licenses/by/2.0>), which permits unrestricted use, distribution, and reproduction in any medium, provided the original work is properly cited.**Abstract**

Introduction Increased mammographic density is a strong risk factor for breast cancer. The reasons for this are not clear; two obvious possibilities are increased epithelial cell proliferation in mammographically dense areas and increased breast epithelium in women with mammographically dense breasts. We addressed this question by studying the number of epithelial cells in terminal duct lobular units (TDLUs) and in ducts, and their proliferation rates, as they related to local breast densities defined histologically within individual women.

Method We studied deep breast tissue away from subcutaneous fat obtained from 12 healthy women undergoing reduction mammoplasty. A slide from each specimen was stained with the cell-proliferation marker MIB1. Each slide was divided into (sets of) areas of low, medium and high density of connective tissue (CT; highly correlated with mammographic densities). Within each of the areas, the numbers of epithelial cells in TDLUs and ducts, and the numbers MIB1 positive, were counted.

Results The relative concentration (RC) of epithelial cells in high compared with low CT density areas was 12.3 (95% confidence interval (CI) 10.9 to 13.8) in TDLUs and 34.1 (95% CI 26.9 to 43.2) in ducts. There was a much smaller difference between medium and low CT density areas: RC = 1.4 (95% CI 1.2 to 1.6) in TDLUs and 1.9 (95% CI 1.5 to 2.3) in ducts. The relative mitotic rate (RMR; MIB1 positive) of epithelial cells in high compared with low CT density areas was 0.59 (95% CI 0.53 to 0.66) in TDLUs and 0.65 (95% CI 0.53 to 0.79) in ducts; the figures for the comparison of medium with low CT density areas were 0.58 (95% CI 0.48 to 0.70) in TDLUs and 0.66 (95% CI 0.44 to 0.97) in ducts.

Conclusion Breast epithelial cells are overwhelmingly concentrated in high CT density areas. Their proliferation rate in areas of high and medium CT density is lower than that in low CT density areas. The increased breast cancer risk associated with increased mammographic densities may simply be a reflection of increased epithelial cell numbers. Why epithelium is concentrated in high CT density areas remains to be explained.

Introduction

On a mammogram, fat appears radiolucent or dark, whereas stromal and epithelial tissue appears radio-dense or white. The amount of mammographic density is a strong independent predictor of breast cancer risk [1,2]. The biological basis for this increased risk is poorly understood. A critical question is

whether densities are directly related to risk or are simply a marker of risk. We addressed this question recently by studying the location of small ductal carcinoma *in situ* (DCIS) lesions as revealed by microcalcifications, and showed that such DCIS occurs overwhelmingly in the mammographically dense areas of the breast [3]. Most DCIS lesions in our study

a_H, a_L, a_M = the areas of the slide classified as being of high, low and medium CT density (in μm^2); CI = confidence interval; CT = connective tissue; DAB = 3,3'-diaminobenzidine tetrahydrochloride; DCIS = ductal carcinoma *in situ*; n_H, n_L, n_M = the numbers of epithelial cells staining positive for MIB1 within high, low and medium CT density areas; RC = relative concentration; RMR = relative mitotic rate; TDLU = terminal duct lobular unit; t_H, t_L, t_M = the numbers of epithelial cells within high, low and medium CT density areas;

Table 1**Relation between relative concentration of epithelial cells and connective tissue density**

CT density	RC	95% CI	<i>p</i>
TDLUs			
Low	1.0		
Medium	1.4	1.2–1.6	<0.001
High	12.3	10.9–13.8	<0.001
Ducts			
Low	1.0		
Medium	1.9	1.5–2.3	<0.001
High	34.1	26.9–43.2	<0.001

CI, confidence interval; CT, connective tissue; RC, relative concentration (per unit area); TDLUs, terminal duct lobular units.

occurred in the lateral-superior quadrant, as has been found in previous studies [4], and 'correlated strongly with the average percentage density in the different mammographic quadrants' [3]. Pre-DCIS mammograms that were taken on average about two years previously showed that the areas subsequently exhibiting DCIS were clearly dense at the time of the earlier mammogram, and this suggests that this relationship was not brought about by the presence of the DCIS. The reasons for these findings are not clear; two obvious possibilities are increased epithelial cell proliferation in mammographically dense areas of the breast and increased breast epithelium in women with mammographically dense breasts. Two groups have investigated the relationship between the amount of mammographic density of a woman and the amount of her breast epithelial tissue [5,6]. Alowami and colleagues [5] used tissue obtained from biopsies investigating breast lesions that were subsequently diagnosed as benign or pre-invasive breast disease; they studied tissue 'distant from the diagnostic lesion' without reference to its location as regards mammographic density (that is, 'random' tissue). They found that the median density of duct lobular units was 28% higher in breasts whose overall mammographic density was 50% or more ($n = 27$) than in breasts whose overall mammographic density was less than 25% ($n = 35$); this result was not statistically significant and the result was described as showing 'no difference in the density of epithelial components' [5]. Li and colleagues [6] also found in their much larger study ($n = 236$) of 'random' breast tissue collected from normal women by Bartow and colleagues [7] in their autopsy study of accidental deaths in New Mexico that women with high mammographic density had greater amounts of epithelial tissue (as measured by area of epithelial nuclear staining) and the result was highly statistically significant. Breast epithelial proliferation rates as they relate to mammographic densities in healthy women have not been well studied [8]. We have addressed these questions by studying the number of epithelial cells in terminal duct lobular units (TDLUs) and in breast ducts, and their respective prolif-

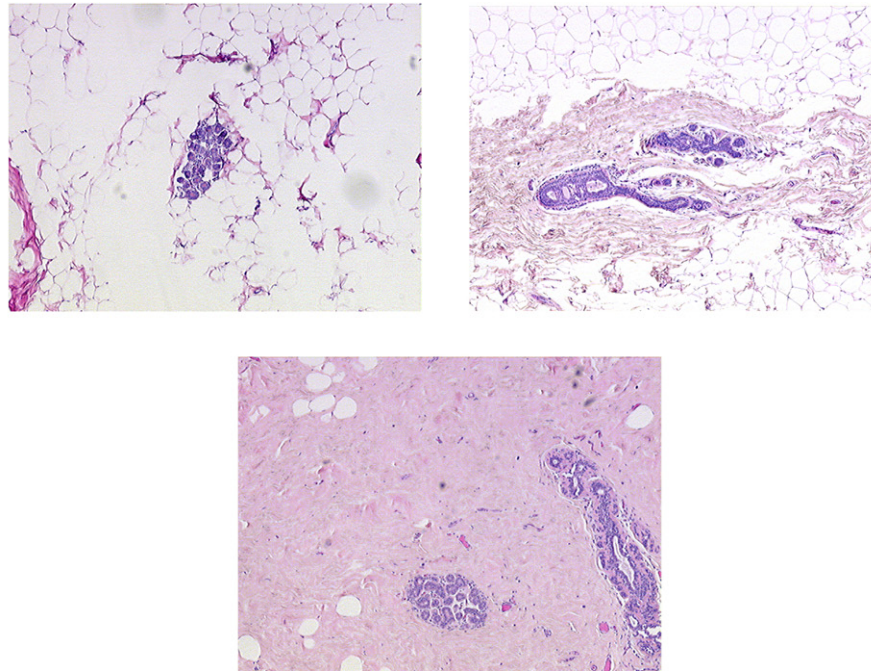
eration rates as they relate to local histological breast densities within individual women.

Materials and methods

We retrospectively identified 15 consecutive healthy women who had undergone a reduction mammoplasty performed by one of us (SD) at the University of Southern California medical facilities. The study protocol was approved by the Institutional Review Board of the University of Southern California School of Medicine.

For each participant we obtained the formalin-fixed paraffin-embedded block of tissue that had been routinely processed and saved from her surgery. A single slide was cut from each block and stained with the proliferation marker MIB1 (BioGenex Laboratories, San Ramon, CA, USA). The slides were prepared in accordance with our previously published protocol [9]; the chromogen used was 3,3'-diaminobenzidine tetrahydrochloride (DAB). On microscopic examination one of the slides contained skin and two other slides showed areas of disintegration; all three were deemed unsuitable for study.

Each of the remaining 12 slides was divided into (sets of) areas of low, medium and high density of connective tissue (CT) (highly correlated with densities as defined by mammographic criteria [10]); see Figure 1. The total size of each of the three areas (in μm^2), and within each of the three areas the numbers of epithelial cells in TDLUs and ducts and the numbers that were MIB1 positive, were counted with the help of an automated microscope system that digitized the images and permitted the outlining of relevant areas on a high-resolution computer screen (ACIS II; Clariant, Inc., San Juan Capistrano, CA, USA). The total numbers of epithelial cells in different outlined areas within the CT density-defined areas was then automatically counted by the ACIS II nuclear counting software program, which is based on color identification. Hematoxylin was used to counterstain the MIB1-negative nuclei blue, and the DAB chromogen marked the MIB1-positive nuclei brown.

Figure 1

Example of areas of low, medium (upper right) and high (lower center) CT density.

The software calculated the numbers of MIB1-negative and MIB1-positive cells on the basis of these color differences.

Statistical analysis

For each slide, and separately for TDLU and ductal cells, three sets of values were obtained: first, the areas of the slide classified as being of low, medium or high CT density (a_L , a_M and a_H in μm^2); second, the numbers of epithelial cells within these areas (t_L , t_M and t_H); and third, the numbers of these epithelial cells staining positive for MIB1 (n_L , n_M and n_H). On the null hypothesis of no association between the t 's and the a 's – that is, no association between the numbers of epithelial cells and the CT density of the local tissue – the expected value of the t 's is simply proportional to the related a 's, so that, for example, the expected value of t_H is $(t_L + t_M + t_H) \times a_H / (a_L + a_M + a_H)$. Similarly, on the null hypothesis of no association between MIB1 positivity as a proportion of epithelial cells and the CT density of the local tissue, the expected value of the n 's is simply proportional to the related t 's, so that, for example, the expected value of n_H is $(n_L + n_M + n_H) \times t_H / (t_L + t_M + t_H)$. We analyzed these data with standard statistical software as implemented in the STATA statistical software package (procedure cs; Stata Corporation, Austin, TX, USA); the ratios of epithelial concentration (cells per unit area) and the ratios of proportions of epithelial cells staining positive for MIB1 are the measures of effect. All statistical significance levels (p values) quoted are two-sided.

Results

The 12 subjects included in the analysis were aged 18 to 60 years with a median age of 33 years; only one subject was aged 50 years or older.

Areas of the slides of low CT density comprised on average 44% of the total of areas of low plus medium plus high CT density ($a_L / (a_L + a_M + a_H)$), whereas areas of high CT density comprised on average 35% of the total area ($a_H / (a_L + a_M + a_H)$).

Table 1 shows the summary relative concentrations (RCs; ratios of cells per unit area) of epithelial cells in the three areas defined by CT density separately for TDLU cells and for ductal cells. The concentration of TDLU epithelial cells is slightly greater in the areas of medium CT density than in the areas of low CT density (RC = 1.4, 95% confidence interval (CI) 1.2 to 1.6; $p < 0.001$) but is much greater in the areas of high CT density (RC = 12.3, 95% CI 10.8 to 13.8; $p < 0.001$). The TDLU results for the individual slides (women) comparing areas of high CT density with areas of low CT density are shown in Figure 2. Although the results from individual subjects do differ somewhat, the RCs were not correlated with age (the only variable available on these women) and the summary RC seems to be a fair representation of the overall results. The results for ducts were similar.

Table 2 shows the summary relative mitotic rates (RMRs) of epithelial cells staining MIB1 positive in the three areas defined by CT density separately for TDLU cells and for ductal

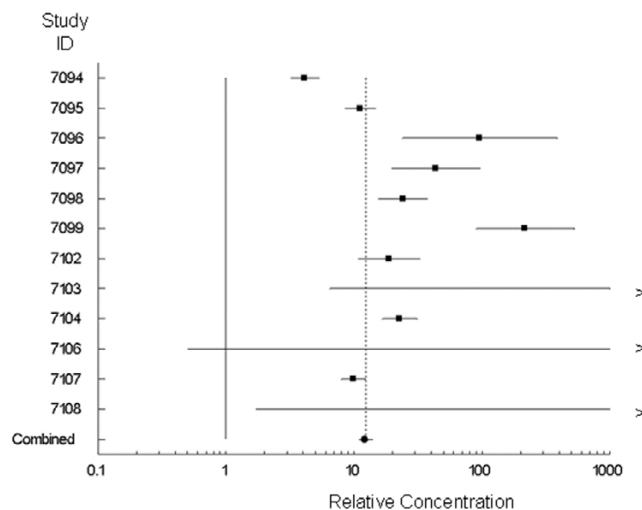
Table 2

Relation between relative mitotic rate (MIB1 positive) of epithelial cells and connective tissue density

CT density	RMR	95% CI	p
TDLUs			
Low	1.00		
Medium	0.58	0.48–0.70	<0.001
High	0.59	0.53–0.66	<0.001
Ducts			
Low	1.00		
Medium	0.66	0.44–0.97	0.035
High	0.65	0.53–0.79	<0.001

CI, confidence interval; CT, connective tissue; RMR, relative mitotic rate; TDLUs, terminal duct lobular units.

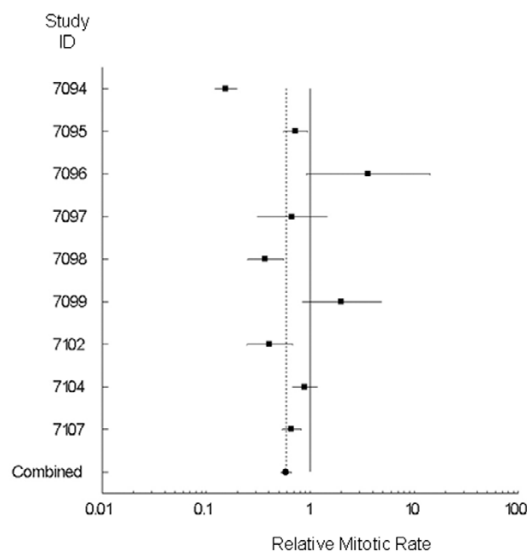
Figure 2



RCs (with 95% CIs) of TDLU epithelial cells in high and low CT areas.

cells. The proportion of TDLU epithelial cells staining MIB1 positive is statistically significantly less (RMR \approx 0.6) both in the areas of medium CT density ($p < 0.001$) and in the areas of high CT density ($p < 0.001$) than in the areas of low CT density. The median MIB1-positive proportion was about 4%. Almost all the women in this study were premenopausal on the basis of their age; this figure is close to the Ki67 figure of 4.5% given for healthy premenopausal women in the study of Hargreaves and colleagues [11]. The TDLU results for the individual slides (women) comparing areas of high CT density with areas of low CT density are shown in Figure 3. Again, although the results from individual subjects do differ somewhat, the RMRs were not correlated with age (the only variable available on these women) and the summary RMR seems to be a fair representation of the overall results. The results for ducts were again similar. There was no difference in the proliferation rates of epithelial cells in TDLUs and ducts within the same CT den-

Figure 3



RMRs (with 95% CIs) of TDLU epithelial cells in high and low CT areas.

density area of individual women (RMR = 1.01, 95% CI 0.98 to 1.04; $p = 0.42$).

More details of the results are provided in the Additional file.

Discussion

Mammographic density is a very strong risk factor for breast cancer. The two groups of investigators [5,6] that studied random biopsies (single slides) from women with different mammographic densities found that the extent of mammographic densities was most strongly correlated with the amount of collagen on the slide. A weaker correlation was found with the amount of epithelial tissue. The findings reported here suggest that the relation between the extent of mammographic density and the amount of epithelial tissue is directly related to the increased concentration of collagen (the main component of

'connective tissue' as shown by collagen staining; see Figure 1) in women with high mammographic densities, because breast epithelium is overwhelmingly confined to areas of high CT density. In the earlier studies of random biopsies [5,6] the weaker relationship between mammographic density and epithelium concentration than between mammographic density and collagen concentration could be simply due to the much greater statistical variability of epithelial tissue in a random slide than one would see for collagen, which occupies a much greater extent of the slide. These results suggest that the increasing breast cancer risk associated with increasing mammographic density might be simply a reflection of more breast epithelial tissue.

We found that the proliferation rate of epithelial cells in areas of high CT density was much lower than in areas of low CT density, arguing against the possibility that dense stroma has a growth factor role in the increased breast cancer risk of women with mammographically dense breasts. In the study of Stomper and colleagues [8], comparison was made between single biopsies of either fat or dense areas in different women; they found no difference in the proliferation rates in the dense and fat areas. Further work is warranted but there is clearly no evidence that areas of high CT density are associated with increased proliferation.

Our results were obtained by conducting a comprehensive count of all the cells in each slide per subject (instead of counting a selected region) and allowed the comparison of proliferation rates in areas of differing CT density within an individual. This permitted us to control completely automatically for factors such as age, menopausal status, or time in the menstrual cycle in the analysis. This gave us great statistical power so that highly statistically significant results could be obtained even with small numbers of subjects.

This study used tissue obtained at reduction mammoplasty performed on women with large breasts. We do not believe that this affects the validity of our findings because the tissue samples were taken deep in the breast away from the subcutaneous fat, but this requires confirmation in future studies. Further studies are also needed relating the CT densities to such risk factors as parity and to understand the biology of the relationship between CT densities and breast epithelium.

Conclusion

The basis of the strong relationship between mammographic density and breast cancer risk may be simply that mammographically dense breasts contain more breast epithelial tissue. Why breast epithelial tissue should be associated with CT densities is not known. Does breast epithelium induce densities? Alternatively, can breast epithelium effectively survive only in areas of densities? Understanding the nature of the interaction between dense CT stroma and epithelial tissue should be a major focus of breast cancer research.

Competing interests

The authors declare that they have no competing interests.

Authors' contributions

DH, AHW, CLP and MCP participated in the design of the study. DH supervised the preparation of the slides and analyzed the slides with the ACIS II system. SD performed all the reduction mammoplasties that provided the tissues used in this analysis and consulted on the tissue obtained from reduction mammoplasties. SB consulted on the interpretation of the results and provided insight into the relationship between mammographic densities and tissue characteristics. CLP coordinated the study. MCP supervised the statistical analysis which was carried out by PW. AHW, CLP and MCP conceived of the study. MCP, DH and AHW drafted the manuscript; all authors read and approved the final manuscript.

Additional files

The following Additional files are available online:

Additional File 1

A Word file containing two tables of detailed results from this study.

See <http://www.biomedcentral.com/content/supplementary/bcr1408-S1.doc>

Acknowledgements

This work was supported by a Department of Defense Congressionally Mandated Breast Cancer Program Grant BC 044808, by the USC/Norris Comprehensive Cancer Center Core Grant P30 CA14089, and by generously donated funds from the endowment established by Flora L Thornton for the Chair of Preventive Medicine at the USC/Norris Comprehensive Cancer Center. The funding sources had no role in this report.

References

1. Saftlas AF, Szklo M: **Mammographic parenchymal patterns and breast cancer risk.** *Epidemiol Rev* 1987, **9**:146-174.
2. Boyd NF, Lockwood GA, Byng JW, Titchler DL, Yaffe MJ: **Mammographic densities and breast cancer risk.** *Cancer Epidemiol Biomarkers Prev* 1998, **7**:1133-1144.
3. Ursin G, Hovanessian-Larsen L, Parisky YR, Pike MC, Wu AH: **Greatly increased occurrence of breast cancers in areas of mammographically dense tissue.** *Breast Cancer Res* 2005, **7**:R605-R608.
4. Perkins CI, Hotes J, Kohler BA, Howe HL: **Association between breast cancer laterality and tumor location, United States, 1994-1998.** *Cancer Causes Control* 2004, **15**:637-645.
5. Alowami S, Troup S, Al-Haddad S, Kirkpatrick I, Watson PH: **Mammographic density is related to stroma and stromal proteoglycan expression.** *Breast Cancer Res* 2003, **5**:R129-R135.
6. Li T, Sun L, Miller N, Nicklee T, Woo J, Hulse-Smith L, Tsao M-S, Khokha L, Martin L, Boyd N: **The association of measured breast tissue characteristics with mammographic density and other risk factors for breast cancer.** *Cancer Epidemiol Biomarkers Prev* 2005, **14**:343-349.
7. Bartow SA, Pathak DR, Black WC, Key CR, Teaf SR: **The prevalence of benign, atypical and malignant breast lesions in pop-**

- ulations at different risk for breast cancer. *Cancer* 1987, **60**:2751-2760.
8. Stomper PC, Penetrante RB, Edge SB, Arredondo MA, Blumen-son LE, Stewart CC: **Cellular proliferative activity of mammo-graphic normal dense and fatty tissue determined by DNA S phase percentage.** *Breast Cancer Res Treat* 1996, **37**:229-236.
 9. Shi S-R, Cote R, Chaiwun B, Young LL, Shi Y, Hawes D, Chen T, Taylor CR: **Standardization of immunochemistry based on anti-gen retrieval technique for routine formalin-fixed tissue sections.** *Appl Immunohistochem* 1998, **6**:89-96.
 10. Bartow SA, Mettler FA, Black WC, Moskowitz M: **Correlations between radiographic patterns and morphology of the female breast.** *Prog Surg Path* 1982, **4**:263-275.
 11. Hargreaves DF, Potten CS, Harding C, Shaw LE, Morton MS, Rob-erts SA, Howell A, Bundred NJ: **Two-week dietary soy supple-mentation has an estrogenic effect on normal premenopausal breast.** *J Clin Endocrinol Metab* 1999, **84**:4017-4024.

Progesterone and estrogen receptors in pregnant and premenopausal non-pregnant normal human breast

DeShawn Taylor · Celeste Leigh Pearce · Linda Hovanessian-Larsen · Susan Downey · Darcy V. Spicer · Sue Bartow · Malcolm C. Pike · Anna H. Wu · Debra Hawes

Received: 28 April 2008 / Accepted: 16 January 2009 / Published online: 10 February 2009
© Springer Science+Business Media, LLC. 2009

Abstract We report here our studies of nuclear staining for the progesterone and estrogen receptors (PRA, PRB, ER α) and cell proliferation (MIB1) in the breast terminal duct lobular unit epithelium of 26 naturally cycling premenopausal women and 30 pregnant women (median 8.1 weeks gestation). Square root transformations of the PRA, PRB and ER α values, and a logarithmic transformation of the MIB1 values, were made to achieve more normal distributions of the values. PRA expression decreased from a mean of 17.8% of epithelial cells in cycling subjects to 6.2% in pregnant subjects ($P = 0.013$). MIB1 expression increased from 1.7% in cycling subjects to 16.0% in pregnant subjects ($P < 0.001$). PRB and ER α expression was slightly lower in pregnant subjects but the differences were

not statistically significant. Sixteen of the non-pregnant subjects were nulliparous and ten were parous so that we had limited power to detect changes associated with parity. PRA was statistically significantly lower in parous women than in nulliparous women (32.2% in nulliparous women vs. 10.2%; $P = 0.014$). PRB (23.5 vs. 12.9%), ER α (14.4 vs. 8.6%) and MIB1 (2.2 vs. 1.2%) were also lower in parous women, but the differences were not statistically significant. The marked decreases in PRA in pregnancy and in parous women has also been found in the rat. A reduction in PRA expression may be a useful marker of the reduction in risk with pregnancy and may be of use in evaluating the effect of any chemoprevention regimen aimed at mimicking pregnancy. Short-term changes in PRA expression while the chemoprevention is being administered may be a more useful marker.

DeShawn Taylor, Celeste Leigh Pearce, Linda Hovanessian-Larsen, Susan Downey are to be considered joint first authors of this report based on their pivotal contributions to the studies reported here.

D. Taylor
Department of Obstetrics and Gynecology, Keck School of Medicine, University of Southern California, Los Angeles, CA 90033, USA

C. L. Pearce · M. C. Pike · A. H. Wu
Department of Preventive Medicine, Keck School of Medicine, University of Southern California, Los Angeles, CA 90033, USA

L. Hovanessian-Larsen
Department of Radiology, Keck School of Medicine, University of Southern California, Los Angeles, CA 90033, USA

S. Downey
Department of Surgery, Keck School of Medicine, University of Southern California, Los Angeles, CA 90033, USA

D. V. Spicer
Department of Medicine, Keck School of Medicine, University of Southern California, Los Angeles, CA 90033, USA

S. Bartow
Department of Pathology, University of New Mexico, Albuquerque, NM 87131, USA

Present Address:
S. Bartow
107 Stark Mesa, Carbondale, CO 81623, USA

D. Hawes
Department of Pathology, Keck School of Medicine, University of Southern California, Los Angeles, CA 90033, USA

M. C. Pike (✉)
USC/Norris Comprehensive Cancer Center, 1441 Eastlake Avenue, Los Angeles, CA 90033, USA
e-mail: mcpike@usc.edu

Keywords Breast · Estrogen receptor · Progesterone receptor · Parity · Pregnancy

Introduction

The progesterone receptor (PR) is expressed in two isoforms, progesterone receptor A (PRA) and progesterone receptor B (PRB) [1]. Kariagina et al. [2] described the varying expression of these two receptors in the breast epithelium of nulliparous and parous rats at differing ages, and noted that the results differed radically from the results seen in mice [3]. Their major findings in rats were: (a) The percentage of lobular cells expressing PRA (PRA + cells) declined steadily from 6 weeks of age (puberty) to 14 weeks of age in nulliparous rats, was much lower during pregnancy (8–10 days of pregnancy) and only partly recovered after involution. (b) The percentage of PRB + lobular cells was relatively constant from 3 to 14 weeks of age in nulliparous rats, and was not altered during pregnancy or after involution. These authors suggested that, since human and rat mammary glands share many features [4, 5], their finding might be applicable to the human breast. These findings in rats suggested that measuring PRA may be a simple method of distinguishing a parous from a nulliparous breast, which, if substantiated in the human breast, may be most helpful as a relatively easily obtained biomarker of possible success in chemoprevention efforts aimed at achieving the protection associated with an early pregnancy.

There are few data available on PRA and PRB expression in normal human breast tissue. We report here our findings regarding PRA and PRB expression in normal human breast tissue obtained from women undergoing reduction mammoplasties as well as from women immediately after a pregnancy termination (within 10 min of the termination). We also report here our findings for estrogen receptor α (ER α) and cell proliferation in these same breast samples.

Materials and methods

Specimen collection

We retrospectively identified 13 healthy naturally cycling premenopausal women who had undergone a reduction mammoplasty and for whom we could obtain the formalin-fixed paraffin-embedded (FFPE) block of tissue saved from her surgery that had been routinely processed at the University of Southern California Department of Pathology. We also prospectively collected breast tissue (frozen within 30 min of excision) from 8 healthy premenopausal women

who were undergoing reduction mammoplasty and 5 healthy volunteers and processed this tissue in a similar manner. The mammoplasty surgeries were all performed by one of us (SD) either at the University of Southern California medical facilities or at the Pacific SurgiCenter, while the tissue from the volunteers were obtained using ultrasound guided 14-gauge core needle biopsies (LHL). Women who reported current use of hormonal contraception were excluded from the current analyses.

Ultrasound guided 14-gauge core needle breast biopsy tissue was also prospectively collected from 33 women who had undergone a pregnancy termination within the preceding 10 min. Samples of these tissues were processed in a similar manner to that described above, i.e., FFPE in a routine manner at the University of Southern California Department of Pathology. Thirty samples were suitable for analysis.

An in-person interview was conducted with the prospectively recruited mammoplasty subjects, the healthy volunteers and the pregnancy termination subjects, and a telephone interview was conducted with the retrospectively recruited mammoplasty subjects. The interview collected detailed information on reproductive and menstrual factors using a structured questionnaire.

The study protocols were approved by the Institutional Review Board (IRB) of the University of Southern California Keck School of Medicine, and as appropriate, with the IRBs of St. John's Hospital and Health Center (for Pacific SurgiCenter) and of the Department of Defense Congressionally Directed Breast Cancer Research Program. The prospectively collected samples were obtained after the women had signed an informed consent agreeing to participate in this research. The women from whom the retrospectively collected samples were obtained also provided verbal informed consent agreeing to participate in this research.

Immunohistochemistry

Immunohistochemical (IHC) analysis was performed as follows: For all studies, multiple adjacent FFPE sections were cut at 5 μ m, deparaffinized and hydrated. All slides were also subject to antigen retrieval which was performed by heating the slides in 10 mmol/l sodium citrate buffer (pH 6) at 110°C for 30 min in a pressure cooker in a microwave oven [6]. Endogenous peroxidase activity was blocked by incubation in 3% H₂O₂ in phosphate-buffered saline for 10 min, followed by blocking of nonspecific sites with SuperBlock blocking buffer (Pierce, Rockford, IL, USA) for 1 h both at room temperature [7].

For the single marker studies, the sections were incubated for analysis with the following antibodies: PRA, the mouse monoclonal antibody NCL-PGR-312 (Novocastra

Laboratories Ltd, Newcastle upon Tyne, UK) at a concentration of 1:5,000; PRB, the mouse monoclonal antibody NCL-PGR-B (Novocastra Laboratories Ltd, Newcastle upon Tyne, UK) at a concentration of 1:100; ER α , the mouse monoclonal antibody ER Ab-12 (Clone 6F11) (Neomarkers, Kalamazoo, MI, USA) at a concentration of 1:100; and MIB1, a proliferation marker, the mouse monoclonal antihuman Ki67 antibody (Dako Cytomation, Carpinteria, CA, USA) at a concentration of 1:500. After incubation with the primary antibodies, antibody binding was localized with the ABC staining kit from Vector Laboratories (Burlingame, CA, USA) according to the manufacturer's instructions and peroxidase activity was detected using 3,3'-diaminobenzidine substrate solution (DAB; Biocare, Concord, CA, USA). A wash step with phosphate buffer solutions (PBS) for 10 min was carried out between each step of the immunostaining. Slides were counterstained with hematoxylin and mounted in mounting medium for examination.

A selection of the slides were also double-stained to permit luminal-epithelial and myoepithelial tissue to be clearly distinguished and to evaluate the co-expression of different markers. The myoepithelial cells were detected using an antibody for smooth muscle actin (SMA; Dako Cytomation, Carpinteria, CA, USA) at a concentration of 1:4000. SMA is localized in the cytoplasm of the cells and is easily distinguished from nuclear staining; on double-stained slides actin was detected using DAB. Ferengi blue was the second chromogen for both PRA and PRB. In slides that were double-stained for PRA and PRB, PRA was stained with Ferengi Blue (Biocare, Concord, CA, USA) and PRB with DAB. No hematoxylin counterstain was applied to the double-stained slides.

In the single-marker slides, we used the Automated Cellular Imaging System II (ACIS II, Clariant, Aliso Viejo, CA, USA) to assess all terminal duct lobular units (TDLUs) on a single slide or the first 100 target areas containing TDLUs selected systematically from left to right and top to bottom on the slide if there were an excessive number of epithelial cells present. A clear distinction between luminal-epithelial cells and myoepithelial cells in TDLUs is frequently difficult to make on conventionally stained slides. For this reason we counted the total numbers of luminal-epithelial + myoepithelial cells (referred to as epithelial cells) and the percentage of them positive for the relevant marker using the ACIS II which is a cellular imaging system that digitizes the images and permits the user to identify and quantitate relevant areas on a high-resolution computer screen based on color differentiation. The ACIS II software program does not function optimally when both nuclear and cytoplasmic staining is present. Due to some cytoplasmic staining in addition to nuclear positivity found in the ER α slides from the pregnant subjects

we used conventional light microscopy and manual counting methods for assessing the TDLUs in these cases. If scant epithelial tissue was present all epithelial cells were counted, in most cases we randomly identified 300 epithelial cells, in cases with a large amount of epithelium present we counted 500 epithelial cells to avoid sampling bias. The percentage of cells positive was determined by identifying the number of cells with nuclear positivity for the selected marker versus those negative or positive.

In the double-marker slides we used the Nuance FLEXTM spectral imaging system (Cambridge Research & Instrumentation, Inc., Woburn, MA, USA) to assess the co-expression of markers on a single slide.

Statistical analysis

We analyzed these data using standard statistical software (Stata, Stata Corporation, Austin, TX, USA). Differences in expression and tests for trend in expression were tested for significance by standard *t*-tests and regression tests after adjustment for age and ethnicity (African American, Hispanic Whites, non-Hispanic Whites) and after transformation of the variables to achieve more normal distributions of values (square root transformations of PRA, PRB and ER α , and logarithmic transformation of MIB1). The comparison of non-pregnant to pregnant results was also adjusted for prior parity (nulliparous/parous). All statistical significance levels (*P* values) quoted are two sided.

Results

Non-pregnant subjects

The means (and 95% confidence intervals) of the proportion of epithelial cells with positive nuclear staining for PRA, PRB, ER α and MIB1 in non-pregnant subjects subclassified by parity (nulliparous vs. parous) are given in Table 1. The individual values are shown in Fig. 1.

Table 1 Mean (\pm 95% CI) percentages of PRA, PRB, ER α and MIB1 nuclear staining in premenopausal non-pregnant nulliparous and parous subjects

	Nulliparous (<i>N</i> = 16)	Parous (<i>N</i> = 10)	<i>P</i> value
PRA	32.2 (22.6–43.4)	10.2 (3.3–20.9)	0.014
PRB	23.5 (14.6–34.5)	12.9 (4.9–24.7)	0.20
ER α	14.4 (10.4–19.0)	8.6 (4.7–13.6)	0.11
MIB1	2.2 (1.3–3.7)	1.2 (0.6–2.6)	0.26

Comparison of parous and nulliparous subjects with square root transformation of PRA, PRB and ER α values, and logarithmic transformation of MIB1 values, and adjusted for ethnicity and age

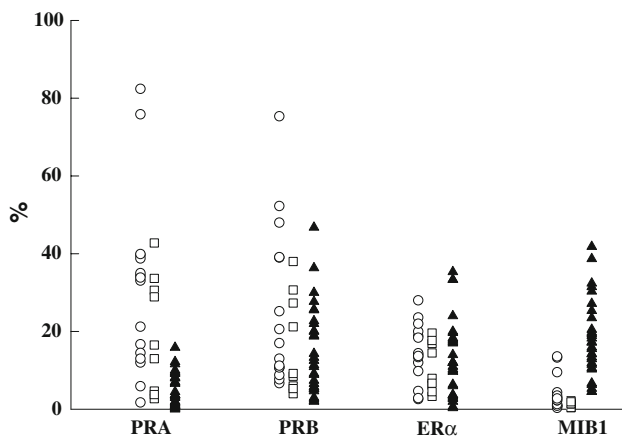


Fig. 1 Percentage of cells expressing nuclear PRA, PRB, ER α and MIB1 in premenopausal nulliparous (○), premenopausal parous (□) and pregnant (▲) women

PRA and PRB

A higher proportion of cells were positive for PRA in nulliparous compared to parous women (mean values: 32.2 vs. 10.2%; $P = 0.014$). There was also a higher proportion of cells positive for PRB in nulliparous compared to parous women (23.5 vs. 12.9%), but this difference was not statistically significant ($P = 0.20$).

PRA was expressed in the luminal epithelium but almost never expressed in the myoepithelium (Fig. 2A). PRB was expressed in both luminal epithelium and myoepithelium (Fig. 2B). The proportion of cells expressing PRB in the luminal epithelium was greater than the proportion expressing PRB in the myoepithelium, although this was difficult to assess completely satisfactorily due to the morphology of the myoepithelial cells which does not permit clear nuclear visualization in many cases.

ER α

A higher proportion of cells were positive for ER α in nulliparous compared to parous women (mean values: 14.4 vs. 8.6%), but this was also not statistically significant ($P = 0.11$). ER α was not expressed in the myoepithelium.

MIB1

A higher proportion of cells were positive for MIB1 in nulliparous women compared to parous women (mean values: 2.2 vs. 1.2%), but this was again not statistically significant ($P = 0.26$).

MIB1 expression was much lower in the myoepithelium than in the luminal epithelium.

We found no evidence that weight affected these results.

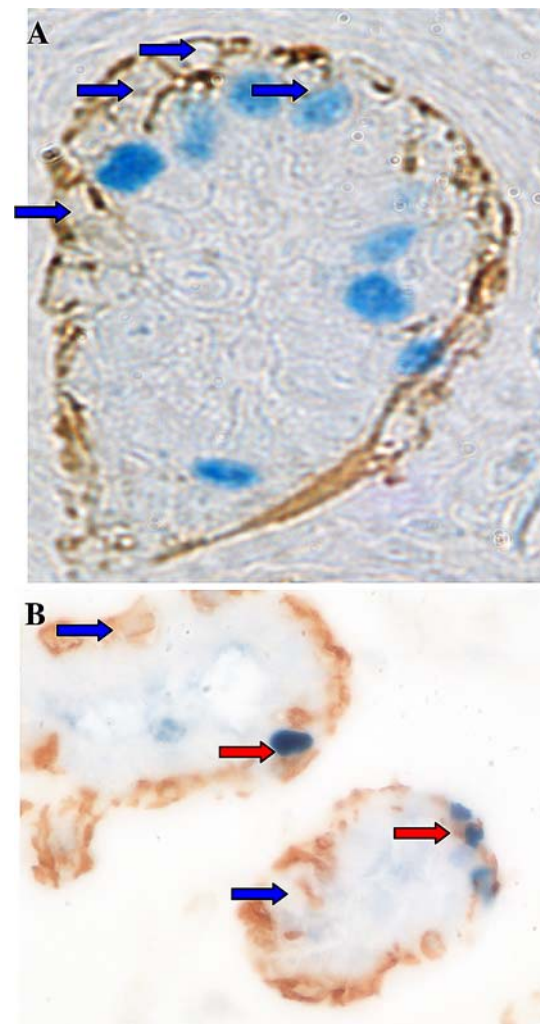


Fig. 2 **A** Double staining for PRA (blue) and SMA (brown) showing myoepithelial cells are negative for PRA (blue arrows). **B** Double staining for PRB (blue) and SMA (brown) showing myoepithelial cells positive (red arrows) and negative (blue arrows) for PRB

Pregnant subjects

The gestational age of the pregnant subjects varied from 5 to 23 weeks (median 8.1 weeks, interquartile range 7.2–12.0 weeks). Results are presented in Table 2.

PRA and PRB

A mean of 6.2% of epithelial cells expressed nuclear PRA. A mean of 14.2% of epithelial cells expressed nuclear PRB. As in the non-pregnant subjects, PRA was almost never expressed in the myoepithelium while PRB was expressed in both luminal epithelium and myoepithelium. In the luminal epithelium almost all cells expressing PRA expressed PRB, but many luminal epithelial cells expressed PRB without expressing PRA (Fig. 3).

Table 2 Mean ($\pm 95\%$ CI) percentages of PRA, PRB, ER α and MIB1 nuclear staining in naturally cycling premenopausal and pregnant subjects

	Non-pregnant ($N = 26$)	Pregnant ($N = 30$)	P value
PRA	17.8 (11.5–25.6)	6.2 (3.1–10.3)	0.013
PRB	17.3 (10.9–25.2)	14.2 (9.1–20.5)	0.57
ER α	12.3 (8.1–17.5)	10.6 (7.1–14.8)	0.63
MIB1	1.7 (1.1–2.6)	16.0 (11.0–23.3)	<0.001

Comparison of pregnant and non-pregnant subjects with square root transformation of PRA, PRB, and ER α values, and logarithmic transformation of MIB1 values; and adjusted for ethnicity, age and prior parity (parous/nulliparous)

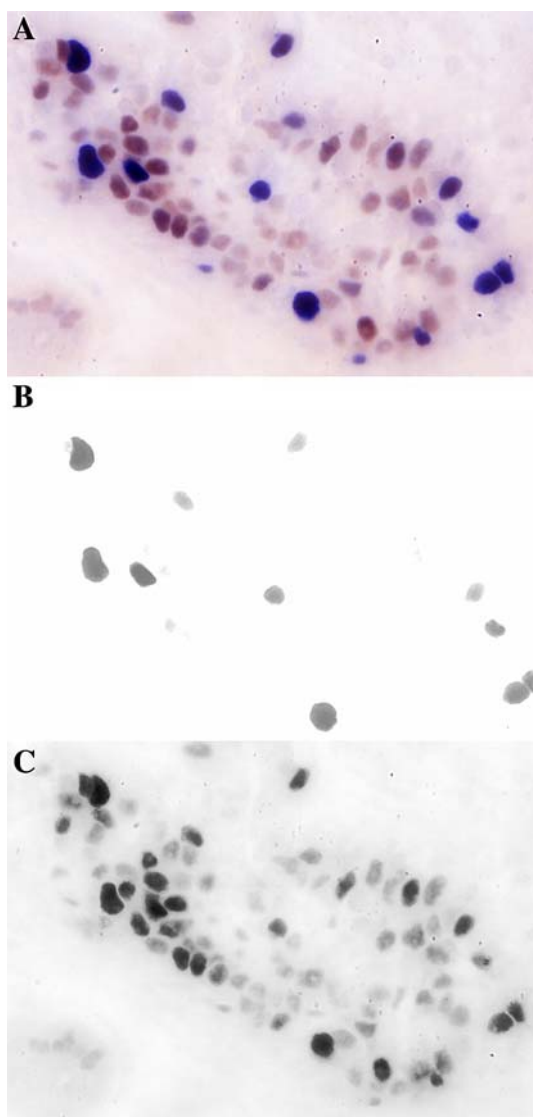


Fig. 3 **A** Composite spectral image showing PRA (blue) and PRB (brown) positive cells in a pregnant subject. **B** PRA positive cells only. **C** PRB positive cells only. There are many PRB positive cells that do not co-express PRA

ER α

A mean of 10.6% of epithelial cells expressed nuclear ER α . As in non-pregnant subjects, ER α was not expressed in the myoepithelium.

MIB1

A mean of 16.0% of epithelial cells expressed nuclear MIB1. As in non-pregnant subjects, MIB1 expression was much lower in the myoepithelium than in the luminal epithelium.

There was statistically significant evidence ($P_{\text{trend}} = 0.043$) of a decline in PRA expression with gestational age; a mean of 8.4% of cells were PRA + at a gestational age of <12 weeks vs. 1.8% at a gestational age of ≥ 12 weeks (Fig. 4). There was also a statistically significant ($P_{\text{trend}} = 0.004$) decline in ER α expression with gestational age; a mean of 13.4% at a gestational age of <12 weeks vs. 4.6% at a gestational age of ≥ 12 weeks (Fig. 4). PRB expression also declined with gestational age, but the effect was smaller and not statistically significant ($P = 0.65$). There was no effect of gestational age on MIB1 expression.

The results for PRA and MIB1 in pregnant women were markedly different from the results in non-pregnant women. PRA expression was much decreased in pregnant women [mean values: 17.8% in non-pregnant subjects vs. 6.2% in pregnant subjects ($P = 0.013$)], and MIB1 was much increased [1.7 vs. 16.0% ($P < 0.001$)].

As can be seen in Fig. 1, the results for PRA, PRB, ER α and MIB1 varied widely between different subjects. The results frequently also varied widely within a single slide; this was due in part to the positive cells tending to cluster within single TDLUs as is illustrated in Fig. 5 for ER α

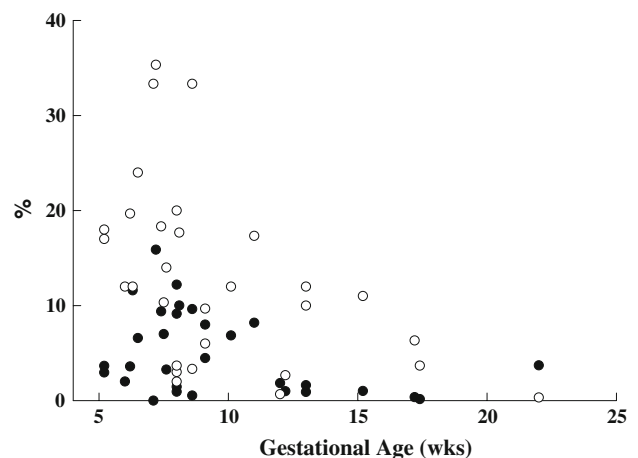


Fig. 4 Nuclear PRA (●) and ER α (○) expression in pregnant women by gestational age

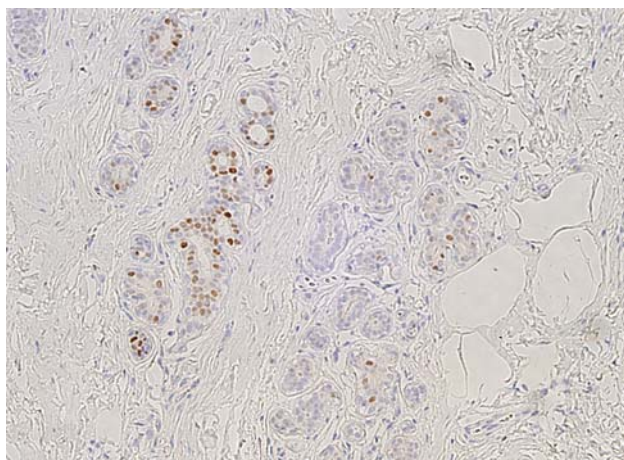


Fig. 5 Number of ER positive cells (*brown nuclei*) can vary significantly between TDLUs as seen in this photomicrograph

in a non-pregnant subject and as has previously been reported [8].

PRA, PRB, ER α and MIB1 were not expressed in the non-pregnant or pregnant breast stromal fibroblasts.

Discussion

In women, a full-term birth at a young age is associated with a long-term significantly reduced risk of breast cancer and induced abortions also provide protection although to a lesser extent [9]. A clear goal for breast cancer chemoprevention efforts is to mimic the protective effect of such early pregnancies. In order to evaluate the effectiveness of any such chemoprevention effort, a biomarker indicative of achieving the desired effect must be identified.

Data from studies in rats show that expression of PRA is substantially decreased during and following pregnancy, suggesting that PRA levels may be such a marker. We have clearly shown a similar reduction in PRA expression in the human breast. PRA expression was decreased from a mean of 32.2% in nulliparous non-pregnant subjects to 6.2% in pregnant subjects, and only rose to 10.2% in parous non-pregnant subjects. PRA expression was decreased early on in pregnancy (<8 weeks gestation, see Fig. 4) and decreased further with increasing gestational age.

There was little or no change in PRB expression in pregnant subjects; this is precisely as seen in the rat [2]. PRB expression was lower in parous subjects but the difference was not statistically significant, and there was no difference in PRB expression between nulliparous and parous rats [2].

PRB was frequently expressed in myoepithelial cells as well as in luminal epithelial cells, whereas PRA expression was almost exclusively confined to luminal epithelial cells.

This effective restriction of PRA to luminal cells, while PRB was expressed in both types of epithelium, was also found in the rat [2]. In the rat, Kariagina et al. [2] found that PRB was more frequently expressed in myoepithelial cells than in luminal cells (~95 vs. ~60% for all epithelial cells). We did not see this. The proportion of cells expressing PRB in the luminal epithelium appeared to be greater than the proportion expressing it in the myoepithelium.

These results differ from the results reported by Mote et al. [10] who found that PRA and PRB were co-expressed at similar levels. Their study was performed on FFPE breast tissue samples from autopsies of premenopausal women obtained some 20 years previously by one of us [11]. We were unsuccessful at staining these autopsy specimens for PRA or PRB.

Overall there was little difference in ER α expression between non-pregnant and pregnant subjects, but the results shown in Fig. 4 strongly suggest that ER α expression is increased early on in pregnancy (<8 weeks gestation) and then declines to lower levels than are seen in non-pregnant subjects. ER α expression was also lower in parous subjects but the difference was again not statistically significant. Although estrogen receptor β , ER β , is present in a high proportion of luminal and myoepithelial cells in the normal human breast, knock-out studies have shown that ER α is the key ER in the breast [12, 13]. ER α is found in the luminal epithelium but not in any other cell type in the breast [14, 15]. Although it has been stated that all cells expressing PR also express ER α [13], this was not seen in the non-pregnant human breast in a number of studies [16–20] that found that PR was expressed more frequently than ER, although the reverse has also been reported [21, 22]. We also found that PRA was much more frequently expressed than ER α . We found some evidence of a decrease in ER α expression in parous women, but this difference was not statistically significant, and was not seen in the study of Battersby et al. [19].

MIB1 expression increased from 1.7% in non-pregnant women to 16.0% in pregnant women. The increase in breast cell proliferation in early pregnancy is, of course, well known [16, 23, 24]. MIB1 expression was also lower in parous subjects but the difference was again not statistically significant. Olsson et al. [25] also found a decrease in MIB1 expression in parous women in a small study, but this was not found in the studies reported by Longacre and Bartow [26], Anderson et al. [27] or Williams et al. [28]. Freudenhake et al. [29] reported lower MIB1 expression in parous women but their results were completely confounded with an age effect. Our finding of lower MIB1 expression in myoepithelium than in luminal epithelium confirms the results reported by Joshi et al. [30].

Epithelial staining for PRA, PRB, ER α and MIB1 were all nuclear in the non-pregnant subjects as has been

previously reported [14, 16, 23, 24]. The same held for PRA, PRB and MIB1 in pregnant subjects, but ER α showed a diffuse cytoplasmic blush in a large proportion of the pregnant subjects along with the nuclear positivity staining. Our finding of no staining of fibroblasts for PR or ER α confirms results from earlier studies [21, 31].

Experiments in mice and observations from human breast tumor studies both suggest that PRA has a deleterious effect on breast tissue [32]. In the mouse, breast development is normal in the absence of PRA, but overexpression of PRA results in a hyperplastic state [33]. Also, in PR-positive breast cancer tissue, the PRA to PRB ratio is increased with two-thirds of the tumors studied showing more PRA and a quarter showing a fourfold increase of PRA [34]. This suggests that an overabundance of PRA is a harmful characteristic and this is in line with parity being associated with a decreased risk of breast cancer and our observation of pregnancy appearing to induce long-term reductions in the expression of PRA.

A reduction in PRA expression may be a useful marker of the reduction in risk with pregnancy. However, the extent of the overlap (Fig. 1) between the results from nulliparous and parous women mean that large numbers of subjects will likely be required if it is to be used to establish such an effect with any chemoprevention regimen aimed at mimicking pregnancy. If before and after treatment samples can be obtained a change may be easier to detect. Short-term changes in PRA expression while the chemoprevention is being administered may be a more useful marker.

Acknowledgments We wish to express our sincerest gratitude to the women who agreed to be part of these studies. We also wish to express our thanks to Ms. Peggy Wan and Ms. A. Rebecca Anderson for extensive help with the management of the study and the statistical analysis. Drs. Christine Clarke and Patricia Mote provided very valuable advice on certain aspects of immunohistochemistry and pointed us to the best antibody for detection of PRB; we are most grateful for this help. This work was supported by a Department of Defense Congressionally Directed Breast Cancer Research Program Grant BC 044808, by the USC/Norris Comprehensive Cancer Center Core Grant P30 CA14089, funds from the endowment established by Flora L. Thornton for the Chair of Preventive Medicine at the Keck School of Medicine of USC and an anonymous donor grant to DT. The funding sources had no role in this report. Disclosure statement: The authors declare that they have nothing to disclose.

References

1. Vegeto E, Shahbaz MM, Wen DX, Goldman ME, O'Malley BW, McDonnell DP (1993) Human progesterone receptor A form is a cell- and promoter-specific repressor of human progesterone receptor B function. *Mol Endocrinol* 7:1244–1255. doi:10.1210/me.7.10.1244
2. Kariagina A, Aupperlee MD, Haslam SZ (2007) Progesterone receptor isoforms and proliferation in the rat mammary gland during development. *Endocrinology* 148:2723–2736. doi:10.1210/en.2006-1493
3. Aupperlee MD, Smith KT, Kariagina A, Haslam SZ (2005) Progesterone receptor isoforms A and B: temporal and spatial differences in expression during murine mammary gland development. *Endocrinology* 146:3577–3588. doi:10.1210/en.2005-0346
4. Russo J, Russo IH (1996) Experimentally induced mammary tumors in rats. *Breast Cancer Res Treat* 39:7–20. doi:10.1007/BF01806074
5. Russo IH, Russo J (1998) Role of hormones in mammary cancer initiation and progression. *J Mammary Gland Biol Neoplasia* 3:49–61. doi:10.1023/A:1018770218022
6. Taylor CR, Shi SR, Chen C, Young L, Yang C, Cote RJ (1996) Comparative study of antigen retrieval heating methods: microwave, microwave and pressure cooker, autoclave, and steamer. *Biotech Histochem* 71:263–270. doi:10.3109/10520299609117171
7. Kumar SR, Singh J, Xia G, Krasnoperov V, Hassanieh L, Ley EJ, Scheinet J, Kumar NG, Hawes D, Press MF (2006) Receptor tyrosine kinase EphB4 is a survival factor in breast cancer. *Am J Pathol* 169:279–293. doi:10.2353/ajpath.2006.050889
8. Shoker BS, Jarvis C, Sibson DR, Walker C, Sloane JP (1999) Oestrogen receptor expression in the normal and pre-cancerous breast. *J Pathol* 188:237–244. doi:10.1002/(SICI)1096-9896(199907)188:3<237::AID-PATH343>3.0.CO;2-8
9. Collaborative Group on Hormonal Factors in Breast Cancer (2004) Breast cancer and abortion: collaborative reanalysis of data from 53 epidemiological studies, including 83,000 with breast cancer from 16 countries. *Lancet* 363:1007–1016. doi:10.1016/S0140-6736(04)15835-2
10. Mote PA, Bartow S, Tran N, Clarke CL (2002) Loss of coordinate expression of progesterone receptors A and B is an early event in breast carcinogenesis. *Breast Cancer Res Treat* 72:163–172. doi:10.1023/A:1014820500738
11. Longacre TA, Bartow SA (1986) A correlative morphologic study of human breast and endometrium in the menstrual cycle. *Am J Surg Pathol* 10:382–393. doi:10.1097/0000478-198606000-00003
12. Speirs V, Skliris GP, Burdall SE, Carder PJ (2002) Distinct expression patterns of ER alpha and ER beta in normal human mammary gland. *J Clin Pathol* 55:371–374
13. Couse JF, Korach KS (1999) Estrogen receptor null mice: what have we learned and where will they lead us? *Endocr Rev* 20:358–417. doi:10.1210/er.20.3.358
14. Petersen OW, Hoyer PE, van Deurs B (1987) Frequency and distribution of estrogen receptor-positive cells in normal, non-lactating human breast tissue. *Cancer Res* 47:5748–5751
15. Clarke RB, Howell A, Potten CS, Anderson E (1997) Dissociation between steroid receptor expression and cell proliferation in the human breast. *Cancer Res* 57:4987–4991
16. Bartow SA (1998) Use of the autopsy to study ontogeny and expression of the estrogen receptor gene in human breast. *J Mammary Gland Biol Neoplasia* 3:37–48. doi:10.1023/A:1026641401184
17. Jacquemier JD, Hassoun J, Torrente M, Martin P-M (1990) Distribution of estrogen and progesterone receptors in healthy tissue adjacent to breast lesions at various stages-Immunohistochemical study of 107 cases. *Breast Cancer Res Treat* 15:109–117. doi:10.1007/BF01810783
18. Williams G, Anderson E, Howell A, Watson R, Coyne J, Roberts SA, Potten CS (1991) Oral contraceptive (OCP) use increases proliferation and decreases oestrogen receptor content of epithelial cells in the normal human breast. *Int J Cancer* 48:206–210. doi:10.1002/ijc.2910480209
19. Battersby S, Robertson BJ, Anderson TJ, King RJB, McPherson K (1992) Influence of menstrual cycle, parity and oral contraceptive use on steroid hormone receptors in normal breast. *Br J Cancer* 65:601–607

20. Söderqvist G, von Schoultz B, Tani E, Skoog L (1993) Estrogen and progesterone receptor content in breast epithelial cells from healthy women during the menstrual cycle. *Am J Obstet Gynecol* 168:874–879
21. Russo J, Ao X, Grill C, Russo IH (1999) Pattern of distribution of cells positive for estrogen receptor alpha and progesterone receptor in relation to proliferating cells in the mammary gland. *Breast Cancer Res Treat* 53:217–227. doi:[10.1023/A:1006186719322](https://doi.org/10.1023/A:1006186719322)
22. Lee S, Mohsin SK, Mao S, Hilsenbeck SG, Medina D, Allred DC (2006) Hormones, receptors, and growth in hyperplastic enlarged lobular units: early potential precursors of breast cancer. *Breast Cancer Res* 8:R6. doi:[10.1186/bcr1367](https://doi.org/10.1186/bcr1367)
23. Battersby S, Anderson TJ (1988) Proliferative and secretory activity in the pregnant and lactating human breast. *Virchows Archiv A Pathol Anat* 413:189–196
24. Suzuki R, Atherton AJ, O'Hare MJ, Entwistle A, Lakhani SR, Clarke C (2000) Proliferation and differentiation in the human breast during pregnancy. *Differentiation* 66:106–115. doi:[10.1046/j.1432-0436.2000.660205.x](https://doi.org/10.1046/j.1432-0436.2000.660205.x)
25. Olsson H, Jernström H, Alm P, Kreipe H, Ingvar C, Jönsson PE, Rydén S (1996) Proliferation of the breast epithelium in relation to menstrual cycle phase, hormonal use, and reproductive factors. *Breast Cancer Res Treat* 40:187–196. doi:[10.1007/BF01806214](https://doi.org/10.1007/BF01806214)
26. Longacre TA, Bartow SA (1986) A correlative morphologic study of human breast and endometrium in the menstrual cycle. *Am J Surg Pathol* 10:382–393. doi:[10.1097/00000478-198606000-00003](https://doi.org/10.1097/00000478-198606000-00003)
27. Anderson TJ, Battersby S, King RJB, McPherson K, Going JJ (1989) Oral contraceptive use influences resting breast proliferation. *Hum Pathol* 20:1139–1144. doi:[10.1016/0046-8177\(89\)90049-X](https://doi.org/10.1016/0046-8177(89)90049-X)
28. Williams G, Anderson E, Howell A, Watson R, Coyne J, Roberts SA, Potten CS (1991) Oral contraceptive (OCP) use increases proliferation and decreases oestrogen receptor content of epithelial cells in the normal human breast. *Int J Cancer* 48:206–210. doi:[10.1002/ijc.2910480209](https://doi.org/10.1002/ijc.2910480209)
29. Feuerhake F, Sigg W, Höfter EA, Unterberger P, Welsch U (2003) Cell proliferation, apoptosis, and expression of Bcl-2 and Bax in non-lactating human breast epithelium in relation to the menstrual cycle and reproductive history. *Breast Cancer Res Treat* 77:37–48. doi:[10.1023/A:1021119830269](https://doi.org/10.1023/A:1021119830269)
30. Joshi K, Smith JA, Perusinghe N, Monaghan P (1986) Cell proliferation in the human mammary epithelium. *Am J Pathol* 124:199–206
31. Mote PA, Leary JA, Avery KA, Sandelin K, Chenevix-Trench G, kConfab Investigators, Kirk JA, Clarke CL (2004) Germ-line mutations in BRCA1 or BRCA2 in the normal breast are associated with altered expression of estrogen-responsive proteins and the predominance of progesterone receptor A. *Genes Chromosomes Cancer* 39:236–248. doi:[10.1002/gcc.10321](https://doi.org/10.1002/gcc.10321)
32. Jacobsen BM, Richer JK, Sartorius CA, Horwitz KB (2003) Expression profiling of human breast cancers and gene regulation by progesterone receptors. *J Mammary Gland Biol Neoplasia* 8:257–268. doi:[10.1023/B:JOMG.0000010028.48159.84](https://doi.org/10.1023/B:JOMG.0000010028.48159.84)
33. Shyamala G, Yang X, Silberstein G, Barcellos-Hoff MH, Dale E (1998) Transgenic mice carrying an imbalance in the native ratio of A to B forms of progesterone receptor exhibit developmental abnormalities in mammary glands. *Proc Natl Acad Sci USA* 95:696–701. doi:[10.1073/pnas.95.2.696](https://doi.org/10.1073/pnas.95.2.696)
34. Graham JD, Yeates C, Balleine RL, Harvey SS, Milliken JS, Bilous AM, Clarke CL (1995) Characterization of progesterone receptor A and B expression in human breast cancer. *Cancer Res* 55:5063–5068

Breast epithelial cell proliferation is markedly increased with short-term high levels of endogenous estrogen secondary to controlled ovarian hyperstimulation

Karine Chung · Linda J. Hovanesian-Larsen · Debra Hawes · DeShawn Taylor · Susan Downey · Darcy V. Spicer · Frank Z. Stanczyk · Sherfaraz Patel · A. Rebecca Anderson · Malcolm C. Pike · Anna H. Wu · Celeste Leigh Pearce

Received: 31 October 2011 / Accepted: 1 November 2011
© The Author(s) 2011. This article is published with open access at Springerlink.com

Abstract Oocyte donors have high serum estradiol (E2) levels similar to the serum levels seen in the first trimester of pregnancy. We report in this article our studies comparing cell proliferation, Ki67 (MIB1), and estrogen and progesterone receptor levels (ER α , PRA, and PRB) in the breast terminal duct lobular units of oocyte donors, women in early pregnancy, and in normally cycling women. Breast tissue and blood samples were obtained from 10 oocyte donors, and 30 pregnant women at 5–18 weeks of gestation. Breast tissue samples were also obtained from 26 normally cycling women. In the oocyte donors: peak E2 (mean \sim 15,300 pmol/l) was reached on the day before oocyte (and tissue) donation; peak progesterone (P4; mean 36.3 nmol/l) was reached on the day of donation; Ki67 was positively associated with level of E2, and the mean Ki67 was 7.0% significantly greater than the mean 1.8% of cycling women. In the pregnant women: mean E2 rose

from \sim 2,000 pmol/l at 5 weeks of gestation to \sim 27,000 pmol/l at 18 weeks; mean P4 did not change from \sim 40 nmol/l until around gestational week 11 when it increased to \sim 80 nmol/l; mean Ki67 was 15.4% and did not vary with gestational age or E2. Oocyte donors have greatly increased levels of E2 and of breast-cell proliferation, both comparable in the majority of donors to the levels seen in the first trimester of pregnancy. Whether their short durations of greatly increased E2 levels are associated with any long-term beneficial effects on the breast, as occurring in rodent models, is not known.

Keywords Oocyte donors · Breast epithelium · Estradiol · Pregnancy

Introduction

Estradiol (E2) and progesterone (P4) are critically important in the pathogenesis of breast cancer [1, 2]. Infertility

Drs. Chung, Hovanesian-Larsen, Hawes and Taylor are to be joint first authors of this report based on their pivotal contributions to the studies reported here.

K. Chung · D. Taylor · F. Z. Stanczyk · S. Patel
Department of Obstetrics and Gynecology, Keck School of Medicine, University of Southern California, Los Angeles, CA 90033, USA

L. J. Hovanesian-Larsen
Department of Radiology, Keck School of Medicine, University of Southern California, Los Angeles, CA 90033, USA

D. Hawes
Department of Pathology, Keck School of Medicine, University of Southern California, Los Angeles, CA 90033, USA

S. Downey
Department of Surgery, Keck School of Medicine, University of Southern California, Los Angeles, CA 90033, USA

D. V. Spicer
Department of Medicine, Keck School of Medicine, University of Southern California, Los Angeles, CA 90033, USA

F. Z. Stanczyk · A. R. Anderson · M. C. Pike · A. H. Wu · C. L. Pearce
Department of Preventive Medicine, Keck School of Medicine, University of Southern California, Los Angeles, CA 90033, USA

M. C. Pike (✉)
Department of Epidemiology and Biostatistics, Memorial Sloan-Kettering Cancer Center, 307 E. 63rd Street, New York, NY 10065, USA
e-mail: pikem@mskcc.org

treatments involving controlled ovarian hyperstimulation are known to cause a transient large increase in serum E2 comparable to the levels seen in the first trimester of pregnancy, whereas P4 levels are no greater than those that are seen in the luteal phase of the menstrual cycle [3, 4]. The effects of this short-term high endogenous E2 exposure on normal breast tissue are unknown.

As part of studies of the changes in human breast associated with pregnancy, we have studied breast tissue from naturally cycling nulliparous and parous women and from women immediately after a pregnancy termination [5]. We report here our studies of the epithelium of the breast terminal duct lobular unit (TDLU) at the end of the ovarian stimulation phase in 10 oocyte donors (women having ovarian hyperstimulation to donate oocytes for use by other women). We report on proliferation (Ki67), estrogen receptor α (ER α), and progesterone receptors A and B (PRA and PRB) in these oocyte donors, and compare these results to those obtained from 30 women sampled between 5 and 22 weeks of gestation (weeks since last menstrual period, LMP) [5] and to the results obtained from 26 cycling women.

Materials and methods

All study protocols described here were approved by the Institutional Review Boards (IRBs) of the USC Keck School of Medicine and where appropriate of the Department of Defense Congressionally Directed Breast Cancer Research Program. The prospectively collected samples were obtained after the women had signed an informed consent. The samples obtained retrospectively from the cycling women were used after the women had been contacted and given consent for their samples to be used.

Oocyte donors

Women attending the In vitro Fertilization Clinic at the University of Southern California (USC) to donate oocytes for the use of other women were invited to volunteer for this study. Women who expressed a desire to participate underwent a routine clinical breast examination; no abnormalities were found. The research-related procedures included a menstrual and reproductive history questionnaire, a blood sample on the day of oocyte retrieval and a breast biopsy immediately after the oocyte retrieval or on the day before if necessary.

Subjects underwent standard clinical protocols for ovarian stimulation. Daily subcutaneous injections of follicle stimulating hormone for approximately 10–14 days with regular monitoring of serum E2 and ultrasound measurement of ovarian follicles. When the follicles were

determined to be mature, human chorionic gonadotropin (10,000 IU) was administered by subcutaneous injection and oocytes were retrieved under intravenous sedation by trans-vaginal ultrasound guided needle aspiration approximately 36 h later.

Ultrasound guided 14-gauge core-needle breast biopsy tissue was collected from a region of ultrasonographically normal dense breast tissue in the upper outer quadrant of the breast. Samples of these tissues were formalin fixed paraffin embedded (FFPE) in a routine manner at the USC Department of Pathology.

Pregnant women

The recruitment of pregnant women has been described previously [5]. Briefly, the pregnant samples were collected from women who had undergone a pregnancy termination within the preceding 10 min; and the blood and tissue samples were collected and processed in like manner to that described above for oocyte donors.

Normally cycling women

The recruitment of normally cycling women has also been described previously [5]. Briefly, the samples from cycling women were obtained from women undergoing a reduction mammoplasty; some of these samples were collected prospectively and others from FFPE tissue blocks, that had been routinely processed at the USC Department of Pathology. These were much larger tissue samples than are obtained at core-needle biopsy but were processed in like manner. No blood samples were obtained at the time of surgery from the retrospectively identified women and hormone values are not reported on here for the cycling women.

Immunohistochemistry

Immunohistochemical (IHC) analysis of the FFPE samples was performed as follows: Multiple adjacent FFPE sections were cut at 5 μ m, deparaffinized and hydrated. All slides were subject to antigen retrieval which was performed by heating the slides in 10 mmol/l sodium citrate buffer (pH 6) at 110°C for 30 min in a pressure cooker in a microwave oven. Endogenous peroxidase activity was blocked by incubation in 3% H₂O₂ for 20 min, followed by blocking of nonspecific sites with SuperBlock blocking buffer (Pierce, Rockford, IL, USA) for 1 h both at room temperature (see [5]).

The sections were incubated with the following antibodies: MIB1, a proliferation marker, the mouse monoclonal antihuman Ki67 antibody (Dako Cytomation, Carpinteria, CA, USA) at a concentration of 1:500; PRA,

the mouse monoclonal antibody NCL-PGR-312 (Novocastra Laboratories Ltd, Newcastle upon Tyne, UK) at a concentration of 1:5,000; PRB, the mouse monoclonal antibody NCL-PGR-B (Novocastra Laboratories Ltd, Newcastle upon Tyne, UK) at a concentration of 1:100; and ER α , the mouse monoclonal antibody ER Ab-12 (Clone 6F11) (Neomarkers, Kalamazoo, MI, USA) at a concentration of 1:100. After incubation with the primary antibodies, antibody binding was localized with the secondary antibody for 45 min and then with the ABC staining kit from Vector Laboratories (Burlingame, CA, USA) according to the manufacturer's instructions, and peroxidase activity was detected using 3,3'-diaminobenzidine substrate solution (DAB; Biocare, Concord, CA, USA). A wash step with phosphate buffer solution (PBS) for 10 min was carried out between each step of the immunostaining. Slides were counterstained with hematoxylin and mounted in mounting medium for examination.

We generally assessed all TDLUs on a single slide. A clear distinction between luminal-epithelial cells and myoepithelial cells in TDLUs is frequently difficult to make on conventionally stained slides. For this reason we counted the total numbers of luminal-epithelial + myoepithelial cells (epithelial cells) and the percentage of them positive for the relevant marker using the Automated Cellular Imaging System II (ACIS II, Clariant, Aliso Viejo, CA, USA), which digitizes the images and permits the user to identify and quantitate relevant areas on a high-resolution computer screen based on color differentiation. The ACIS II software program does not function optimally when both nuclear and cytoplasmic staining is present. Due to some background cytoplasmic staining in addition to nuclear positivity found in the ER α slides from the pregnant subjects, we used conventional light microscopy and manual counting for assessing the TDLUs in these cases; we counted 500 epithelial cells except in a few cases with scant epithelial tissue. Only nuclear staining was regarded as positive staining.

Blood specimens

The blood specimens obtained during oocyte stimulation and at breast biopsy were processed in a standard manner and the serum frozen at -20°C . E2 and P4 were quantified by specific radioimmunoassay as described previously [6, 7]. SHBG was measured by a chemiluminescent immunoassay on the Immulite Analyzer (Siemens Medical Solutions Diagnostics, Malvern, PA, USA). The coefficients of variation for E2, P4 and SHBG were 14.7, 7.8, and 3.7%, respectively. No serum results were given in our previous publication on pregnant and naturally cycling women [5]. Non-SHBG-bound E2 was calculated by the

method of Södergård et al. [8] using the parameters given by Dunn et al. [9].

Statistical analysis

We analyzed these data using the standard statistical package program, Stata 11 (Stata Corporation, College Station, TX, USA). Differences in expression and tests for trend in expression were tested for significance by standard *t* tests and regression tests after transformation of the variables to achieve more normal distributions of values (square root transformations of ER α , PRA, and PRB; and logarithmic transformation of MIB1) [5]. E2, P4, and SHBG values were logarithmically transformed. Testing for the effects of prior births, age and ethnicity on the results were carried out by inclusion of terms for these in regression analyses. All statistical significance levels (*P* values) quoted are two sided.

Results

We recruited 13 oocyte donors who provided informed consent. One decided to withdraw from the study prior to undergoing the breast biopsy. The remaining 12 completed the study protocol. The biopsies from two of the women had no epithelium in the specimen—these women were excluded from further study. Of the remaining 10, eight had their biopsy on the day of oocyte donation and two on the day before due to their unavailability on the donation day.

Figure 1 shows the E2 and P4 values of the individual subjects in the 7 days before oocyte retrieval. E2 increased steadily in each subject until the day before oocyte retrieval—on the day of retrieval, E2 had fallen from a mean of $\sim 15,300$ to $\sim 6,000$ pmol/l. P4 also increased steadily in each subject; the mean value increased from 1.1 nmol/l at 7 days before oocyte retrieval to 4.1 nmol/l at 2 days before retrieval, and then, after hCG treatment, to 18.0 nmol/l on the day before oocyte retrieval, and to 36.3 nmol/l on the day of retrieval. For comparison, in naturally cycling women, the follicular phase maximum E2 is $\sim 1,100$ pmol/l, the luteal phase maximum E2 is ~ 510 pmol/l, and the luteal phase maximum P4 is ~ 40 nmol/l [10].

Figure 2 shows the relationships of serum E2 and P4 to gestational age in the pregnant women [5]. E2 increased steadily with gestational age, from $\sim 2,000$ pmol/l at 5 weeks to $\sim 27,000$ pmol/l at 18 weeks of gestation. P4 did not change from the mid-luteal peak of ~ 40 nmol/l until around week 11 of gestation, after which it increased to ~ 80 nmol/l.

Figure 3 shows the relation between Ki67 (MIB1) for the oocyte donors plotted against their E2 on the day before

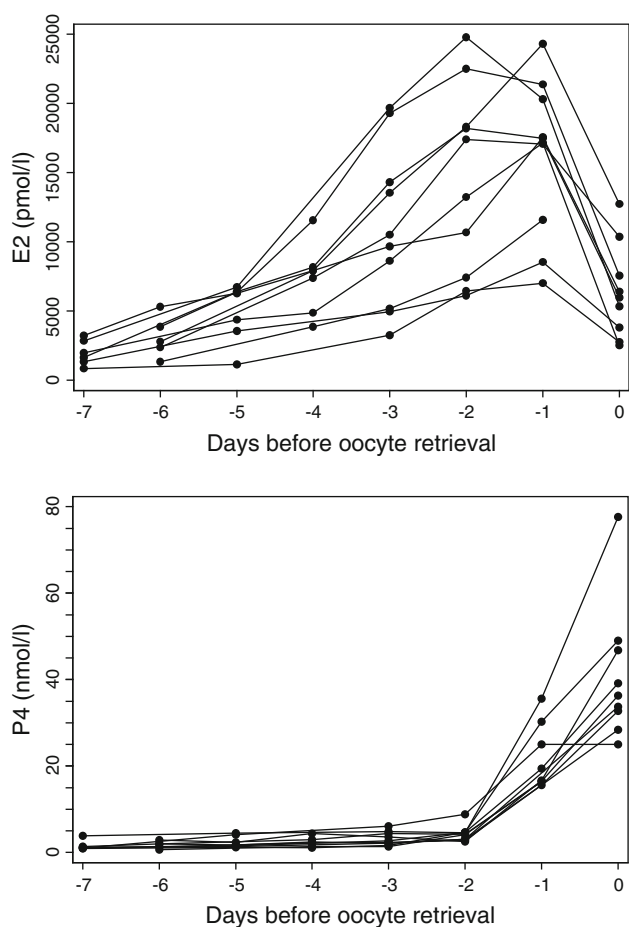


Fig. 1 Individual oocyte donor estradiol (E2) and progesterone (P4) values in the week before oocyte retrieval

biopsy, and for the 30 pregnant women plotted against their E2 on the day of biopsy, while Fig. 4 shows the relation between Ki67 for the 10 oocyte donors and the 30 pregnant women plotted against their P4 on the day of biopsy.

For the oocyte donors, there was a strong positive relationship between Ki67 and E2 on the day before biopsy (see Fig. 3)—correlation, $r = 0.76$ ($P = 0.010$); while the correlation between Ki67 and E2 on the day of biopsy was much weaker— $r = 0.17$ ($P = 0.65$) (data not shown). For the oocyte donors, there was no significant relationship between Ki67 and P4 on the day of biopsy or P4 on the day before biopsy. For the pregnant women, there was no relationship between Ki67 and E2 or P4.

The means (and 95% confidence intervals) of the proportion of epithelial cells with positive nuclear staining for Ki67, ER α , PRA, and PRB are given in Table 1.

The Ki67 mean value was increased from 1.8% in the cycling women to 7.0% in the oocyte donors ($P = 0.003$). The Ki67 mean value in the seven oocyte donors whose serum E2 values on the day before biopsy exceeded 10,000 pmol/l was 14.1%, very close to the mean value of 15.4% seen in the pregnant women.

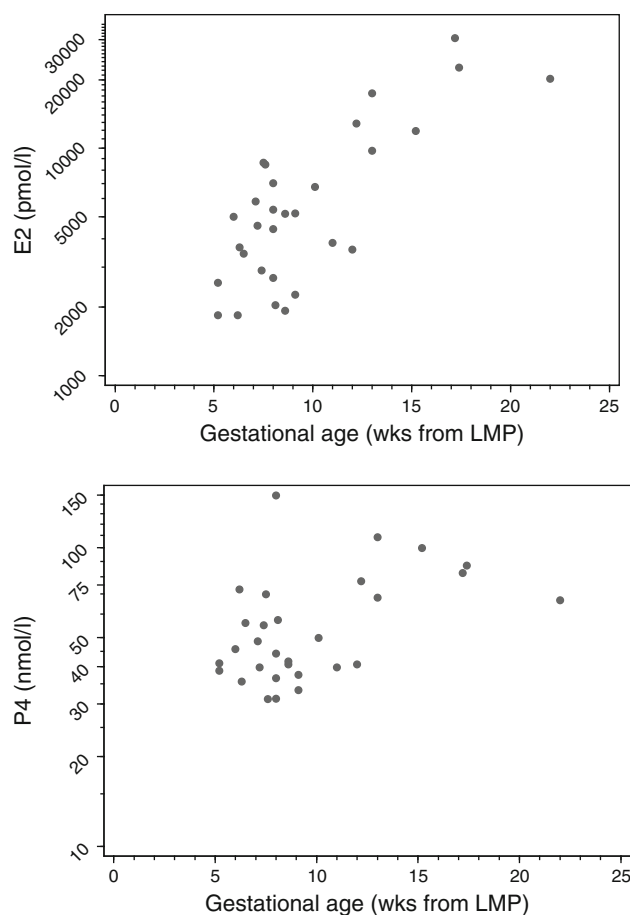


Fig. 2 Individual pregnant woman estradiol (E2) and progesterone (P4) values versus gestational age

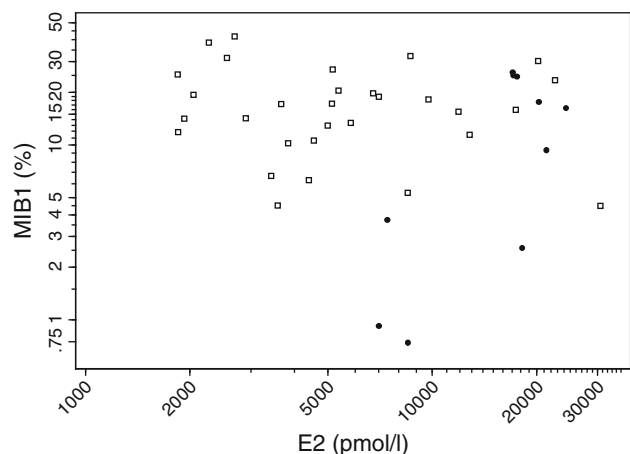


Fig. 3 Individual woman TDLU epithelial cell MIB1 values versus estradiol (E2) values—E2 values for oocyte donors on the day before biopsy (filled circle); E2 values for “pregnant” women on the day of biopsy (open square)

The ER α mean value was lower in oocyte donors (6.8%) than in cycling women (12.0%). The PRA mean value was slightly lower in the oocyte donors (17.8%) than in the cycling women (23.5%), but was not as low as in the

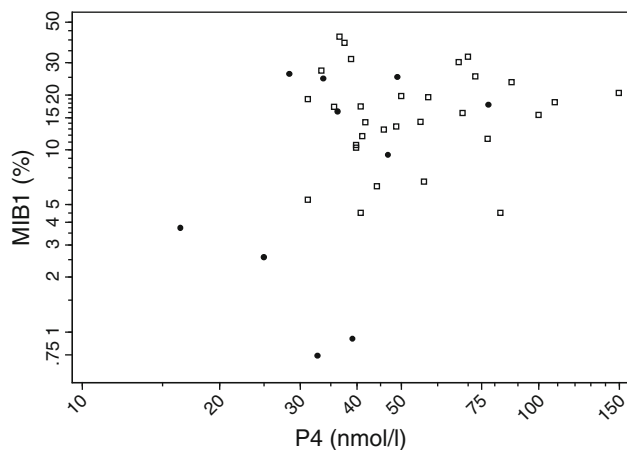


Fig. 4 Individual woman TDLU epithelial cell MIB1 values versus progesterone (P4) values on day of biopsy—oocyte donors (filled circle); “pregnant” women (open square)

Table 1 Mean (with 95% confidence limits) percentages of Ki67, PRA, PRB, and ER α in oocyte donors, pregnant women, and naturally cycling women

Group		Mean ^a	lcl ^a	ucl ^a	P value ^b
Ki67	Oocyte donor (N = 10)	7.0	3.0	16.5	
	Pregnant (N = 30)	15.4	12.4	19.1	0.016
	Cycling (N = 26)	1.8	1.2	2.7	0.003
ER α	Oocyte donor	6.8	4.3	9.9	
	Pregnant	11.0	7.9	14.6	0.15
	Cycling	12.0	9.2	15.2	0.034
PRA	Oocyte donor	17.8	13.4	22.9	
	Pregnant	3.9	2.5	5.5	<0.001
	Cycling	23.5	16.2	32.2	0.37
PRB	Oocyte donor	16.9	11.3	23.6	
	Pregnant	12.8	9.4	16.8	0.31
	Cycling	19.2	13.3	26.0	0.67

^a Calculations were made with transformed values—logarithmic for MIB1, and square root for ER α , PRA, and PRB values. lcl and ucl are lower and upper 95% confidence interval values, respectively

^b P values are for comparisons with oocyte donors

pregnant women (3.9%). The difference between the oocyte donors and the cycling women was not statistically significant. The PRB mean values were similar in all three groups of women.

The results shown in Table 1 are the values as measured without adjustment for the potential confounders of parity, age, or ethnicity. Adjustment for ethnicity and age had little effect on any of the values shown. We previously reported that parous naturally cycling women had significantly lower PRA values than nulliparous naturally cycling women [5], and lower values of Ki67, ER α , and PRB, but the differences for these factors were not statistically significant. Parity had no effect on Ki67, ER α , and PRA in

pregnant women, but the PRB mean was marginally statistically significantly greater in the parous group ($P = 0.049$). Eight of the 10 oocyte donors were nulliparous, so that we had no power to investigate the effects of parity in the oocyte donors. Adjustment for parity made little difference to the comparisons shown in Table 1 and no differences to the statistical significance of the comparisons.

Discussion

This is the first study, to our knowledge, to evaluate the immediate effects of short-term exposure to high levels of endogenous estrogen on the breast epithelium of women. In oocyte donors, the level of breast-cell proliferation was positively associated with their serum E2, and a large increase in breast-cell proliferation, similar to the increase seen in pregnant women, occurred in six of the seven oocyte donors whose serum E2 exceeded 10,000 pmol/l. In contrast, the pregnant women demonstrated the same level of breast-cell proliferation over the whole range of observed serum E2 values from $\sim 1,800$ pmol/l to $\sim 30,000$ pmol/l with no evidence of a dose–response.

When we re-plotted Fig. 3 using non-SHBG-bound E2 rather than E2, a very similar picture was seen. It is unlikely that the contribution of estriol (E3) and estetrol (E4) to the overall estrogenic milieu in pregnant women explains their higher proliferation because these two hormones are at very low levels through gestational week 8 where most of our subjects with E2 concentrations below 10,000 pmol/l lie (Fig. 3 [11–13]). Higher levels of proliferation in pregnant women may be due to their longer exposure to high levels of E2 and to longer exposure to luteal (or higher) levels of P4, it may also be due to their higher ER α expression (see below).

Prolactin is a breast-cell mitogen and prolactin levels increase starting around week 5 of gestation [14]. The proliferation effect of E2 may be enhanced as prolactin has been reported to induce estrogen receptor expression in the breast [15, 16]. Prolactin levels vary greatly during the day with a maximum during sleep and a rapid fall-off on waking. Time of blood draw was not recorded for our study subjects and therefore does not provide useful information on the comparison of prolactin levels in oocyte donors and pregnant women.

We previously reported that PRA decreased steadily with gestational age in pregnant women [5] and although there was already some decrease early on in pregnancy, PRA only reached very low levels ($\sim 1\%$) after week 12 of gestation. There was a non-statistically significant 24% reduction of PRA in oocyte donors compared with naturally cycling women, but this was small relative to the

reduction seen in pregnant women. We also previously reported that “overall there was little difference in ER α expression between non-pregnant and pregnant subjects,” but the data strongly suggested that “ER α expression is increased early on in pregnancy (<8 weeks of gestation) and then declines to lower levels than are seen in non-pregnant subjects.” In contrast, ER α expression in oocyte donors was low.

Based on a strictly limited amount of epidemiological data but considerable data from rodent experiments (see below), it is possible that a short-term pregnancy and short-term relatively high levels of estrogen may provide some long-term protection against breast cancer. However, the fetoplacental unit in pregnant women is responsible for major endocrinologic changes which are not present in women undergoing ovarian stimulation. Thus, a number of factors in a pregnant woman may contribute to long-term protection against breast cancer. The effects of the high levels of endogenous E2 and P4 achieved during human full-term pregnancy are twofold: a transient increase in breast cancer risk and this is followed by a significant long-term permanent decrease in risk if the pregnancy occurs before around age 32, with the protective effect being greater the earlier the age at which the pregnancy occurs [16–21]. The mechanism for the protective effect remains unclear, but has been attributed in part to hormonal changes, in particular, a reduction in prolactin levels [1], and may possibly be due to hormone-induced changes in breast function leading to lower breast-cell proliferation and possibly other effects. Breast-tissue mRNA expression differences between parous and nulliparous rodents have been observed [22, 23], but whether such changes occur in humans has not been satisfactorily established. There is some evidence that terminated pregnancies may also provide some degree of protection against breast cancer [24]. There are no data available on the effects of a terminated pregnancy on long-term prolactin levels, breast-cell proliferation, or any other possibly relevant factors.

Full-term pregnancy-induced protection against mammary carcinogenesis is consistently observed in rats [25–27]. There is again some evidence that terminated pregnancies may also provide protection [26], but this has not been found consistently [27]. The protective effect in the rat can also be achieved by administration of exogenous E2 and P4 [25, 28–30], and two studies have found that with E2 + P4 substantial protection could be achieved with as little as 7–10 days of administration [29, 30].

There are large differences in the effects of pregnancy in women and in the rat: the ovary is the sole source of serum estrogen and the major source of serum progesterone in pregnancy in the rat, while in women, the main source of estrogen and progesterone moves from the ovary to the

placenta during the latter part of the first trimester [31, 32]. The serum E2 levels in pregnant rats only exceed the values seen in cycling rats during the third week of pregnancy, when it approximately doubles [33–37]. In contrast, the levels of serum E2 are greatly increased in pregnant women—they are increased some fivefold in the first trimester, some 20-fold in the second trimester, and some 40-fold in the third trimester [31]. Whether the results in the rat of short-term E2 exposure at only twice the maximum estrus serum E2 level are of any relevance to the human situation is, thus, not at all clear.

The serum P4 levels in cycling rats vary from 45 to 160 nmol/l [34–36]; the levels steadily increase during pregnancy and reach a maximum of 320 nmol/l in the second week, approximately double the maximum seen in the estrus cycle, and then decline in the third week [38, 39]. The levels of serum P4 in cycling women are lower, at 1.5–40 nmol/l, than the levels in the cycling rat [10]. Serum P4 levels in women increase steadily during pregnancy—they are increased some twofold in the first trimester, some fourfold in the second trimester, and some 10-fold in the third trimester compared to the maximum of around 40 nmol/l at the luteal-phase serum P4 peak [31]. The maximum seen during pregnancy in women is thus not greatly increased over the maximum level seen in the rat estrus cycle, and the results in the rat of short-term P4 exposure at the maximum estrus cycle serum P4 level could possibly be of more relevance to the human situation.

If short-term high levels of serum E2 do provide long-term protection against breast cancer, then we might expect that the breast would change in oocyte donors in a way similar to that seen in pregnant women. The short-term high levels of endogenous E2 did cause a dramatic increase in breast-cell proliferation similar to that associated with pregnancy, but the reduction in PRA was much less than that seen in pregnant women. Studies comparing nulliparous oocyte donors at some time after donation to parous women should be informative.

Acknowledgments The authors wish to express their sincerest gratitude to the women who agreed to be part of the studies discussed in this article. The authors also wish to express their thanks to Ms. Peggy Wan for her extensive help with data handling and statistical analysis. This study was supported by the Department of Defense Congressionally Directed Breast Cancer Research Program Grant BC 044808 to MCP, by the USC/Norris Comprehensive Cancer Center Core Grant P30 CA14089, by funds from the endowment established by Flora L. Thornton for the Chair of the Department of Preventive Medicine at the Keck School of Medicine of USC, and funds from an anonymous donor grant to DT.

Disclosures The authors declare that they do not have financial relationships with any of the organizations that sponsored the research, and they do not have any other real or apparent conflict(s) of interest that may have a direct bearing on the subject matter of the article.

Open Access This article is distributed under the terms of the Creative Commons Attribution Noncommercial License which permits any noncommercial use, distribution, and reproduction in any medium, provided the original author(s) and source are credited.

References

- Bernstein L, Ross RK (1993) Endogenous hormones and breast cancer risk. *Epidemiol Rev* 15:48–65
- Pike MC, Wu AH, Spicer DV, Lee S, Pearce CL (2007) Estrogens, progestins, and risk of breast cancer. *Ernst Scher Found Symp Proc* 1:127–150
- Papageorgiou T, Guibert J, Goffinet F, Patrat C, Fulla Y, Janssens Y, Zorn JR (2002) Percentile curves of serum estradiol levels during controlled ovarian stimulation in 905 cycles stimulated with recombinant FSH show that high estradiol is not detrimental to IVF outcome. *Hum Reprod* 17:2846–2850. doi:10.1093/humrep/17.11.2846
- Peña JE, Chang PL, Chan LK, Zeitoun K, Thornton MH 2nd, Sauer MV (2002) Supraphysiological estradiol levels do not affect oocyte and embryo quality in oocyte donation cycles. *Hum Reprod* 17:83–87. doi:10.1093/humrep/17.1.83
- Taylor D, Pearce CL, Hovanessian-Larsen L, Downey S, Spicer DV, Bartow S, Pike MC, Wu AH, Hawes D (2009) Progesterone and estrogen receptors in pregnant and pre-menopausal non-pregnant normal human breast. *Breast Cancer Res Treat* 118:161–168. doi:10.1007/s10549-009-0322-4
- Probst-Hensch NM, Ingles SA, Diep AT, Haile RW, Stanczyk FZ, Kolonel LN, Henderson BE (1999) Aromatase and breast cancer susceptibility. *Endocr Relat Cancer* 6:165–173. doi:10.1677/erc.0.0060165
- Scott JZ, Stanczyk FZ, Goebelsmann U, Mishell DR (1978) A double-antibody radioimmunoassay for serum progesterone using progesterone-3-(0-carboxymethyl) oximino-[125I]-iodo-histamine as radioligand. *Steroids* 31:393–405
- Södergård R, Bäckström T, Shanbhag V, Carstensen H (1982) Calculation of free and bound fractions of testosterone and estradiol-17 beta to human plasma proteins at body temperature. *J Steroid Biochem* 16:801–810. doi:10.1016/0022-4731(82)90038-3
- Dunn JF, Nisula BC, Rodbard D (1981) Transport of steroid hormones: binding of 21 endogenous steroids to both testosterone-binding globulin and corticosteroid-binding globulin in human plasma. *J Clin Endocrinol Metab* 53:58–68. doi:10.1210/jcem-53-1-58
- Goebelsmann U, Mishell DR (1979) The menstrual cycle. In: Mishell DR, Davajan V (eds) *Reproductive endocrinology, infertility and contraception*. FA Davis, Philadelphia, pp 67–89
- Lobo RA (1997) Endocrinology of pregnancy. In: Lobo RA, Mishell DR, Paulson RJ, Shoupe D (eds) *Mishell's textbook of infertility, contraception, and reproductive endocrinology*, 4th edn. Blackwell Science, Malden, pp 183–206
- Levitz M, Young BK (1977) Estrogens in pregnancy. *Vitam Horm* 35:109–147
- Goebelsmann U (1979) Protein and steroid hormones in pregnancy. *J Reprod Med* 23:166–177
- Barberia JM, Abu-Fadl S, Kletzky OA, Nakamura RM, Mishell DR (1975) Serum prolactin patterns in early gestation. *Am J Obstet Gynecol* 121:1107–1110
- Das R, Vonderhaar BK (1997) Prolactin as a mitogen in mammary cells. *J Mammary Gland Biol Neoplasia* 2:29–39
- Gutzman JH, Miller KK, Schuler LA (2004) Endogenous human prolactin and not exogenous human prolactin induces estrogen receptor alpha and prolactin receptor expression and increases estrogen responsiveness in breast cancer cells. *J Steroid Biochem Mol Biol* 88:69–77. doi:10.1016/j.jsbmb.2003.10.008
- Trichopoulos D, Hsieh CC, MacMahon B, Lin TM, Lowe CR, Mirra AP, Ravnihar B, Salber EJ, Valaoras VG, Yuasa S (1983) Age at any birth and breast cancer risk. *Int J Cancer* 31:701–704. doi:10.1002/ijc.2910310604
- Pike MC, Krailo MD, Henderson BE, Casagrande JT, Hoel DG (1983) 'Hormonal' risk factors, 'breast tissue age' and the age-incidence of breast cancer. *Nature* 303:767–770. doi:10.1038/303767a0
- Wohlfahrt J, Melbye M (2001) Age at any birth is associated with breast cancer risk. *Epidemiology* 12:68–73
- Albrektsen G, Heuch I, Hansen S, Kvale G (2005) Breast cancer risk by age at birth, time since birth and time intervals between births: exploring interaction effects. *Br J Cancer* 92:167–175. doi:10.1038/sj.bjc.6602302
- Schedin P (2006) Pregnancy-associated breast cancer and metastasis. *Nat Rev Cancer* 9:281–291. doi:10.1038/nrc1839
- Ginger MR, Gonzalez-Rimbua MF, Gay JP, Rosen JM (2001) Persistent changes in gene expression induced by estrogen and progesterone in the rat mammary gland. *Mol Endocrinol* 15:1993–2009. doi:10.1210/me.15.11.1993
- Blakely CM, Stoddard AJ, Belka GK, Dugan KD, Notarfrancesco KL, Moody SE, D'Cruz CM, Chodosh LA (2006) Hormone-induced protection against mammary tumorigenesis is conserved in multiple rat strains and identifies a core gene expression signature induced by pregnancy. *Cancer Res* 66:6421–6431; erratum in 2007; 67:844–846. doi:10.1158/0008-5472.CAN-05-4235
- Collaborative Group on Hormonal Factors in Breast Cancer (2004) Breast cancer and abortion: collaborative reanalysis of data from 53 epidemiological studies, including 83,000 with breast cancer from 16 countries. *Lancet* 363:1007–1016. doi:10.1016/S0140-6736(04)15835-2
- Medina D (2004) Breast cancer: the protective effect of pregnancy. *Clin Cancer Res* 10:380S–384S
- Sinha DK, Pazik JE, Dao TL (1988) Prevention of mammary carcinogenesis in rats by pregnancy: effect of full-term and interrupted pregnancy. *Br J Cancer* 57:390–394
- Russo J, Russo IH (1980) Susceptibility of the mammary gland to carcinogenesis: II. Pregnancy interruption as a risk factor in tumor incidence. *Am J Pathol* 100:497–512
- Grubbs CJ, Farnell DR, Hill DL, McDonough KC (1985) Chemoprevention of *N*-nitroso-*N*-methylurea-induced mammary cancers by pretreatment with 17 β -estradiol and progesterone. *J Natl Cancer Inst* 74:927–931
- Guzman RC, Yang J, Rajkumar L, Thordarson G, Chen X, Nandi S (1999) Hormonal prevention of breast cancer: mimicking the protective effect of pregnancy. *Proc Natl Acad Sci USA* 96:2520–2525. doi:10.1073/pnas.96.5.2520
- Medina D, Peterson LE, Moraes R, Gay J (2001) Short-term exposure to estrogen and progesterone induces partial protection against *N*-nitroso-*N*-methylurea-induced mammary tumorigenesis in Wistar-Furth rats. *Cancer Lett* 169:1–6. doi:10.1016/S0304-3835(01)00507-9
- O'Leary P, Boyne P, Flett P, Beilby J, James I (1991) Longitudinal assessment of changes in reproductive hormones during normal pregnancy. *Clin Chem* 37:667–672
- Numan M (1994) Maternal behavior. In: Knobil E, Neill JD (eds) *The physiology of reproduction*. Raven Press, New York, pp 221–302
- Kalra PS, Kalra SP (1977) Temporal changes in the hypothalamic and serum luteinizing hormone-releasing hormone (LH-RH) levels and the circulating ovarian steroids during the rat oestrous cycle. *Acta Endocrinol* 85:449–455
- Nequin LG, Alvarez J, Schwartz NB (1979) Measurement of serum steroid and gonadotropin levels and uterine and ovarian

- variables throughout the 4 day and 5 day estrous cycles in the rat. *Biol Reprod* 20:659–670
35. Haim S (2003) Serum levels of sex hormones and corticosterone throughout 4- and 5-day estrous cycles in Fischer 344 rats and their simulation in ovariectomized females. *J Endocrinol Invest* 26:1013–1022
36. Strange R, Westerlind KC, Ziemiecki A, Andres A-C (2007) Proliferation and apoptosis in mammary epithelium during the rat oestrus cycle. *Acta Physiol* 190:137–149. doi:[10.1111/j.1748-1716.2007.01704.x](https://doi.org/10.1111/j.1748-1716.2007.01704.x)
37. Guzman RC, Rajkumar L, Thordarson G, Nandi S (2005) Pregnancy levels of estrogen prevents mammary cancers. In: Li JJ, Li SA, Llombart-Bosch A (eds) *Hormonal carcinogenesis IV*. Springer, New York, pp 427–430
38. Sanyal MK (1978) Secretion of progesterone during gestation in the rat. *J Endocrinol* 79:179–190. doi:[10.1677/joe.0.0790179](https://doi.org/10.1677/joe.0.0790179)
39. Macdonald GJ, Matt DW (1984) Adrenal and placental steroid secretion during pregnancy in the rat. *Endocrinology* 114:2068–2073. doi:[10.1210/endo-114-6-2068](https://doi.org/10.1210/endo-114-6-2068)

Original research article

Lowering oral contraceptive norethindrone dose increases estrogen and progesterone receptor levels with no reduction in proliferation of breast epithelium: a randomized trial^{☆,☆☆,★,★★}

Linda Hovanessian-Larsen^{a,1}, DeShawn Taylor^{b,1}, Debra Hawes^{c,1}, Darcy V. Spicer^d,
Michael F. Press^c, Anna H. Wu^e, Malcolm C. Pike^{e,f,*}, C. Leigh Pearce^e

^aDepartment of Radiology, Keck School of Medicine, University of Southern California, Los Angeles, CA 90033, USA

^bDepartment of Obstetrics and Gynecology, Keck School of Medicine, University of Southern California, Los Angeles, CA 90033, USA

^cDepartment of Pathology, Keck School of Medicine, University of Southern California, Los Angeles, CA 90033, USA

^dDepartment of Medicine, Keck School of Medicine, University of Southern California, Los Angeles, CA 90033, USA

^eDepartment of Preventive Medicine, Keck School of Medicine, University of Southern California, Los Angeles, CA 90033, USA

^fDepartment of Epidemiology and Biostatistics, Memorial Sloan-Kettering Cancer Center, New York, NY 10065, USA

Received 10 October 2011; revised 22 December 2011; accepted 27 December 2011

Abstract

Background: This study was conducted to compare breast epithelial-cell proliferation and estrogen and progesterone receptor levels in women taking one of two oral contraceptives (OCs) containing the same dose of estrogen but different doses of the progestin norethindrone (NET). **Study Design:** Thirty-three women were randomly assigned 1:1 to one of two OCs with 35-mcg ethinylestradiol (EE2) but different doses of NET — 1 or 0.4 mg. At the end of the active pill phase of the third OC cycle, a breast biopsy was performed and the percentages of epithelial cells of the terminal duct lobular units were measured for Ki67 (MIB1), progesterone receptors A and B (PRA and PRB, respectively), and estrogen receptor α (ER α).

Results: The biopsies from 27 women had sufficient epithelium for analysis. The percentages of cells positive for PRA, PRB and ER α were approximately double with the lower progestin dose (PRA: $p=.041$; PRB: $p=.030$; ER α : $p=.056$). The Ki67 percentage was not reduced with the lower progestin dose (12.5% for 0.4-mg NET vs. 7.8% for 1.0-mg NET).

Conclusions: The increase in PRA-, PRB- and ER α -positive cells with the 60% lower progestin dose OC appears likely to account for its failure to decrease breast-cell proliferation. This breast-cell proliferation result is contrary to that predicted from the results of lowering the medroxyprogesterone acetate dose in menopausal hormone therapy.

© 2012 Elsevier Inc. All rights reserved.

Keywords: Breast epithelial cells; Combined oral contraceptives; Estrogen receptor; Progesterone receptor; Progestin dose; Proliferation markers

[☆] Authorship: DT, DVS, MCP, AHW and CLP participated in the design of the study. DH supervised the preparation of the slides and analyzed the slides with the ACIS II system. DH, DVS and MFP consulted on the interpretation of issues arising in the IHC analysis. MFP performed the review of the biopsy material to ensure that there was no evidence of any abnormalities requiring further clinical evaluation. LHL performed all the biopsies that provided the tissues used in this study. CLP coordinated the study. MCP supervised the statistical analysis. DVS, MCP, AHW and CLP conceived of the study. MCP, AHW and CLP drafted the manuscript. All authors critically read the manuscript and approved the final draft.

^{☆☆} Disclosure: The authors declare that they have no competing interests.

[★] Funding: This work was supported by a Department of Defense Congressionally Directed Breast Cancer Research Program Grant BC 044808, by the USC/Norris Comprehensive Cancer Center Core Grant P30 CA14089 and by generously donated funds from the endowment established by Flora L Thornton for the Chair of Preventive Medicine at the USC/Norris Comprehensive Cancer Center. The funding sources had no role in this report.

^{★★} Trial Registration: ClinicalTrials.gov NCT00972439.

* Corresponding author. Department of Epidemiology and Biostatistics, Memorial Sloan-Kettering Cancer Center, 307 East 63rd Street, New York, NY 10065, USA. Tel.: +1 646 735 8139; fax: +1 646 735 0011.

E-mail address: pikem@mskcc.org (M.C. Pike).

¹ Linda Hovanessian-Larsen, DeShawn Taylor and Debra Hawes are to be considered joint first authors of this report based on their pivotal contributions to the study reported here.

1. Introduction

Breast epithelial-cell proliferation is higher in women on menopausal estrogen–progestin therapy (MEPT) than in women on menopausal estrogen therapy (MET) [1], and epidemiological studies have shown that MEPT significantly increases a postmenopausal woman's risk of breast cancer and that the effect is greater than with MET [2,3]. Analysis of the studies of the effects of MEPT on breast cancer risk showed that a lowering of the dose of the progestin, medroxyprogesterone acetate (MPA), from 10 to 2.5 mg significantly reduced the increased breast cancer risk from the MEPT despite extending the number of days the MPA was given from ~10 per 28-day cycle (sequential MEPT) to every day (continuous-combined MEPT) [2].

The large comprehensive meta-analysis conducted by the Collaborative Group on Hormonal Factors in Breast Cancer found that breast cancer risk was slightly increased in current and recent users of oral contraceptives (OCs) [4], but how much of this increase is due to earlier diagnosis because of more frequent contact with the medical system is not completely clear. OCs effectively block ovulation and are thus associated with profoundly reduced levels of serum progesterone. Since the progestin exposure of the breast of a woman on an OC is thus almost solely from the OC progestin, the MEPT results discussed above would predict that the level of progestin in an OC would be positively associated with its effect on breast cancer risk. This was not seen in the Collaborative Groups' analysis, and the results of more recent studies have not been able to provide definitive results on the effect of progestin type or dose either [5–9]. In order to gain an understanding of the biology behind this, we decided that it would likely be informative to study the effect of progestin dose on the breast directly by studying the effects on cell proliferation and steroid receptor levels in breast epithelium of two commonly prescribed Food and Drug Administration (FDA)-approved OCs containing the same dose of estrogen but different doses of the progestin norethindrone (NET): Ortho Novum 1/35[®] contains 35-mcg ethinyl-estradiol (EE2) and 1-mg NET, and Ovcon 35[®] contains the same dose of EE2 (35 mcg) but only 0.4-mg NET, a 60% reduced dose of progestin. A 10-mg dose of MPA is generally considered as approximately equivalent to a 1-mg dose of NET [10], so the doses being considered in these OCs are roughly comparable to the doses of MPA in sequential and continuous-combined EPT.

The results of lowering the progestin dose in MEPT predicted that the 0.4-mg NET OC would be associated with a marked reduction in breast-cell proliferation compared to the 1-mg NET OC.

2. Materials and methods

The study protocol was approved by the Institutional Review Board (IRB) of the University of Southern

California Keck School of Medicine and by the IRB of the Department of Defense Congressionally Directed Breast Cancer Research Program prior to the enrollment of any participants. All participants gave written informed consent and, in particular, were fully informed in detail concerning the potential risks associated with the ultrasound-guided core breast biopsy sample collection (see below).

2.1. Study participants

Women attending clinics at Los Angeles County/University of Southern California Women's and Children's Hospital who were being prescribed an OC solely for contraception were invited to volunteer for this study.

To be eligible for the study, a subject had to be premenopausal aged 18–34 years; currently taking and willing to switch type of OC or wishing to start taking an OC for contraception; a nonsmoker; and willing to refrain from consumption of grapefruit or grapefruit juice during the study (grapefruit interferes with metabolism of exogenously administered OCs) [11]. Subjects with any of the following were ineligible: abnormal breast examination; history or current therapeutic or prophylactic use of anticoagulants; known bleeding disorder or history of unexplained bleeding or bruising; history of breast cancer or previous diagnostic breast biopsy; known allergy to local anesthetic; currently pregnant or pregnant within the previous 6 months; or having any standard contraindication to being prescribed an OC [12].

Women, who expressed a possible desire to participate, were fully informed in detail concerning the potential risks and, in particular, with the risks associated with the ultrasound-guided core breast biopsy procedure. If they continued to express a desire to participate, they were requested to sign an informed consent. After providing written informed consent, the participants underwent a routine clinical breast examination. If there was an abnormal finding on the breast examination, the subject would have been excluded from the study, but no such abnormalities were found. Eligible subjects were administered a menstrual and reproductive history questionnaire, and height and weight were measured. Subjects were provided with three 28-day cycle packs of Ortho Novum 1/35[®] or Ovcon 35[®] with instructions to take the pills each evening. The sequence for the 1:1 treatment allocation was determined using a random-number table constrained by the use of randomly permuted blocks. The brand name was provided to the attending physician in a sealed envelope only to be opened after the subject had been enrolled and had completed the above procedures.

A breast biopsy was performed during the third consecutive OC cycle at the end of the third week of active OC pill use. The radiologist performing the biopsy was blinded to OC type.

2.2. Tissue procurement

An ultrasound-guided 14-gauge core-needle breast biopsy was performed in a region of ultrasonographically normal-

dense breast tissue in the upper-outer quadrant of the breast. After anesthetizing the breast with 1% lidocaine, a 4-mm incision was made to facilitate entry of the biopsy needle. Multiple core biopsy samples were obtained through the same single incision. The biopsy specimens were formalin fixed and paraffin embedded (FFPE) in a routine manner at the University of Southern California Department of Pathology.

2.3. Immunohistochemistry

Immunohistochemical (IHC) analysis of the FFPE samples was performed for Ki67 (MIB1; a proliferation marker), progesterone receptor A (PRA), progesterone receptor B (PRB) and estrogen receptor α (ER α). Multiple adjacent FFPE sections were cut at 5 μ m, deparaffinized and hydrated. All slides were subjected to antigen retrieval which was performed by heating the slides in 10 mmol/L sodium citrate buffer (pH 6) at 110°C for 30 min in a pressure cooker in a microwave oven [13]. Endogenous peroxidase activity was blocked by incubation in 3% H₂O₂ in phosphate-buffered saline for 10 min, followed by blocking of nonspecific sites with SuperBlock blocking buffer (Pierce, Rockford, IL, USA) for 1 h both at room temperature [14].

The sections were incubated for analysis with the following antibodies: MIB1, the mouse monoclonal anti-human Ki67 antibody (Dako Cytomation, Carpinteria, CA, USA) at a concentration of 1:500; PRA, the mouse monoclonal antibody NCL-PGR-312 (Novocastra Laboratories, Newcastle upon Tyne, UK) at a concentration of 1:5000; PRB, the mouse monoclonal antibody NCL-PGR-B (Novocastra Laboratories) at a concentration of 1:100; and ER α , the mouse monoclonal antibody ER Ab-12 (Clone 6FH) (Neomarkers, Kalamazoo, MI, USA) at a concentration of 1:100. After incubation with the primary antibodies, antibody binding was localized with the ABC staining kit from Vector Laboratories (Burlingame, CA, USA) according to the manufacturer's instructions and peroxidase activity was detected using 3,3'-diaminobenzidine substrate solution (DAB; Biocare, Concord, CA, USA). A wash step with phosphate-buffer solution for 10 min was carried out between each step of the immunostaining. Slides were counterstained with hematoxylin and mounted in mounting medium for examination. A clear distinction between luminal-epithelial cells and myoepithelial cells in terminal duct lobular units (TDLUs) is frequently difficult to make on conventionally stained slides. In these IHC studies, we counted the total numbers of luminal-epithelial+myoepithelial cells (together referred to as epithelial cells) and the percentage of them positive for the relevant marker in the TDLUs.

The markers MIB1, PRA, PRB and ER α are all nuclear. For each marker, we used the Automated Cellular Imaging System II (ACIS II; Clariant, Aliso Viejo, CA, USA) to assess all TDLUs on a single slide or the first 100 target areas containing TDLUs selected systematically from left to right and top to bottom on the slide if there were a large number of epithelial cells present. The ACIS II is a cellular imaging

system that digitizes the images and permits the user to identify and quantitate relevant areas on a high-resolution computer screen based on color differentiation. The pathologist conducting the IHC was blinded to OC type.

2.4. Statistical analysis

We analyzed these data using the statistical package program Stata 11 (Stata Corporation, College Station, TX, USA). Differences in expression and tests for trend in expression were tested for significance by standard *t* tests and regression tests after adjustment for age and ethnicity (African American, Hispanic whites, non-Hispanic whites) and after transformation of the variables to achieve more normal distributions of values (logarithmic transformation of MIB1 and square root transformations of PRA, PRB and ER α). All statistical significance levels (*p* values) quoted are two-sided. In this pilot study, we planned on obtaining tissue samples from 30 women, 15 in each of the two OC groups. This sample size afforded us 80% power with a one-sided alpha of 5% to detect a 50% reduction in breast-cell proliferation in the 0.4-mg OC group based on an estimated standard deviation as observed by Anderson et al. [15]. The results in women who had not taken a hormonal contraceptive for at least 10 weeks before starting the study were checked to see whether their results differed from the overall results.

3. Results

Thirty-three women were enrolled in the study with 17 and 16 randomly assigned to Ortho Novum 1/35[®] and Ovcon 35[®], respectively. Fig. 1 shows the flow of participants through the study. All 33 completed the study including contributing a breast-biopsy specimen. Five of the breast-biopsy specimens contained insufficient TDLU epithelial tissue for analysis and one of the remaining women was diagnosed with a follicular cyst on the day of biopsy, leaving 27 evaluable patients — 14 on Ortho Novum 1/35[®] and 13 on Ovcon 35[®]. The means (and 95% confidence intervals) of the proportion of epithelial cells with positive nuclear staining for Ki67, PRA, PRB and ER α for the 27 women are given in Table 1.

The Ki67 mean value increased 60% from 7.8% to 12.5% with the reduction in NET dose from 1.0 to 0.4 mg, although this increase in breast-cell proliferation was not statistically significant (*p*=.27). PRA, PRB and ER α also increased with the reduction in NET dose. PRA and PRB were statistically significantly higher in the lower-dose progestin OC group. The PRA mean value increased 120% from 7.6% in the 1.0-mg NET group to 16.7% in the 0.4-mg NET group (*p*=.041). The PRB mean value increased 98% from 12.0% in the 1.0-mg NET group to 23.7% in the 0.4-mg NET group (*p*=.030). The ER α mean value increased 102% from 9.0% in the 1.0-mg NET group to 18.2% in the 0.4-mg OC group, although this difference was only of borderline statistical significance (*p*=.056).

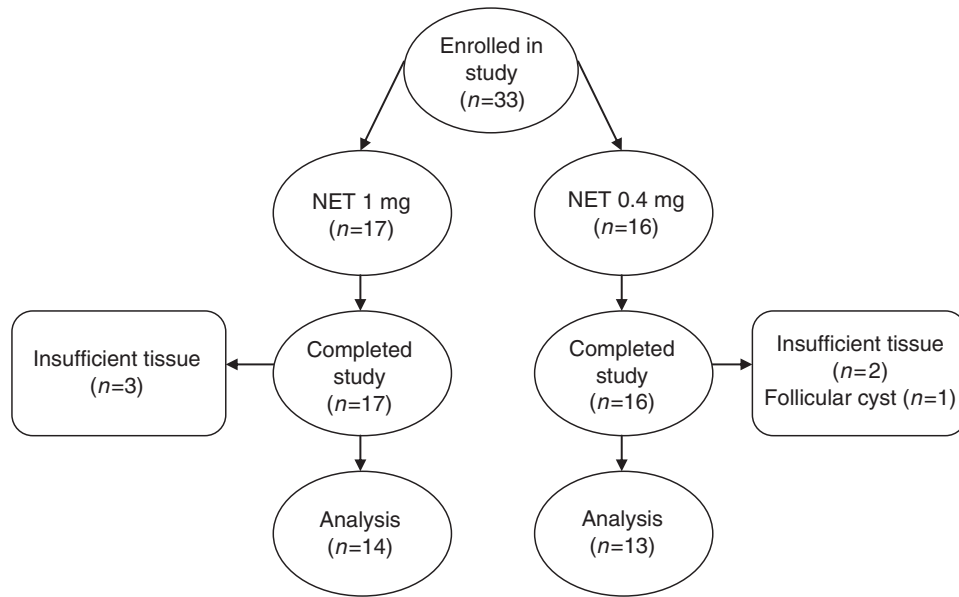


Fig. 1. Flowchart of participants.

The results in the 21 women who had not taken a hormonal contraceptive for at least 10 weeks before starting the study were very similar to the overall results shown in Table 1.

4. Discussion

The predicted reduction in TDLU breast epithelial-cell proliferation with the 60% reduction in progestin dose was not observed. Although the observed mean value of Ki67 was higher in the lower progestin dose group, it was not statistically significant. This failure to observe a simple dose–effect relationship of this progestin on breast epithelial-cell proliferation is likely to be at least part of the explanation of why epidemiological studies have, in general, failed to identify differences in risk of breast cancer by dose of progestin in the OC [4–9].

Studies of breast-cell proliferation in OC users (Supplementary Table 1) [15–27] have contained a wide range of estrogen and progestin doses: no study reported an effect of progestin dose (although these were ‘combined’ doses across various progestins) and only the Anderson et al. [15] study

reported lower proliferation in OCs with lower EE2. It is of interest to note that early studies reported by Anderson et al. [15] and Williams et al. [16] found little difference between OC users and normally cycling women in TDLU breast-cell proliferation as measured by thymidine labeling index. The more recent studies of Olsson et al. [22] and Isaksson et al. [24] using Ki67 as the marker of cell proliferation have each found some evidence that average proliferation on OCs is greater than over the menstrual cycle — 10.6% vs 9.0%, and 4.8% vs 2.2%, respectively. The Ki67 figure of 7.8% we observed with the much more commonly used 1-mg NET OC should not be taken as an average figure for the OC cycle since there is clear evidence that proliferation is lower in the placebo week and there is some evidence that proliferation may be at its maximum towards the end of the active pill phase when we took our breast-biopsy samples [15].

Concomitantly with this failure to observe a decrease in Ki67 with the reduction in NET dose, the levels of each of PRA, PRB and ERα approximately doubled. This is the first report of an effect of NET dose on PRA, PRB and ERα expression levels in the breast. Whether this increase in the proportion of cells expressing steroid receptor with decreasing progestin dose explains the failure to see a decrease in Ki67 is unclear. We did not measure the pharmacokinetics of EE2 and NET in these women and were thus not able to see whether these values together with the proportion of cells expressing receptor were associated with the Ki67 values. The proportion of cells expressing receptors themselves (within an OC type) was not associated with the Ki67 values. It is not known whether this effect of NET dose on receptor levels holds true for other progestins. Increasing progesterone levels after ovulation in the normal menstrual cycle are associated with markedly lower ER expression in almost all studies (Supplementary Table 2) [16,28–33], but the changes

Table 1
Ki67, PRA, PRB and ERα percentage associated with two 35-mcg EE2 OCs with different NET doses

Measure	NET dose		p ^a
	1 mg	0.4 mg	
Ki67	7.8 (4.4–13.9)	12.5 (7.0–22.3)	.27
PRA	7.6 (5.3–10.4)	16.7 (8.6–27.3)	.041
PRB	12.0 (8.8–15.8)	23.7 (14.1–35.7)	.030
ERα	9.0 (5.5–13.3)	18.2 (10.0–28.8)	.056

Values shown are means with 95% confidence limits.

^a Two-sided significance level for difference between NET doses.

in PR expression over the menstrual cycle in the same studies are inconsistent (Supplementary Table 3) [16,28–33].

Studies of ER expression in the breast during an OC cycle have found lower levels in the 3 weeks on active estrogen–progestin than in the week on placebo, and the levels during OC use are lower than the levels seen during the menstrual cycle (Supplementary Table 2). However, studies of PR expression have found higher levels in the 3 weeks on active estrogen–progestin than in the week on placebo, and the results from the three studies that have investigated how the PR expression levels during OC use compared to the levels seen during the menstrual cycle have produced inconclusive results (Supplementary Table 3). There have been no reports on the effects of dose of EE2 or on the effects of the dose and type of progestin in the OC on these findings.

The results presented here provide clear evidence that decreasing the dose of the progestin NET in an OC from 1 to 0.4 mg increases ER α , PRA and PRB in the breast epithelium. There is indirect evidence suggesting that decreasing the dose of EE2 in an OC will decrease PR, but it may increase ER [1]. It is possible that an OC with the same NET dose but lower EE2 dose may be associated with a decreased proliferation of breast epithelium. We are currently investigating this possibility in a trial similar to the one reported here. Whether it is possible to adjust the doses in OCs to achieve an average breast-cell proliferation rate which is the same as or less than that occurring in a normal menstrual cycle is unknown.

5. Conclusions

Lowering the NET dose by 60% from 1 to 0.4 mg in a 35-mcg EE2 OC did not decrease breast-cell proliferation and approximately doubled the proportion of breast-epithelial cells expressing PRA, PRB and ER α . These latter results demonstrate that a simple dose–effect relationship between progestin dose and breast-cell proliferation is not to be expected. The breast-cell proliferation result is contrary to that predicted from the results of lowering the MPA dose from 10 to 2.5 mg in MEPT. This MEPT result strongly suggests that further investigation of the dose–effect relationship between other progestins in OCs is warranted. Investigating the dose–effect relationship with EE2 may also be informative. The long-term aim of such studies is to find an estrogen–progestin combination that will decrease the breast cancer risk of OC users– it is clear that simply reducing the progestin dose, at least of some progestins, is insufficient to achieve this aim.

Supplementary materials related to this article can be found online at [doi:10.1016/j.contraception.2011.12.015](https://doi.org/10.1016/j.contraception.2011.12.015).

Acknowledgments

We wish to express our sincerest gratitude to the women who agreed to be part of this study. We also wish to express

our thanks to Ms. A. Rebecca Anderson and Ms. Peggy Wan for extensive help with the management of the study and the statistical analysis.

References

- [1] Hofseth LJ, Raafat AM, Osuch JR, et al. Hormone replacement therapy with estrogen or estrogen plus medroxyprogesterone acetate is associated with increased epithelial proliferation in the normal postmenopausal breast. *J Clin Endocrinol Metab* 1999;84:4559–65.
- [2] Lee SA, Ross RK, Pike MC. An overview of menopausal oestrogen–progestin hormone therapy and breast cancer risk. *Br J Cancer* 2005;92:2049–58.
- [3] Prentice RL, Manson JE, Langer RD, et al. Benefits and risks of postmenopausal hormone therapy when it is initiated soon after menopause. *Am J Epidemiol* 2009;170:12–23.
- [4] Collaborative Group on Hormonal Factors in Breast Cancer. Breast cancer and hormonal contraceptives: collaborative reanalysis of individual data on 53,297 women with breast cancer and 100,239 women without breast cancer from 54 epidemiological studies. *Lancet* 1996;347:1713–27.
- [5] Marchbanks PA, McDonald JA, Wilson HG, et al. Oral contraceptives and the risk of breast cancer. *N Engl J Med* 2002;346:2025–32.
- [6] Rosenberg L, Zhang Y, Coogan PF, Strom BL, Palmer JR. A case-control study of oral contraceptive use and incident breast cancer. *Am J Epidemiol* 2009;169:473–9.
- [7] Kumle M, Weiderpass E, Braaten T, Persson I, Adami HO, Lund E. Use of oral contraceptives and breast cancer risk: the Norwegian–Swedish Women’s Lifestyle and Health Cohort Study. *Cancer Epidemiol Biomarkers Prev* 2002;11:1375–81.
- [8] Althuis MD, Brogan DR, Coates RJ, et al. Hormonal content and potency of oral contraceptives and breast cancer among young women. *Br J Cancer* 2003;88:50–7.
- [9] Hunter DJ, Colditz GA, Hankinson SE, et al. Oral contraceptive use and breast cancer: a prospective study of young women. *Cancer Epidemiol Biomarkers Prev* 2010;19:2496–502.
- [10] Stanczyk FZ. All progestins are not created equal. *Steroids* 2003;68:879–90.
- [11] Medical Letter. Drug interactions with grapefruit juice. *Obstet Gynecol* 2005;105:429–31.
- [12] World Health Organization Department of Reproductive Health and Research. Medical eligibility criteria for contraceptive use. 3rd edition. Geneva: World Health Organization; 2004.
- [13] Taylor CR, Shi SR, Chen C, Young L, Yang C, Cote RJ. Comparative study of antigen retrieval heating methods: microwave, microwave and pressure cooker, autoclave, and steamer. *Biotech Histochem* 1996;71:263–70.
- [14] Kumar SR, Singh J, Xia G, et al. Receptor tyrosine kinase EphB4 is a survival factor in breast cancer. *Am J Pathol* 2006;169:279–93.
- [15] Anderson TJ, Battersby S, King RJB, McPherson K, Going JJ. Oral contraceptive use influences resting breast proliferation. *Hum Pathol* 1989;20:1139–44.
- [16] Williams G, Anderson E, Howell A, et al. Oral contraceptive (OCP) use increases proliferation and decreases oestrogen receptor content of epithelial cells in the normal human breast. *Int J Cancer* 1991;48:206–10.
- [17] Masters JR, Drife JO, Scarisbrick JJ. Cyclic variation of DNA synthesis in human breast epithelium. *J Natl Cancer Inst* 1977;58:1263–5.
- [18] Meyer JS. Cell proliferation in normal human breast ducts, fibroadenomas, and other ductal hyperplasias measured by nuclear labeling with tritiated thymidine. *Hum Pathol* 1977;8:67–81.
- [19] Anderson TJ, Ferguson DJ, Raab GM. Cell turnover in the “resting” human breast: influence of parity, contraceptive pill, age and literacy. *Br J Cancer* 1982;46:376–82.

- [20] Longacre TA, Bartow SA. A correlative morphologic study of human breast and endometrium in the menstrual cycle. *Am J Surg Pathol* 1986;10:382–93.
- [21] Nazário AC, De Lima GR, Simões MJ, Novo NF. Cell kinetics of the human mammary lobule during the proliferative and secretory phase of the menstrual cycle. *Bull Assoc Anat* 1995;79:23–7.
- [22] Olsson H, Jernström H, Alm P, et al. Proliferation of the breast epithelium in relation to menstrual cycle phase, hormonal use, and reproductive factors. *Breast Cancer Res Treat* 1996;40:187–96.
- [23] Söderqvist G, Isaksson E, von Schoultz B, Carlström K, Tani E, Skoog L. Proliferation of breast epithelial cells in healthy women during the menstrual cycle. *Am J Obstet Gynecol* 1997;176:123–8.
- [24] Isaksson E, von Schoultz E, Odland V, et al. Effects of oral contraceptives on breast epithelial proliferation. *Breast Cancer Res Treat* 2001;65:163–9.
- [25] Feuerhake F, Sigg W, Höfner EA, Unterberger P, Welsch U. Cell proliferation, apoptosis, and expression of Bcl-2 and Bax in non-lactating human breast epithelium in relation to the menstrual cycle and reproductive history. *Breast Cancer Res Treat* 2003;77:37–48.
- [26] Navarrete MA, Maier CM, Falzoni R, et al. Assessment of the proliferative, apoptotic and cellular renovation indices of the human mammary epithelium during the follicular and luteal phases of the menstrual cycle. *Breast Cancer Res* 2005;7:R306–13.
- [27] Garcia y Narvaiza D, Navarrete MA, Falzoni R, Maier CM, Nazário AC. Effect of combined oral contraceptives on breast epithelial proliferation in young women. *Breast J* 2008;14:450–5.
- [28] Jacquemier JD, Hassoun J, Torrente M, Martin PM. Distribution of estrogen and progesterone receptors in healthy tissue adjacent to breast lesions at various stages — Immunohistochemical study of 107 cases. *Breast Cancer Res Treat* 1990;15:109–17.
- [29] Ricketts D, Turnbull L, Ryall G, et al. Estrogen and progesterone receptors in the normal female breast. *Cancer Res* 1991;51:1817–22.
- [30] Battersby S, Robertson BJ, Anderson TJ, King RJ, McPherson K. Influence of menstrual cycle, parity and oral contraceptive use on steroid hormone receptors in normal breast. *Br J Cancer* 1992;65:601–7.
- [31] Söderqvist G, von Schoultz B, Tani E, Skoog L. Estrogen and progesterone receptor content in breast epithelial cells from healthy women during the menstrual cycle. *Am J Obstet Gynecol* 1993;168:874–9.
- [32] Isaksson E, Sahlin L, Söderqvist G, et al. Expression of sex steroid receptors and IGF-1 mRNA in breast tissue — effects of hormonal treatment. *J Steroid Biochem Mol Biol* 1999;70:257–62.
- [33] Hallberg G, Persson I, Naessén T, Magnusson C. Effects of pre- and postmenopausal use of exogenous hormones on receptor content in normal human breast tissue: a randomized study. *Gynecol Endocrinol* 2008;24:475–80.

Mammographic density, MRI background parenchymal enhancement and breast cancer risk

Malcolm C. Pike^{1,2*} & C. Leigh Pearce¹

¹*Department of Epidemiology and Biostatistics, Memorial Sloan-Kettering Cancer Center, New York, New York;* ²*Department of Preventive Medicine, Keck School of Medicine, University of Southern California, Los Angeles, California;*

*Correspondence to: Dr. M. C. Pike, Memorial Sloan-Kettering Cancer Center, 307 East 63rd Street, New York, NY 10065, USA. Tel: 01-646-735-8139. E-mail: pikem@mskcc.org

Abstract: Mammographic density (MD), representing connective and epithelial tissue (fibroglandular tissue, FGT) is a major risk factor for breast cancer. In an analysis of an autopsy series [1] [2], MD was found to be strongly correlated with the collagen and epithelial content of the breast [3], and another report showed that breast epithelium was highly concentrated in the areas of collagen concentration [4]. Collagen comprises the overwhelming majority of the FGT, occupying an area on the slides obtained from the autopsy series some 15 times the area of glandular tissue. The relationship of MD to breast cancer risk appears likely to be due to a major extent to increased epithelial cell numbers. FGT is also seen in breast magnetic resonance imaging (breast MRI) and, as expected, it has been shown that this measure of FGT (MRI-FGT) is highly correlated with MD. Contrast enhanced breast MRI shows that *normal* FGT 'enhances' (background parenchymal enhancement, BPE) after contrast agent is administered [5] [6], and a recent study suggests that BPE is also a major breast cancer risk factor, possibly as important as, and independent of, MD [7]. BPE is much more sensitive to the effects of menopause and tamoxifen than is FGT [8] [9]. Changes in MD and BPE may be most useful in predicting response to chemopreventive agents aimed at blocking breast cell proliferation. More study of the biological basis of the effects of MD and BPE are needed if we are to fully exploit these factors in developing chemopreventive approaches to breast cancer.

Key words: breast cancer, breast background parenchymal enhancement, breast MRI, mammographic density

introduction

The extent of mammographic density (MD), i.e., the white areas on a mammogram representing connective and epithelial tissue (fibroglandular tissue; FGT) in contrast to fat, is a major breast cancer risk factor with the risk of breast cancer in women of the same age being close to directly proportional to the amount of MD as well as to the percent MD (i.e., MD as a proportion of the area of breast on the mammogram, MD%) [10]. FGT can also be measured using breast magnetic resonance imaging (breast MRI) and it has been shown that this measure of FGT (MRI-FGT) is highly correlated with MD [11]. Breast MRI when used with a contrast agent (contrast breast MRI) is a more sensitive method than mammography in detecting early breast tumors. In contrast breast MRI one compares a baseline MRI to one taken shortly after the contrast agent is administered; and breast tumors show marked 'enhancement' in the post contrast MRI. Some degree of enhancement is also seen in normal breast tissue – termed background parenchymal enhancement (BPE). The 'extent' of BPE varies quite markedly between different women, and in a case-control study completed at Memorial Sloan-Kettering Cancer Center a woman's risk of breast cancer appeared to be at least as markedly affected by the extent of BPE as it was by the amount of MRI-FGT [7]. Furthermore, this risk from BPE appeared to be close to independent of the risk from MRI-FGT and presumably from MD.

mammographic density

On a mammogram, connective and epithelial tissue (fibroglandular tissue, FGT) appear white ('dense'), whereas fat appears dark ('non-dense'). A strong association between mammographic parenchymal pattern and breast cancer risk was first proposed by Wolfe in 1976 [12] [13] [14]. Since that time it has been shown that the extent of dense tissue on the mammogram (mammographic density, MD), i.e., the area of the mammogram considered to be 'white', is a reproducible and major risk factor for breast cancer [10]. To permit comparisons between different mammographic methods, MD was often reported as a proportion (percentage) of the area of the breast on the mammogram (mammographic density percent, MD%).

Table 1 shows the relationship between MD% and breast cancer risk in a classic study [15]. Risk increases steadily with increasing MD% and some 4.6-fold between women with an MD% $\geq 75\%$ compared to a woman with an MD% of $<10\%$.

MD and MD% are highly correlated with each other and Table 2 shows that they are almost equally connected with risk of breast cancer [16]. For a given MD, MD% is reduced with increasing BMI and

studies of the effect of MD% are almost invariably improved by adjustment for BMI. In a study where the effects of MD and MD% were examined in detail, the fit of MD% with breast cancer risk was somewhat improved with adjustment for the non-dense area of the mammogram whereas the fit of MD was unaffected and the authors concluded that MD was to be preferred on grounds of simplicity [16].

Similar to mammographic density, FGT can be seen on breast magnetic resonance imaging (MRI-FGT). Studies have shown that the extent of MRI-FGT correlates strongly with MD, and, since breast MRI is three-dimensional, MRI-FGT or MRI-FGT% (based on volume of the breast) may provide a better measure of breast cancer risk than MD, but this has not been demonstrated [17] [18] [19] [20].

Mammographic density has a large genetic component [21] [22], but is also clearly related to various breast cancer risk factors. This is most clearly seen by considering the effect of menopause on breast cancer risk. Figure 1 shows the age incidence of breast cancer in US white females before the introduction of extensive screening programs which distorted the curve by the inclusion of very early lesions [23] [24]. For most non-hormone dependent cancers incidence increases exponentially with increasing age and a straight line is obtained if we plot the logarithm of incidence against the logarithm of age, but as is clear from Figure 1 there is a clear slowing down of the rate of increase of breast cancer around age 50; this has been demonstrated to be an effect of menopause [25]. The lower estrogen and particularly progesterone levels in postmenopausal women are less stimulating to the breast than the hormonal profile of premenopausal women [26]. This change in the rate of increase in breast cancer and the lower level of proliferation of the breast tissue is reflected in a decrease of MD after the decline in ovarian function and the onset of menopause and this decline is reversed by use of menopausal estrogen-progestin therapy [10] [27]. MD density is also less in parous women and declines further with increasing numbers of live births [28].

Association of MD with Breast Tissue Components

Using breast tissue samples from a large non-selected forensic autopsy series compiled by Bartow and her colleagues [1] [2], Boyd and colleagues [3] showed that MD% – measured in this case by Bartow and her colleagues in an overall assessment of the Faxitron images of the breast slices made of the whole breast and named Faxitron Density % – was strongly correlated with the proportion of tissue area on the associated ‘random’ microscope slide occupied by collagen. Faxitron Density % was also strongly correlated with the proportion of tissue area occupied by the nuclei of breast epithelia and by glandular tissue. Collagen comprised the greatest quantity of fibroglandular tissue in the breast [28]; collagen

occupied an area some 15 times the area occupied by glandular tissue. This latter result is not generally recognized.

We initially reported that very early DCIS lesions in the breast were invariably in areas of the breast containing significant densities [29]; and moreover found in a study of breast tissue from women having a reduction mammoplasty that normal breast epithelium was highly concentrated in the areas of the breast containing a high concentration of inter-lobular collagen [4] and subsequently confirmed this in large studies of breast tissue from normal weight women [30, 31]. Taken together with the results reported by Boyd and his colleagues [3], these results show that the number of epithelial cells varies many-fold between different women mirroring the wide variation in MD, so that the relationship of MD to breast cancer risk may be due to a significant extent simply to increased epithelial cell numbers. We found that normal breast epithelial cell proliferation was higher in those areas where there was little associated collagen [4]; this is evidence against the densities as such being an important modifier of breast cancer risk, but other evidence does suggest a direct effect and this is an area of intense research [32, 33].

The biological basis of the relationship of collagen in the human breast to epithelium is unclear. Blocking ovarian function with a GnRH analog reduces MD by approximately one-third [34] [35] [36], which then returns when the GnRH analog is withdrawn [37]. Some densities appear, therefore, to be closely related to current hormone exposure with its associated greater breast cell proliferation, while others change only slowly with increasing age after the menopause. Differences between these types of density have not been elucidated.

Breast Background Parenchymal Enhancement

Breast MRI when used with a contrast agent (contrast breast MRI) is a more sensitive method than mammography in detecting early breast tumors as a consequence of the different behavior of the contrast agent in tumors as compared to normal breast tissue. Background parenchymal enhancement (BPE) refers to the volume and intensity that *normal* fibroglandular tissue 'enhances' after intravenous contrast agent administration [5] [6]. BPE is categorized in the BIRADS system as Minimal, Mild, Moderate or Marked. BPE is thought to be a measure of the amount of blood flow in the dense tissue and may represent breast activity. As we noted earlier, baseline breast MRI before the administration of the contrast agent can also be used to measure the extent of FGT in the breast. MRI-FGT is categorized in the BIRADS system as Fatty (<25% of breast comprises fibroglandular tissue), Scattered (25% - 50% of

breast comprises fibroglandular tissue), Heterogeneously Dense (51% - 75% of breast comprises fibroglandular tissue) or Dense (>75% of breast comprises fibroglandular tissue).

Table 3 shows the relationship between BPE and MRI-FGT and breast cancer risk in a case-control study we recently carried out at Memorial Sloan-Kettering Cancer Center [7]. BPE varies markedly between different women, and risk increases steadily with increasing BPE. The risks associated with BPE are large, of the same order of magnitude as are found with mammographic density. As we would expect, risk also increases steadily with increasing MRI-FGT but possibly not to quite the same extent as with BPE. Adjustment for MRI-FGT resulted in only a slight decrease in the estimated effects of BPE. BPE is therefore a new significant breast cancer risk factor essentially independent of MRI-FGT. Inspection of the results for the control women in Table 3 shows that there is a marked decline in the level of BPE between premenopausal and postmenopausal women: the percentage of controls showing Moderate or Marked BPE declined from 38.5% to 12.2%. Table 3 shows that there is a much smaller decline in MRI-FGT between premenopausal and postmenopausal women: the percentage of controls showing Heterogeneously Dense (HD) or Dense MRI-FGT declined from 69.2% to 63.4%.

We confirmed these lower postmenopausal levels of BPE in a subsequent study that measured BPE in individual women before and after menopause [8]. Table 4 shows that in this study of individual women, the percentage of Moderate and Marked BPE declined from 53.6% to 14.3%. The percentage of HD or Dense MRI-FGT also declined, from 85.7% to 64.2%, but to a lesser extent than BPE.

In a further study we showed that both BPE and MRI-FGT decrease in the contralateral breast of breast cancer patients treated with tamoxifen (Table 5) [9]. With tamoxifen treatment, the percentage of Moderate and Marked BPE declined from 59.0% to 5.7%. The percentage of HD or Dense MRI-FGT also declined, from 85.2% to 73.9%, but again to a much lesser extent than BPE. The decreases in BPE were not associated with the duration of tamoxifen treatment; decreases occurred “even in patients who were on tamoxifen for a short period, as little as 39 days” [9]. In contrast, the proportion of patients showing a decrease in MRI-FGT became larger with longer duration of tamoxifen treatment [9].

The same decreases occurred, but to a lesser extent, in patients treated with the aromatase inhibitor, Anastrozole (Table 6) [38]. With Anastrozole treatment, the percentage of Moderate and Marked BPE declined from 25.7% to 8.3%. The percentage of HD or Dense MRI-FGT also declined but to a very small extent, from 45.9% to 43.2%. The tamoxifen treated patients were, of course, much younger than the Anastrozole treated patients, who were all postmenopausal. This is the reason for the much higher baseline levels of both BPE and MRI-FGT in the tamoxifen treated patients.

Discussion

Tamoxifen has been repeatedly shown to reduce MD [39] [40] [41]. The reduction in MD with tamoxifen use is much more pronounced in younger women. In the report from Brisson et al. [40], the reduction in MD% due to tamoxifen use was 8.5% in women <50 years of age and 2.2% in women ≥50 years of age. In the report from Cuzick et al. [41], the reduction in MD% was 13.4% in women ≤45 years of age and 1.1% in women ≥56 years of age. These results are in close agreement with the results we found with MRI-FGT. In their analysis of the IBIS-I randomized prevention trial of tamoxifen use, Cuzick et al. [42] reported that the benefit in terms of reduced breast cancer incidence in the tamoxifen arm of the trial was restricted to women whose MD% was reduced by at least 10%. It is difficult to reconcile this result with their previous finding that MD% was only reduced by 1.1% in women ≥56 years of age [42], when the NSABP P1 tamoxifen prevention study [43] found that the benefit of tamoxifen use was equally strong in such older women. As Cuzick et al. [42] state in their paper: their results need “confirmation in a separate study”.

The results presented in Table 5 suggest that BPE may be a better marker of the effect of tamoxifen treatment. Validating this in a prevention setting will be difficult if not impossible to do, but it may be possible to show that the extent of the benefit of tamoxifen treatment of breast cancer patients was associated with the degree to which BPE and MRI-FGT (or MD) was changed. The same applies to validating the use of BPE and possibly MRI-FGT with the use of aromatase inhibitors.

Much more study of the biological basis of these major risk factors in normal human breast is needed if we are to exploit them in some way to help in developing chemopreventive approaches to breast cancer.

conflict of interest

The authors have declared no conflicts of interest.

Grant Support

This work was supported by a Department of Defense Congressionally Directed Breast Cancer Research Program Grant BC044808; and by the USC/Norris Comprehensive Cancer Center Core Grant P30 CA14089. The funding sources had no role in this report.

References

1. Bartow SA, Pathak DR, Mettler FA. Radiographic microcalcification and parenchymal patterns as indicators of histologic "high-risk" benign breast disease. *Cancer* 1990; 66: 1721-1725.
2. Bartow SA, Pathak DR, Mettler FA et al. Breast mammographic pattern: a concatenation of confounding and breast cancer risk factors. *Am J Epidemiol* 1995; 142: 813-819.
3. Li T, Sun L, Miller N et al. The association of measured breast tissue characteristics with mammographic density and other risk factors for breast cancer. *Cancer Epidemiol Biomarkers Prev* 2005; 14: 343-349.
4. Hawes D, Downey S, Pearce CL et al. Dense breast stromal tissue shows greatly increased concentration of breast epithelium but no increase in its proliferative activity. *Breast Cancer Res* 2006; 8: R24.
5. Morris EA. Diagnostic breast MR imaging: current status and future directions. *Radiol Clin North Am* 2007; 45: 863-880, vii.
6. Kuhl C. The current status of breast MR imaging. Part I. Choice of technique, image interpretation, diagnostic accuracy, and transfer to clinical practice. *Radiology* 2007; 244: 356-378.
7. King V, Brooks JD, Bernstein JL et al. Background parenchymal enhancement at breast MR imaging and breast cancer risk. *Radiology* 2011; 260: 50-60.
8. King V, Gu Y, Kaplan JB et al. Impact of menopausal status on background parenchymal enhancement and fibroglandular tissue on breast MRI. *Eur Radiol* 2012; 22: 2641-2647.
9. King V, Kaplan J, Pike MC et al. Impact of tamoxifen on amount of fibroglandular tissue, background parenchymal enhancement, and cysts on breast magnetic resonance imaging. *Breast J* 2012; 18: 527-534.
10. Boyd NF, Lockwood GA, Byng JW et al. Mammographic densities and breast cancer risk. *Cancer Epidemiol Biomarkers Prev* 1998; 7: 1133-1144.
11. Lee NA, Rusinek H, Weinreb J et al. Fatty and fibroglandular tissue volumes in the breasts of women 20-83 years old: comparison of X-ray mammography and computer-assisted MR imaging. *AJR Am J Roentgenol* 1997; 168: 501-506.
12. Wolfe JN. Breast patterns as an index of risk for developing breast cancer. *Am J Roentgenol* 1976; 126: 1130-1137.
13. Wolfe JN. Risk for breast cancer development determined by mammographic parenchymal pattern. *Cancer* 1976; 37: 2486-2492.
14. Wolfe JN. Breast parenchymal patterns and their changes with age. *Radiology* 1976; 121: 545-552.
15. Boyd NF, Byng JW, Jong RA et al. Quantitative classification of mammographic densities and breast cancer risk: results from the Canadian National Breast Screening Study. *J Natl Cancer Inst* 1995; 87: 670-675.
16. Stone J, Ding J, Warren RM et al. Using mammographic density to predict breast cancer risk: dense area or percentage dense area. *Breast Cancer Research* 2010; 12: R97.
17. Wei J, Chan HP, Helvie MA et al. Correlation between mammographic density and volumetric fibroglandular tissue estimated on breast MR images. *Med Phys* 2004; 31: 933-942.

18. Thompson D, Leach M, Kwan-Lim G et al. Assessing the usefulness of a novel MRI-based breast density estimation algorithm in a cohort of women at high genetic risk of breast cancer: the UK MARIBS study. *Breast Cancer Res* 2009; 11: R80.
19. Klifa C, Carballido-Gamio J, Wilmes L et al. Magnetic resonance imaging for secondary assessment of breast density in a high-risk cohort. *Magn Reson Imaging* 2010; 28: 8-15.
20. Nie K, Chen JH, Chan S et al. Development of a quantitative method for analysis of breast density based on three-dimensional breast MRI. *Med Phys* 2008; 35: 5253-5262.
21. Boyd NF, Dite GS, Stone J et al. Heritability of mammographic density, a risk factor for breast cancer. *N Engl J Med* 2002; 347: 886-894.
22. Steinberg KK, Smith SJ, Stroup DF et al. Comparison of effect estimates from a meta-analysis of summary data from published studies and from a meta-analysis using individual patient data for ovarian cancer studies. *Am J Epidemiol* 1997; 145: 917-925.
23. Pike MC, Krailo MD, Henderson BE et al. 'Hormonal' risk factors, 'breast tissue age' and the age-incidence of breast cancer. *Nature* 1983; 303: 767-770.
24. Pike MC. Age-related factors in cancers of the breast, ovary, and endometrium. *J Chronic Dis* 1987; 40 Suppl 2: 59S-69S.
25. Trichopoulos D, MacMahon B, Cole P. Menopause and breast cancer risk. *J Natl. Cancer Inst.* 1972; 48: 605-613.
26. Pike MC, Spicer DV, Dahmouch L, Press MF. Estrogens, progestogens, normal breast cell proliferation, and breast cancer risk. *Epidemiol Rev* 1993; 15: 17-35.
27. Boyd N, Martin L, Stone J et al. A longitudinal study of the effects of menopause on mammographic features. *Cancer Epidemiol Biomarkers Prev* 2002; 11: 1048-1053.
28. Martin LJ, Boyd NF. Mammographic density. Potential mechanisms of breast cancer risk associated with mammographic density: hypotheses based on epidemiological evidence. *Breast Cancer Res* 2008; 10: 201.
29. Ursin G, Hovanessian-Larsen L, Parisky YR et al. Greatly increased occurrence of breast cancers in areas of mammographically dense tissue. *Breast Cancer Res* 2005; 7: R605-608.
30. Cuzick J, Sestak I, Pinder SE et al. Effect of tamoxifen and radiotherapy in women with locally excised ductal carcinoma in situ: long-term results from the UK/ANZ DCIS trial. *Lancet Oncol* 2011; 12: 21-29.
31. Chung K, Hovanessian-Larsen LJ, Hawes D et al. Breast epithelial cell proliferation is markedly increased with short-term high levels of endogenous estrogen secondary to controlled ovarian hyperstimulation. *Breast Cancer Res Treat* 2012; 132: 653-660.
32. Kerlikowske K, Phipps AI. Breast density influences tumor subtypes and tumor aggressiveness. *J Natl Cancer Inst* 2011; 103: 1143-1145.
33. Phipps AI, Buist DS, Malone KE et al. Reproductive history and risk of three breast cancer subtypes defined by three biomarkers. *Cancer Causes Control* 2011; 22: 399-405.
34. Pike MC, Ross RK, Lobo RA et al. LHRH agonists and the prevention of breast and ovarian cancer. *Br J Cancer* 1989; 60: 142-148.
35. Spicer DV, Ursin G, Parisky YR et al. Changes in mammographic densities induced by a hormonal contraceptive designed to reduce breast cancer risk. *J Natl Cancer Inst* 1994; 86: 431-436.
36. Weitzel JN, Buys SS, Sherman WH et al. Reduced mammographic density with use of a gonadotropin-releasing hormone agonist-based chemoprevention regimen in BRCA1 carriers. *Clin Cancer Res* 2007; 13: 654-658.

37. Gram IT, Ursin G, Spicer DV, Pike MC. Reversal of gonadotropin-releasing hormone agonist induced reductions in mammographic densities on stopping treatment. *Cancer Epidemiol Biomarkers Prev* 2001; 10: 1117-1120.
38. King V, Goldfarb SB, Brooks JD et al. Effect of aromatase inhibitors on background parenchymal enhancement and amount of fibroglandular tissue at breast MR imaging. *Radiology* 2012; 264: 670-678.
39. Atkinson C, Warren R, Bingham SA, Day NE. Mammographic patterns as a predictive biomarker of breast cancer risk: effect of tamoxifen. *Cancer Epidemiol Biomarkers Prev* 1999; 8: 863-866.
40. Brisson J, Brisson B, Cote G et al. Tamoxifen and Mammographic Breast Densities. *Cancer Epidemiol Biomarkers Prev* 2000; 9: 911-915.
41. Cuzick J, Warwick J, Pinney E et al. Tamoxifen and breast density in women at increased risk of breast cancer. *J Natl Cancer Inst* 2004; 96: 621-628.
42. Cuzick J, Warwick J, Pinney E et al. Tamoxifen-induced reduction in mammographic density and breast cancer risk reduction: a nested case-control study. *J Natl Cancer Inst* 2011; 103: 744-752.
43. Fisher B, Constantino JP, Wickerham L et al. Tamoxifen for prevention of breast cancer: Report of the National Surgical Adjuvant Breast and Bowel Project P-1 Study. *Journal of the National Cancer Institute* 1998; 90: 1371-1388.

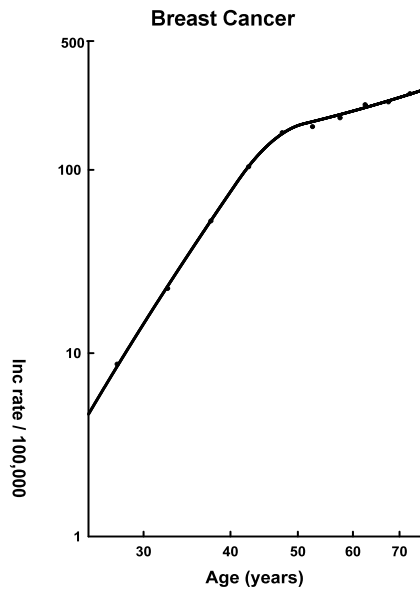


Figure 1. Age-specific incidence rates for breast cancer in US White females (Third National cancer Survey).

Table 1. MD % and relative risk of breast cancer

MD%	RR	Population (%)
None	1.0	7
<10	1.2	17
10-	2.2	21
25-	2.4	27
50-	3.4	19
75+	5.3	9

MD%, mammographic density %; RR, relative risk
From Boyd et al. [15]

Table 2. MD and MD% and relative risk of breast cancer

MD		MD%	
Quintile	RR	Quintile	RR
Q1	1.00	Q1	1.00
Q2	1.41	Q2	1.62
Q3	1.50	Q3	1.46
Q4	1.94	Q4	1.89
Q5	2.85	Q5	2.71

MD, mammographic density; MD%, mammographic density %,
RR, relative risk
From Stone et al. [16]

Table 3. BPE level and relative risk of breast cancer

BPE	Cases N (%)	Controls N (%)	RR	MRI-FGT	Cases N (%)	Controls N (%)	RR
Minimal/Mild	16 (41.0)	63 (80.8)	1.0	Fatty/Scattered	7 (18.0)	26 (33.3)	1.0
Moderate	15 (38.5)	12 (15.4)	8.2	HD	19 (48.7)	35 (44.9)	2.0
Marked	8 (20.5)	3 (3.8)	18.2	Dense	13 (33.3)	17 (21.8)	3.2
Minimal/Mild	16 (41.0)	63 (80.8)	1.0	Fatty/Scattered	7 (18.0)	26 (33.3)	1.0
Moderate/Marked	23 (59.0)	15 (19.2)	10.1	HD/Dense	32 (82.0)	52 (66.7)	2.3
<i>Premenopausal:</i>				<i>Premenopausal:</i>			
Minimal/Mild	4 (23.5)	16 (61.5)	1.0	Fatty/Scattered	1 (5.9)	8 (30.8)	1.0
Moderate/Marked	13 (76.5)	10 (38.5)	5.1	HD/Dense	16 (94.1)	18 (69.2)	5.2
<i>Postmenopausal:</i>				<i>Postmenopausal:</i>			
Minimal/Mild	12 (54.6)	36 (87.8)	1.0	Fatty/Scattered	6 (27.3)	15 (36.6)	1.0
Moderate/Marked	10 (45.4)	5 (12.2)	14.2	HD/Dense	16 (72.7)	26 (63.4)	1.6

CI, confidence interval; RR, relative risk
From King et al. [7]

Table 4. BPE and MRI-FGT change with menopause

BPE	Pre <i>N</i> (%)	Post <i>N</i> (%)
Minimal	4 (14.3)	15 (53.6)
Mild	9 (32.1)	9 (32.1)
Moderate	11 (39.3)	3 (10.7)
Marked	4 (14.3)	1 (3.6)

MRI-FGT	Pre <i>N</i> (%)	Post <i>N</i> (%)
Fatty	0 (0.0)	2 (7.1)
Scattered	4 (14.3)	8 (28.6)
HD	19 (67.9)	16 (57.1)
Dense	5 (17.9)	2 (7.1)

HD, heterogeneously dense; Pre, premenopausal;
Post, postmenopausal
From King et al. [8]

Table 5. BPE and MRI-FGT at baseline and on tamoxifen

BPE	Baseline <i>N</i> (%)	On tamoxifen <i>N</i> (%)
Minimal	14 (15.9)	46 (52.3)
Mild	29 (33.0)	37 (42.0)
Moderate	27 (38.5)	5 (5.7)
Marked	18 (20.5)	0 (0.0)

MRI-FGT	Baseline <i>N</i> (%)	On tamoxifen <i>N</i> (%)
Fatty	2 (2.3)	6 (6.8)
Scattered	11 (12.5)	17 (19.3)
HD	34 (38.6)	41 (46.6)
Dense	41 (46.6)	24 (27.3)

HD, heterogeneously dense

From King et al. [9]

Table 6. BPE and MRI-FGT decrease on Anastrozole

BPE	Baseline <i>N</i> (%)	On AI <i>N</i> (%)
Minimal	17 (15.6)	34 (31.2)
Mild	64 (58.7)	66 (60.6)
Moderate	27 (24.8)	9 (8.3)
Marked	1 (0.9)	0 (0.0)

MRI-FGT	Baseline <i>N</i> (%)	On AI <i>N</i> (%)
Fatty	15 (13.8)	18 (16.5)
Scattered	44 (40.4)	44 (40.4)
HD	35 (32.1)	32 (29.4)
Dense	15 (13.8)	15 (13.8)

AI, Anastrozole; HD, heterogeneously dense
From King et al. [38]

The Relation of Mammographic Density to Breast Collagen and Epithelium

Malcolm Pike^{1,2}, Sue Bartow³, Lisa Martin⁴, Debra Hawes⁵, Dorothy Pathak⁶, Norman F. Boyd⁴

Authors' Affiliations: ¹Department of Preventive Medicine, Keck School of Medicine, University of Southern California, Los Angeles, California; ²Department of Epidemiology and Biostatistics, Memorial Sloan-Kettering Cancer Center, New York, New York; ³Department of Pathology, University of New Mexico, Albuquerque, New Mexico - Current Address: 107 Stark Mesa, Carbondale, CO 81623; ⁴Division of Epidemiology and Statistics, Ontario Cancer Institute, Toronto, Ontario, Canada; ⁵Department of Pathology, Keck School of Medicine, University of Southern California, Los Angeles, California; and ⁶Department of Epidemiology, Michigan State University, East Lansing, Michigan

Corresponding author: Dr. M. C. Pike, Department of Epidemiology and Biostatistics, Memorial Sloan-Kettering Cancer Center, 307 E 63rd Street, New York, NY 10065, USA; e-mail: pikem@mskcc.org.

Keywords Breast, Breast epithelium, Collagen, Mammographic density

Abstract

Background: Mammographic density (MD) is a strong risk factor for breast cancer. In a recent report on an autopsy series MD was found to be correlated with the collagen and epithelial content of the breast (1). Another recent report showed that breast epithelium was highly concentrated in the areas of collagen concentration (2). We have conducted a further analysis of the autopsy series results in the light of the latter finding.

Methods: In the autopsy series the proportions of tissue on a slide occupied by epithelial nuclear area (Epithelial Nuclear Area %), glandular area (Glandular Area %) and collagen area (Collagen Area %) was determined, as was Faxitron density (Faxitron Density %) of the breast. The relationships between these measures were examined. Values for 146 premenopausal and 85 postmenopausal subjects were available for analysis.

Results: Collagen Area % declined from 30.5% in premenopausal women to 12.5% in postmenopausal women. Collagen Area % was approximately 80% of the Faxitron Density %, while Glandular Area % was only ~5.9% and ~3.4% of the Faxitron Density % in premenopausal and postmenopausal women respectively. In postmenopausal women, Epithelial Nuclear Area % was directly proportional to Collagen Area %; but, in premenopausal women, the ratio of Epithelial Nuclear Area % to Collagen Area % declined with increasing Collagen Area %; but whether this was due to a greater concentration of epithelium per unit collagen in low Collagen Area % or a greater concentration in fat is not known and we have no knowledge of how this relates to breast cell proliferation. The ratio of epithelium to a fixed Collagen Area % was much higher in premenopausal than in postmenopausal women, but the relationship of epithelium to collagen was the same in parous and nulliparous women.

Conclusions: The relationship of MD to breast cancer risk appears likely to be due to a major extent to increased epithelial cell numbers. Additional evidence for this conclusion is that the lower MD in parous compared to nulliparous women is reflected in a similar proportional reduction in breast epithelium, as is the lower MD in postmenopausal women.

Impact: Much more study of the biological basis of the major breast cancer risks associated with breast densities are needed if we are to exploit this major risk factor in some way to help in developing chemopreventive approaches to breast cancer.

Introduction

Mammographic density (MD), *i.e.*, the light areas on a mammogram representing connective and epithelial tissue (fibroglandular tissue) in contrast to fat, is a major breast cancer risk factor with the risk of breast cancer being close to directly proportional to the amount of mammographic density as well as to the percent MD (*i.e.*, MD as a proportion of the area of breast on the mammogram, MD%) (3). Using breast tissue samples from a large (n = 236) non-selected forensic autopsy series, compiled by one of us (Bartow) (4,5), Boyd (co-author of this report) and colleagues showed (1) that the percent mammographic density (dense area as a proportion of the total area of the breast in an overall assessment of the Faxitron images of the breast slices made of the whole breast; Faxitron Density % was strongly correlated with the proportion of tissue area on the associated microscope slide occupied by collagen (Collagen Area %). Faxitron Density % was also correlated with the proportion of tissue area occupied by the nuclei of breast epithelia (epithelial nuclear Area %), and with the proportion of tissue area occupied by glandular tissue (Glandular Area %).

In studying the location of breast epithelium in biopsy slides from a small number (n = 12) of women having a reduction mammoplasty, we previously found that breast epithelium was highly concentrated in the areas of the breast containing a high concentration of inter-lobular collagen (2).

We report here our further analysis of the forensic autopsy results presented by Li, Boyd and their colleagues (1) in which we relate their findings to the findings reported by Hawes and colleagues (2), *i.e.*, we investigate the relation of Epithelial Nuclear Area % to Collagen Area % in order to attempt to gain a deeper understanding of the relationship of MD to breast cancer risk.

Materials and Methods

This study used random tissue blocks from the non-selected forensic autopsy series of 236 women collected at the New Mexico Office of the Medical Investigator between 1978 and 1983 by Bartow and colleagues (4,5). The methods used to collect this material have been described in detail elsewhere (4) as have the methods used by Boyd and colleagues (1). Briefly, the women were between 15 and 90 years of age and included 110 non-Hispanic Whites (referred to as 'Anglos' here following the description in the original papers), 81 Hispanics and 45 Native Americans. Bilateral subcutaneous mastectomy was done at autopsy. The specimens were then sectioned at 1 cm intervals and the slices examined radiologically (Faxitron, Wheeling, IL). A Faxitron density based on all slices was estimated by Bartow and her colleague Dr F Mettler (5). Histological sections of a tissue block randomly selected by Bartow and colleagues (4) from the upper outer quadrants were used for the histological measurements described below. If the section showed autolysis another randomly selected block from the same breast was used (1).

Serial sections, 3 μm thick, were cut from formalin-fixed tissue. The first section was stained with routine H&E, the second with Masson's Trichrome; 80 'systematic random' fields of view were selected from each section for analysis (1). Each field was the area covered by the view of a 10 \times 0.25 N.A. Achrostigmat objective on a Zeiss Axioskop light microscope. Areas were measured with the aid of Microcomputer Imaging Device software (Imaging Research Inc., St. Catherines, Ontario, Canada). The collagen area was obtained by setting a threshold to segment out the green-stained collagen on the Trichrome-stained section. Glandular area and epithelial nuclear area were measured by establishing 'masks' through threshold settings over the relevant areas in trichrome-stained and H&E-stained sections respectively. The measurements used in analysis were Collagen Area %, Glandular Area % and

Epithelial Nuclear Area %, *i.e.*, areas of collagen, glandular tissue and epithelial nuclei respectively as a percentage of the total area of the 80 fields examined showing any tissue.

Statistical analysis

Standard linear regression methods were used to examine the relationships between FD%, Collagen Area % and Epithelial Nuclear Area %. Square root transformations were applied to these variables to achieve approximate normality of distribution, as described by Li and colleagues (1). Covariates investigated were ethnicity (non-Hispanic White, Hispanic and Native American); age in 10 year age groups (<20, 20-29, ... ,70+); menopausal status (premenopausal vs postmenopausal – further detail not available); parity (nulliparous vs parous – known for a subset of subjects); body mass index (BMI) recorded as kg/m² and investigated as a continuous variable as well as a categorical variable within three groups (<25, 25 to <30, 30+ kg/m²). The relation between Epithelial Nuclear Area % and both FD% and Collagen Area % differed significantly by menopausal status when we regressed Epithelial Nuclear Area % against Faxitron Density % and against Collagen Area % separately. The other factors were investigated both in the total data with menopausal status modeled as a constant term, and were also investigated separately in premenopausal and postmenopausal subjects. All statistical significance levels (p values) quoted are two-sided.

Results

We initially excluded five subjects from analysis. Four subjects were of unknown menopausal status and one subject had an Epithelial Nuclear Area % that was an extreme outlier. This left values for 146 premenopausal and 85 postmenopausal subjects available for analysis.

Table 1 shows the medians and inter-quartile ranges for Faxitron Density %, Collagen Area %, Glandular Area % and Epithelial Nuclear Area % by menopausal status. In premenopausal women the median value for Faxitron Density % was 40%, for Collagen Area % was 30.5%, for Glandular Area % was 1.67%, and for Epithelial Nuclear Area % was 0.41%. The corresponding figures for postmenopausal women were 20%, 12.5%, 0.68% and 0.10%. In premenopausal women the median ratio of Collagen Area % to Glandular Area % was 14.0, and in postmenopausal women the median ratio was 16.7.

As previously reported Collagen Area % was strongly associated with Faxitron Density % (premenopausal - correlation coefficient, $r = 0.52$, $p < 0.001$; postmenopausal - $r = 0.63$, $p < 0.001$: r and p values given are for square root transformed variables throughout). Fig. 1 shows a Box-plot of Collagen Area % against FD%; the relationship was little affected by menopausal status.

Epithelial Nuclear Area % was significantly related to Collagen Area % in premenopausal women ($r = 0.36$, $p < 0.001$) and in postmenopausal women ($r = 0.52$, $p < 0.001$). The relationship was strongly affected by menopausal status with much higher values for Epithelial Nuclear Area % at a fixed Collagen Area % in premenopausal women (see below). These relationships were stronger than for Epithelial Nuclear Area % and Faxitron Density %, and, when jointly fitted, Collagen Area % remained statistically significant in premenopausal women ($p=0.004$) and postmenopausal women ($p<0.001$), while the relationships with Faxitron Density % were no longer statistically significant.

To increase the ability (power) to detect the influence of other factors on the relationship between Epithelial Nuclear Area % and Collagen Area % we then eliminated from analysis ten subjects whose Epithelial Nuclear Area % was a frank outlier value when plotted against Collagen Area % (nine premenopausal and one postmenopausal subject). Figs. 2a and 2b show the relationships between Epithelial Nuclear Area % and Collagen Area % for the remaining premenopausal and postmenopausal subjects respectively.

The Epithelial Nuclear Area % was close to directly proportional to Collagen Area % in postmenopausal women - Epithelial Nuclear Area % was approximately 0.54% of the Collagen Area %

value. The relationships between Epithelial Nuclear Area % and Collagen Area % were not affected by parity, body mass index or age (within pre- or postmenopausal subjects). Native Americans showed in both premenopausal and postmenopausal women an ~20% greater concentration of Epithelial Nuclear Area % in relation to Collagen Area % than both Anglos and Hispanics but the result did not approach statistical significance ($p=0.29$).

Discussion

Mammographic density is an independent strong risk factor for breast cancer. Mammographic density has a large genetic component (6,7), decreases with increasing parity, with age and at menopause, and in the postmenopausal period is increased by exposure to menopausal estrogen-progestin therapy. The extensive evidence for the effect of these factors has been reviewed in detail by Martin and Boyd (8).

Martin and Boyd (8) also pointed out that “greater amounts of epithelium and/or stroma (were) associated with mammographic density” and that collagen comprised the greatest quantity of fibroglandular tissue in the breast. This latter result is not generally recognized. As we noted above, the ratio of collagen to glandular tissue is ~14 in premenopausal women and ~17 in postmenopausal women.

Hawes et al. (2) showed that breast epithelium was highly concentrated in the areas of collagen concentration. We saw above that the increased epithelium with increased mammographic density can be ‘explained’ by the relationship that exists between epithelium and collagen (Figs. 1 and 2). The number of epithelial cells varies many-fold between different women mirroring the wide variation in mammographic density, so that the relationship of mammographic density to breast cancer risk may be due to a significant extent to increased epithelial cell numbers.

Two other findings are noteworthy. In premenopausal women we observed that the mean Collagen Area % was 83.4% of the mean Faxitron Density % and in postmenopausal women the mean Collagen Area % was 78.0% of the mean Faxitron Density %. These percentages are not significantly different and show that the well-known reduction in mammographic density at menopause (8) is mirrored in a proportional reduction in collagen. The reduction in epithelial tissue in postmenopausal women was however greater than the reduction in Faxitron density or collagen. The other noteworthy finding was that the relationship of epithelium to collagen was the same in parous and nulliparous women. The well-known lower mammographic density in parous compared to nulliparous women is mirrored in the same proportional reduction in both collagen and epithelium.

The biological basis of the relationship of collagen in the human breast to epithelium is unclear. Blocking ovarian function with a GnRH agonist treatment (9) reduces mammographic density by approximately a third (10,11) which then returns when the GnRH is withdrawn (12). Some densities appear therefore to be closely related to current hormone exposure while others change only slowly with increasing age. Differences between these types of density have not been elucidated.

There is an abundant literature on the relationships between the breast stroma and epithelium (13,15). Epithelial and stromal cells, collagen and fat, the tissue components that contribute to mammographic density, are related to each other in several ways. Epithelial and stromal cells communicate by means of paracrine growth factors (16-18). Collagen is a product of stromal fibroblasts, and adipocytes develop from stromal preadipocytes (19). Factors that affect one of these components may therefore affect the others, directly or indirectly, and each component has properties that may influence risk and progression of breast cancer.

Breast cancer arises from epithelial cells, and the number and proliferative state of these cells may influence both the radiological density of the breast, and the probability of genetic damage that may give rise to cancer. In addition, collagen and stromal matrix are products of stromal cells that may

through their mechanical properties facilitate tumor invasion (20). Interactions among epithelial cells, stromal cells, and components of the extracellular matrix regulate the development of tumors (21). Metalloproteinases that regulate stromal matrix can also regulate the activation of growth factors and influence susceptibility to breast cancer (22,23).

To date, few studies have examined the association of mammographic density with the growth factors and stromal matrix proteins that mediate many of these effects in breast tissue. One study, using formalin fixed paraffin blocks of breast tissue (n=92) surrounding benign lesions, compared breasts with little or no radiological density to breasts with extensive density, with the two groups matched for age at the time of biopsy. Similar to the results described above, breast tissue from women with extensive densities had a greater nuclear area, and a larger stained area of collagen. In addition, stained areas by immunohistochemistry for TIMP-3 and IGF-1, were greater in subjects with extensive density compared to those with little breast density (24). Stromal proteoglycans that are expressed in association with breast cancer have also been found to be associated with mammographic density (25).

Three dimensional estimates of the amount of breast density can be made using various methods including MR imaging (26). Although three-dimensional methods have not proved to clearly improve upon the relationship between breast density and breast cancer risk, recent studies of the difference in the intensity of densities on MR imaging after administration of a contrast agent have found a further breast cancer risk factor, breast parenchymal enhancement (BPE) (27-29). The risks associated with BPE are large, of the same order as are found with mammographic density, and adjustment for MRI-measured density resulted in only a slight decrease in the estimated effects of BPE. BPE is thought to be a measure of amount of blood flow in the dense tissue and may represent breast activity.

Much more study of the biological basis of these major risk factors in normal human breast is needed if we are to exploit them in some way to help in developing chemopreventive approaches to breast cancer.

Disclosure of Potential Conflicts of Interest

No potential conflicts of interest were disclosed.

Authors' Contributions

Conception and design: SB, NB, LM, MP

Development of methodology: SB, NB, LM

Acquisition of data: SB, NB, DH, LM, DP

Analysis and interpretation of data: NB, LM, MP

Writing, review, and/or revision of the manuscript: LM, NB, MP

Acknowledgements

The authors wish to gratefully acknowledge Drs. Naomi Miller and Ming-Sound Tsao of the Department of Pathology, Princess Margaret Hospital, Toronto, Canada for carrying out the original immunohistochemistry on the samples discussed here. The authors wish to thank Ms Peggy Wan for data handling and programming help with this project.

Grant Support

This work was supported by a Department of Defense Congressionally Directed Breast Cancer Research Program Grant BC044808, by the USC/Norris Comprehensive Cancer Center Core Grant P30 CA14089, and by the Susan G. Komen Foundation Grant 99-318. The funding sources had no role in this report.

References

1. Li T, Sun L, Miller N, Nicklee T, Woo J, Hulse-Smith L, Tsao MS, Khokha R, Martin L, Boyd N. The association of measured breast tissue characteristics with mammographic density and other risk factors for breast cancer. *Cancer Epidemiol Biomarkers Prev* 2005;14:343-9.
2. Hawes D, Downey S, Pearce CL, Bartow S, Wan P, Pike MC, Wu AH. Dense breast stromal tissue shows greatly increased concentration of breast epithelium but no increase in its proliferative activity. *Breast Cancer Res* 2006;8:R24.
3. Boyd NF, Lockwood GA, Byng JW, Trichler DL, Yaffe MJ. Mammographic densities and breast cancer risk. *Cancer Epidemiol Biomarkers Prev* 1998;7:1133-44.
4. Bartow SA, Pathak DR, Mettler FA. Radiographic microcalcification and parenchymal pattern as indicators of histologic "high-risk" benign breast disease. *Cancer* 1990;66:1721-5.
5. Bartow SA, Pathak DR, Mettler FA, Key CR, Pike MC. Breast mammographic pattern: a concatenation of confounding and breast cancer risk factors. *Am J Epidemiol* 1995;142:813-9.
6. Boyd NF, Dite GS, Stone J, Gunasekara A, English DR, McCredie MR, Giles GG, Trichler D, Chiarelli A, Yaffe MJ, Hopper JL. Heritability of mammographic density, a risk factor for breast cancer. *N Engl J Med* 2002;347:886-94.
7. Stone J, Dite GS, Gunasekara A, English DR, McCredie MR, Giles GG, Cawson JN, Hegele RA, Chiarelli AM, Yaffe MJ, Boyd NF, Hopper JL. The heritability of mammographically dense and nondense breast tissue. *Cancer Epidemiol Biomarkers Prev* 2006;15:612-7.
8. Martin LJ, Boyd NF. Mammographic density. Potential mechanisms of breast cancer risk associated with mammographic density: hypotheses based on epidemiological evidence. *Breast Cancer Res* 2008;10:201.
9. Pike MC, Ross RK, Lobo RA, Key TJ, Potts M, Henderson BE. LHRH agonists and the prevention of breast and ovarian cancer. *Br J Cancer* 1989;60:142-8.
10. Spicer DV, Ursin G, Parisky YR, Pearce JG, Shoupe D, Pike A, Pike MC. Changes in mammographic densities induced by a hormonal contraceptive designed to reduce breast cancer risk. *J Natl Cancer Inst* 1994;86:431-6.
11. Weitzel JN, Buys SS, Sherman WH, Daniels A, Ursin G, Daniels JR, MacDonald DJ, Blazer KR, Pike MC, Spicer DV. Reduced mammographic density with use of a gonadotropin-releasing hormone agonist-based chemoprevention regimen in BRCA1 carriers. *Clin Cancer Res* 2007;13:654-658.
12. Gram IT, Ursin G, Spicer DV, Pike MC. Reversal of gonadotropin-releasing hormone agonist induced reductions in mammographic densities on stopping treatment. *Cancer Epidemiol Biomark Prev* 2001;10:1117-20.
13. Fata JE, Werb Z, Bissell MJ. Regulation of mammary gland morphogenesis by the extracellular matrix and its remodeling enzymes. *Breast Cancer Res* 2004;6:1-11. doi:10.1186/bcr634
14. Barcellos-Hoff M, Medina D. New highlights on stroma-epithelial interactions in breast cancer. *Breast Cancer Res* 2005;7:33-6.
15. Schedin P, Mitrenga T, McDaniel S, Kaeck M. Mammary ECM composition and function are altered by reproductive state. *Molec Carcin* 2004;41:207-20.
16. Cullen KJ, Lippman ME. Stromal-epithelial interactions in breast cancer. In: Dickson RB, Lippman ME, editors. Boston: Kluwer Associates. 1991, pp. 413-31.
17. Dickson RB, Lippman ME. Growth factors in breast cancer. *Endocr Rev* 1995;16:559-89
18. Sakakura T. New aspects of stroma-parenchyma relations in mammary gland differentiation. *Int Rev Cytol* 1991;125:165-202.
19. Zangani D, Darcy KM, Masso-Welch PA, Bellamy ES, Desole MS, Ip MM. Multiple differentiation pathways of rat mammary stromal cells *in vitro*: acquisition of a fibroblast, adipocyte or

endothelial phenotype is dependent on hormonal and extracellular matrix stimulation. *Differentiation* 1999;64:91-101.

20. Provenzano PO, Eliceiri KW, Campbell JM, Inman DR, White JG, Keely PJ. Collagen reorganization at the tumor-stromal interface facilitates local invasion. *BMC Med* 2006;4:38.
21. Tlsty TD, Coussens LM. Tumor stroma and regulation of cancer development. *Annu Rev Pathol* 2006;1:119-50.
22. Bhowmick NA, Neilson EG, Moses HL. Stromal fibroblasts in cancer initiation and progression. *Nature* 2004;432:332-7.
23. Wiseman BS, Werb Z. Stromal effects on mammary gland development and breast cancer. *Science* 2002;296:1046-1049.
24. Guo YP, Martin LJ, Hanna W, Banerjee D, Miller N, Fishell E, Khok R, Boyd NF. Growth factors and stromal matrix proteins associated with mammographic densities. *Cancer Epidemiol Biomarkers Prev* 2001;10:243-8.
25. Alowami S, Troup S, Al-Haddad S, Kirkpatrick I, Watson PH. Mammographic density is related to stroma and stromal proteoglycan expression. *Breast Cancer Res* 2003;5:R129-R135.
26. Aitken Z, McCormack VA, Highnam RP, Martin L, Gunasekara A, Melnichouk O, Maudsley G, Peressotti C, Yaffe M, Boyd NF, dos Santos Silva I. Screen-film mammographic density and breast cancer risk: a comparison of the volumetric standard mammogram form and the interactive threshold measurement methods. *Cancer Epidemiol Biomarkers Prev* 2010;19:418-28.
27. King V, Brooks JD, Bernstein JL, Reiner AS, Pike MC, Morris EA. Background parenchymal enhancement at breast MR imaging and breast cancer risk. *Radiology* 2011;260:50-60.
28. King V, Goldfarb SB, Brooks JD, Sung JS, Nulsen BF, Jozefara JE, Pike MC, Dickler MN, Morris EA. Effect of aromatase inhibitors on background parenchymal enhancement and amount of fibroglandular tissue at breast MR imaging. *Radiology* 2012 Jul 6. (Epub ahead of print).
29. King V, Gu Y, Kaplan JB, Brooks JD, Pike MC, Morris EA. Impact of menopausal status on background parenchymal enhancement and fibroglandular tissue on breast MRI. *Eur Radiol* 2012 Jul 4. (Epub ahead of print).

Table 1 Faxitron, tissue and demographic features of study subjects

	Premenopausal	Postmenopausal
N	146	85
Faxitron Density %	40 (20 – 50) ^a	20 (10 – 40) ^a
Collagen Area %	30.5 (14.0 – 46.8) ^a	12.5 (3.7 – 36.5) ^a
Glandular Area %	1.67 (0.94 – 2.86) ^a	0.68 (0.36 – 1.28) ^a
Epithelial Nuclear Area %	0.41 (0.21 – 0.84) ^a	0.10 (0.00 – 0.24) ^a
Age	32.5 (24 – 39) ^a	60 (52 – 71) ^a
BMI	22.2 (20.1 – 25.2) ^a	22.0 (18.9 – 25.8) ^a
Parity:		
Nulliparous	35	12
Parous	60	54
Not known	51	19
Ethnicity:		
Anglo	60	45
Hispanic	54	27
Native American	32	13

^aMedian and inter-quartile range.

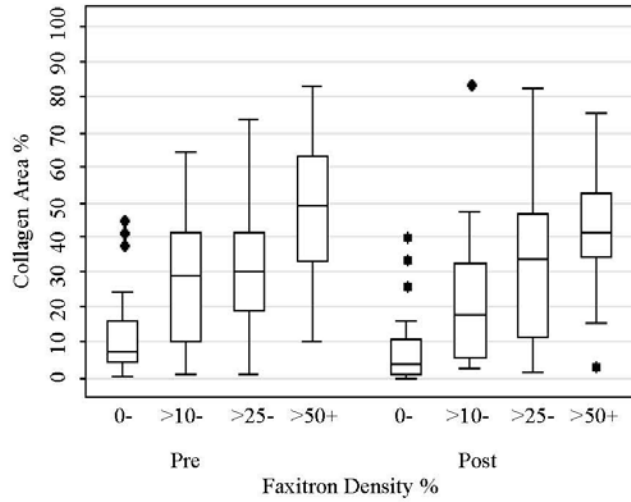


Fig. 1 Box-plot of Collagen Area % vs Faxitron Density % in premenopausal (Pre) and postmenopausal (Post) women. The box shows the 25th and 75th percentile (the interquartile range [IQR]) with the median marked within the box; the 'outliers' marked with ♦ are more than 1.5×IQR below (above) the 25th (75th) percentile; the 'whiskers' indicate the smallest (largest) value that is not an outlier.

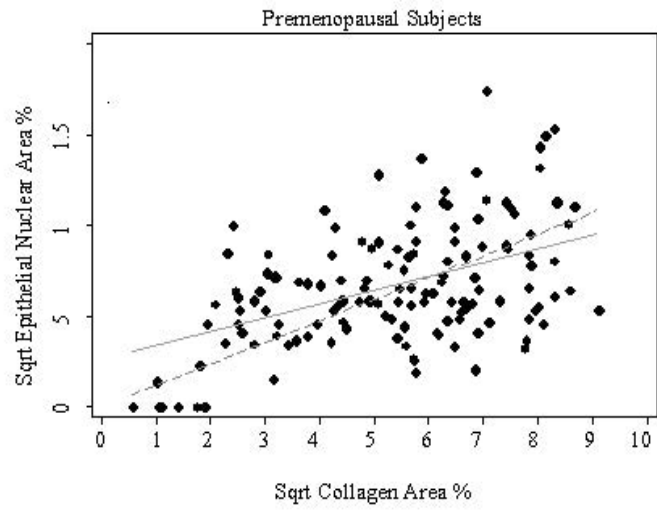


Fig. 2a Scatter plot of Epithelial Nuclear Area % vs Collagen Area %: solid line is fitted regression line, dashed line is regression line forced through the origin.

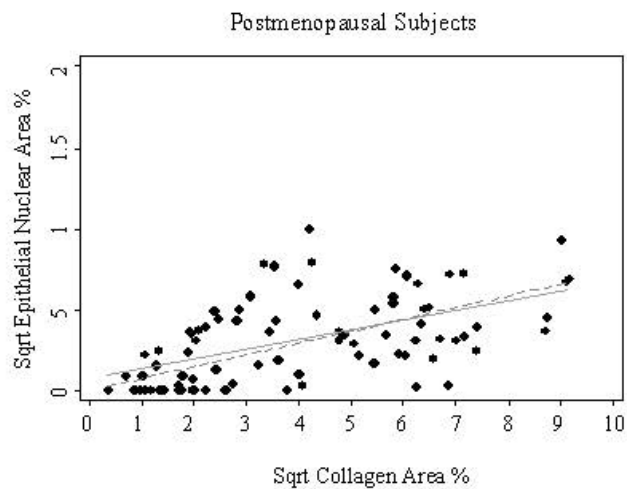


Fig. 2b Scatter plot of Epithelial Nuclear Area % vs Collagen Area %. solid line is fitted regression line, dashed line is regression line forced through the origin.